2022

Investigation of Antibiotic Persistence Mechanisms in Escherichia coli

Joanna Wioletta Urbaniec

Investigation of Antibiotic Persistence Mechanisms in *Escherichia coli*

By Joanna Wioletta Urbaniec

Submitted for the degree of Doctor of Philosophy

Department of Microbial Sciences at the University of Surrey

Department of Civil, Mining and Environmental Engineering at the University of Wollongong

November 2022

Declaration of originality

This thesis and the work to which it refers are the results of my own efforts. Any ideas, data, images, or text resulting from the work of others (whether published or unpublished) are fully identified as such within the work and attributed to their originator in the text, bibliography or in footnotes. This thesis has not been submitted in whole or in part for any other academic degree or professional qualification. I agree that the University has the right to submit my work to the plagiarism detection service Turnitin for originality checks. Whether or not drafts have been so assessed, the University reserves the right to require an electronic version of the final document (as submitted) for assessment as above.

Joanna Urbaniec, November 2022

Abstract

Antibiotic persistence occurs when a subpopulation of isogenic, antibiotic sensitive cells survives prolonged exposure to a bactericidal concentration of an antibiotic. This phenomenon has been shown to contribute to prolonged treatment duration, infection recurrence, as well as accelerated development of genetic resistance. Several molecular mechanisms have been demonstrated to influence formation of persister cells, however, the direct casual links between these mechanisms and persister cell formation remain to be established.

In this thesis we demonstrate that, contrary to previous reports, *E. coli* HipQ, a strain created during an untargeted mutagenesis screen known to produce a high number of antibiotic persisters, does not carry a mutation in the *ydcI* transcription factor. Subsequently, we present evidence suggesting that *ydcI* does not regulate persistence to β-lactams or fluoroquinolones. Furthermore, we show that the HipQ strain carries multiple other non-synonymous substitutions, in contrast to previously reported two single-nucleotide polymorphisms, including mutations in previously reported persistence regulators, which are likely to contribute to its high-persistence phenotype.

Next we demonstrate, with the use of flow cytometry and an [NADH:NAD+ biosensor], that ciprofloxacin exposure results in a high number of viable but non culturable cells (VBNCs). This ciprofloxacin-tolerant VBNC subpopulation has lower intracellular [NADH:NAD+], and therefore undergoes respiration at a lower rate, when compared to the bulk population. Furthermore, we show that *E. coli* HipQ antibiotic-tolerant cells have a significantly lower intracellular [NADH:NAD+] when compared to its parental strain, which likely is a result of a mutation in the glycolysis pathway *gap* gene.

Finally, we assess antibiotic resistance, persistence and biofilm formation capabilities in of a panel of urinary tract infection *E. coli* (UPEC) and demonstrate that in addition to multidrug resistance, high-persistence to critically important antibiotics meropenem and colistin is common amongst clinical isolates. We show that transient colistin resistance develops rapidly when UPEC are incubated in *in vivo* mimicking conditions and that their biofilm formation is dependent on attachment surface, with some isolates being able to form biofilms on the surface of a uroepithelial cell monolayer, but not polystyrene.

‘Altogether, this thesis improves our understanding of molecular mechanisms regulating the formation of *E. coli* antibiotic persisters, and further reaffirms the *in-vivo* relevancy of persistence research.'

Acknowledgements

The road to a PhD is a long and an uphill one. However, having finally reached my destination and looking back on my journey, I can with outmost certainty say that I could not have completed it alone. There were so many people who have helped and guided me along the way that I could not name them all here, but I will always be grateful for their support.

First and foremost, I would like to say an immense thank you to my incredible mentors, Dr Suzie Hingley-Wilson and A/Prof. Martina Sanderson-Smith. You not only helped me to become a much better scientist, but also always supported my personal development and wellbeing. I would also like to express my gratitude to the rest of my supervisory team, Prof. Johnjoe McFadden and Prof. Faisal Hai for their ongoing encouragement, guidance and granting me the opportunity to work on this inspiring project.

Secondly, I would like to thank all my fellow lab members from both UK and Australia, but especially my amazing friends Simone and Winnie. I cannot imagine my PhD journey without our late-night brainstorming sessions and early-morning coffee discussions. You were always there for me when I needed support and I will always be grateful for that.

I would also like to express my gratitude to the incredible technical support staff at both universities, for making my experiments run as smoothly as they could have, and always being understanding of my mistakes.

I would not have made it to where I am without the ongoing support of my non-microbiologist friends, who were always willing to listen to my ramblings when I couldn't get an experiment to work and helped me believe in myself whenever I doubted that a PhD wasn't the right path for me. Kaja, Ola, Michał – you are my absolute rocks.

And last, but certainly not least, I owe a massive thank you to the members of my family who supported my education journey and by doing so opened a world of opportunities for me – I hope that I have made you proud.

Table of contents

List of Figures

Chapter 2

Chapter 3

Chapter 4

Chapter 5

Chapter 6:

List of Tables

Chapter 2:

Chapter 4:

Chapter 5:

Chapter 6:

List of abbreviations:

- AMR: antimicrobial resistance
- AU: artificial urine
- CFU: colony forming unit
- CRISPR: clustered regularly interspaced palindromic repeats
- FBS: foetal bovine serum
- FSC: forward scatter
- KO: knock out
- LB: lysogeny broth
- LPS: lipopolisaccharide
- MDCK: Madin-Darby Canine Kidney
- MH: Mueller-Hinton
- MIC: minimum inhibitory concentration
- MM: Miles and Misra
- NAD: nicotinamide adenine dinucleotide
- NOS: reactive nitrogen species
- PBS: phosphate buffered saline
- PCR: polymerase chain reaction
- PFA: paraformaldehyde
- ROS: reactive oxygen species
- sgRNA: single-guide RNA
- RPI: reduced phenotypic Inheritance
- RPMI: Roswell Park Memorial Institute
- SNP: single nucleotide polymorphism
- SOB: super optimal broth
- SSC: side scatter
- TSS: transport and storage solution
- UPEC: uropathogenic *Escherichia coli*
- VBNCs: viable but non culturable cells

1. INTRODUCTION

1.1 Background

Antibiotic resistance (AMR) occurs when microorganisms acquire genes that render specific antimicrobials ineffective, either through *de novo* mutations in the genome, or horizontal gene transfer. Furthermore, certain bacterial species possess intrinsic resistance to selected antimicrobials. For example Gram negative bacteria are naturally resistant to glycopeptides due to the presence of the outer membrane preventing their diffusion into the cell (Reygaret *et al., 2018)*. AMR remains a growing burden for global public health, threatening to undermine decades of improvements in healthcare achieved since the discovery of antibiotics, a situation which the United Nations organisation has referred to as a 'global health emergency' (WHO, 2019). Concurrently to AMR, antibiotic persistence, as well as antibiotic tolerance, also referred to as 'phenotypic resistance', are alternative survival strategies. Tolerance is a population feature induced by environmental conditions affecting the metabolic state of the entire population, such as starvation or stationary phase of growth. In contrast, antibiotic persistence occurs when a small fraction of a susceptible isogenic population survives exposure to an antibiotic, and is capable of re-growth once it is removed. Both of the aforementioned phenomena differ from genetic resistance as they are reversible and non-heritable (Balaban *et al.*, 2019).

Persistence both increases treatment duration and can contribute to treatment failure. Furthermore, there is a growing array of evidence that it is a 'stepping-stone' which accelerates the development of genetic AMR (Windels *et al.*, 2017).

Antibiotic persistence is thought to stem from intrinsic phenotypic heterogeneity of bacterial populations (Balaban *et al.*, 2004; Hingley-Wilson *et al.*, 2020). Phenotypic heterogeneity occurs through stochastic variation in gene expression (Elowitz, M. B., *et al.* 2002; Cai, L., *et al.* 2006; Levine, E. and T. Hwa 2007), intrinsic asymmetry of cell division (Huh, D. and J. Paulsson 2011) and/or uneven distribution of nutrients in the environment (Stevanovic *et al.,* 2022*)*. Persistence is a complex phenomenon, as any phenotype which temporarily lowers antibiotic efficacy, such as slower cell division (decreased susceptibility to cell-wall synthesis inhibitors) (Hingley-Wilson *et al.*, 2020), downregulation of translation (reduction of target availability) (Semanjski *et al.*, 2018), upregulation of antibiotic efflux pump expression (increased antibiotic efflux) (Pu *et al.,* 2015), changes in cellular membrane permeability (decreased antibiotic uptake) (Allison

and Brynildsen, 2011), or extended lag phase (increased timeframe for antibiotic damage repair) (Mok *et al.,* 2018*)* can contribute to a bacterial cell surviving antibiotic exposure. However, unlike genetic resistance, persistence is not heritable i.e., 'daughter' cells of a persister cell will not necessarily be persisters themselves. Altogether, this makes persistence a challenging phenomenon to investigate as isolation of persister cells requires regrowth, which subsequently results in the loss of the 'persister phenotype' (Balaban *et al.*, 2019). Furthermore, currently there are no biomarkers which would separate persisters from its 'sister' population – viable but non-culturable cells (VBNCs). VBNCs, similarly to persisters remain viable following antibiotic exposure, however, unlike persisters they are not capable of regrowth in standard conditions (Dong *et al.,* 2019). It is hypothesised that these cells could be an extreme variant of persisters, however this remains to be experimentally proven.

Despite the challenges in studying antibiotic persisters, several effective anti-persister drugs have shown promise *in vitro* and in infection models, however so far none were able to completely eradicate this subpopulation. These strategies are based predominantly on altering persister cell metabolism and 'forcing' them into an antibiotic susceptible state (Allison and Brynildsen 2011; Marques *et al.*, 2015) or on by-passing their tolerance mechanisms through combination therapy (Chua *et al.*, 2016; Baek *et al.*, 2020) or direct cell lysis (Mensa *et al., 2011;* Hu and Coates 2013). Nevertheless, improved understanding of molecular mechanisms which allow persistent bacteria to survive exposure to antibiotics would likely inspire new therapeutic regimes capable of killing persisters, and subsequently contribute to the prevention of AMR emergence.

The persister subpopulation is enriched in so-called high-persister (Hip) strains, where a genetic mutation increases the likelihood of persister cell formation. These strains have been used as models for studying molecular mechanisms regulating antibiotic persistence, as they allow for identification of 'persistence-related' genes and investigation of how their function (or misfunction) leads to antibiotic persistence (Korch, Henderson and Hill 2003; Balaban *et al., 2004;* Hingley-Wilson *et al.* 2020). One such strain is *E. coli* HipQ (Wolfson *et al., 1990*), which was found to be highly persistent to β-lactams *and* fluoroquinolones (generating 10 to 1000-fold more persister cells than its parental strain). The mechanism responsible for its increased antibiotic persistence has previously been linked to the phenomenon of 'reduced phenotypic inheritance' i.e., reduced correlation of growth parameters between cells of the same lineage, and the underlying cause was proposed to be a single nucleotide polymorphism in the transcription factor *ydcI*, as this phenotype was also observed in a deletion mutant of this

gene (Hingley-Wilson *et al.*, 2020). *ydcI* is highly conserved across *Enterobacteriaceae* (Solomon *et al., 2014)* and therefore would be considered as a good potential target for target-based drug design pipelines.

1.2 Knowledge gaps

The *ydcI* transcription factor has so far been extensively characterised in *Salmonella enterica* serovar typhimurium, where it is known to regulate acid stress resistance and biofilm formation as a part of the global stress response operon *RpoS* (Solomon *et al. 2014;* Romiyo and Wilson, 2020). In contrast to *Salmonella spp.,* in *E. coli* overexpression of the YdcI protein has been shown to be extremely toxic, and subsequently increase sensitivity to antibiotics (Solomon *et al.,* 2014). However, the mechanism through which *ydcI* regulates antibiotic persistence is poorly understood. As mentioned previously, *ydcI* knock-out strain was shown to display both reduced phenotypic inheritance and increased persistence to ampicillin (Hingley-Wilson *et al. 2020)*. Currently it is unknown whether this phenotype is specific to ampicillin or extends to other antibiotics as well. Furthermore, increased antibiotic persistence of the Δ*ydcI* strain has only been demonstrated on batch level and therefore it is unknown whether it occurs through the same mechanism as in *E. coli* HipQ, where small, slow-growing cells are highly likely to become persisters (Hingley-Wilson *et al., 2020)*. Finally, *ydcI* has been proposed to regulate expression of 16 genes (Gao *et al., 2018)*. Elucidating which of these downstream 'effector' genes contribute to persister cell formation would provide additional alternative therapeutic targets.

Concurrently, a marker which would allow for separation of persister from VBNC cells without the need for regrowth (and therefore loss of the persister phenotype) would facilitate isolation and differential characterisation of these similar, yet functionally distinct subpopulations. Several potential markers (*tolC, tnaC, ptsG)* have been previously suggested by Bamford and colleagues (Bamford *et al.* 2017). However, these markers have only been evaluated in the context of ampicillin, and are only differentially regulated between persisters and VBNCs post antibiotic exposure. A biomarker which is differentially expressed prior to antibiotic exposure would provide a further advantage, as it would allow for sorting and enrichment of either of the subpopulations of interest. In *E. coli* altered reductase activity has previously been shown correlate with persistence (Omar and Brynildsen 2013a, 2015, Mohiuddin *et al.,* 2020), however whether this also applies to the VBNC subpopulation remains poorly understood. Determining whether

disrupted intracellular redox balance is a ubiquitous and specific 'persistence' marker would contribute to improved, regrowth-independent persister isolation protocols.

Finally, the majority of research into antibiotic persistence has been done on laboratory adapted strains. Although there is a degree of evidence supporting the significance of antibiotic persistence in the clinical setting (Bigger, 1944; Luo *et al.,* 2012; Schumacher *et al.* 2015), routine laboratory screening of pathogenic isolates does not determine neither the presence nor the frequency of persister cells. It is important to understand whether high persistence is common amongst clinical isolates and how it relates to the presence of other virulence factors, such as biofilm formation, where presence of persister cells has been suggested to be a key factor governing biofilm virulence (Anderl *et al.,* 2003; Nguyen *et al.,* 2011).

1.3 Research objectives

The primary research objective of this thesis is to investigate the role of the transcription factor *YdcI* in regulating antibiotic persistence in *E. coli*, with the aim of discovering new drug targets effective against persister cells. This will be achieved through functional analysis of *ydcI* and its effector genes on both batch and single-cell level.

The second objective is to investigate disrupted intracellular redox balance as a biomarker for transient antibiotic tolerance, with the aim of providing an improved framework for isolation and characterisation of antibiotic-tolerant subpopulations, i.e., persister and VBNC cells on a single-cell level. This will be achieved through investigation of NADH homeostasis of *E. coli* persisters, VBNCs and antibiotic-susceptible cells prior and post antibiotic exposure with the use of a [NADH:NAD+] biosensor.

The final objective is to phenotypically characterise a panel of uropathogenic *E. coli* isolates with the aim of providing further evidence of high antibiotic persistence in clinically relevant pathogens, and its relationship to other virulence determinants. This will be achieved through investigation of antibiotic resistance, antibiotic persistence, and biofilm formation capability of these isolates in both *in vitro* and *in vivo*-mimicking conditions.

1.4 Thesis outline

This thesis is divided into seven chapters:

Chapter 1 contains the background to, knowledge gaps, and research objectives of this thesis

Chapter 2 contains the literature review of topics relevant to the research objectives of this thesis

Chapter 3 contains general materials and methods

Chapter 4 contains the investigations pertaining to the role of *ydcI* transcription factor in high persistence of *E. coli* HipQ

Chapter 5 contains investigations pertaining to NADH homeostasis of *E. coli* persisters, VBNC cells, and antibiotic susceptible cells prior and post ciprofloxacin exposure

Chapter 6 contains investigations pertaining to characterisation of antibiotic resistance, antibiotic persistence, and biofilm formation capability of a panel of uropathogenic *E. coli*

Chapter 7 contains final conclusions and future work recommendations

2. Literature Review

This chapter has been published as a review article in FEMS Microbiology Reviews (https://doi.org/10.1093/femsre/fuab042) with Ye Xu as a joint first co-author. Both authors contributed equally to writing and editing of this work. The article content has been further edited for relevance and clarity by the author of this thesis.

2.1. Overview of antibiotic persistence

2.1.1. Discovery of persistence

The phenomenon of antibiotic persistence was first observed by American microbiologist Gladys Hobby who observed that a small fraction of *Streptococcus* cells was able to survive penicillin treatment that proved lethal to the rest of the isogenic population (Hobby *et al.*, 1942). Shortly after, in 1944, the phenomenon was named 'bacterial persistence' by Irish academic Joseph Bigger who observed that a small minority of cells (about 1 in 10^6) in cultures of *Staphylococcus aureus*, isolated from patients, could not be eradicated even using high doses of penicillin. Bigger also hypothesised that persistence was induced by environmental stresses, such as pH, and might be caused by slow growth rate of persister cells rather than a heritable resistance (Bigger, 1944). It would be another forty years before the phenomenon of persistence was further investigated through molecular techniques, largely due to the difficulty of studying minority subpopulations using traditional microbiological assays. Alongside molecular advances, increasing evidence has emerged implicating antibiotic persistence as a cause of treatment failure (Cohen *et al.*, 2013) and as a 'stepping-stone' for genetic antibiotic resistance (Windels *et al.*, 2019; Liu *et al.*, 2020). Antibiotic persistence is noted in multiple clinically relevant pathogens from *Mycobacterium tuberculosis* (Manina *et al.*, 2015, Vilcheze and Jacobs, 2019), *Pseudomonas aeruginosa* (Nguyen *et al.*, 2011), *Escherichia coli* (Balaban *et al.*, 2004) and Methicillin-Resistant *S. aureus* (MRSA) (Kim *et al.*, 2018) and is likely to be a cornerstone to disease control and to combatting AMR.

2.1.2. What is a persister?

In this thesis the term ‘persistence’ will refer to a subpopulation of bacterial cells that possess the non-heritable character of surviving prolonged exposure to an antibiotic that kills isogenic sister cells. The key features that distinguish persistence from genetic resistance are that it involves only a subpopulation of isogenic cells that do not carry resistance genes, so the phenomenon is sometimes termed as phenotypic, rather than genetic, resistance (Balaban *et al.,* 2019). It also tends to not be antibiotic-specific; or, at least, persister cells can be detected that are tolerant to a wide variety of antibiotics (Moyed and Bertrand 1983; Wolfson *et al.*, 1990), suggesting that the majority of persistence is a general, rather than antibiotic-specific, phenomenon. However, it appears that there is a subclass of persisters that are antibiotic-specific which we will also describe further in this chapter.

Persisters are also sometimes described as being *tolerant* to an antibiotic, rather than genetically resistant, with the term ‘tolerance’ indicating that the capability of surviving exposure to antibiotics is reversible and non-heritable. In contrast to persistence, antibiotic tolerance can be a feature of an entire population of cells when, for example, it is exposed to stress, starvation, or stationary phase growth, which are conditions that restrict growth of the entire population. In this sense, persisters could also be described as being hetero-tolerant, *i.e*., a subpopulation of antibiotic tolerant cells within a population of mostly sensitive cells (Balaban *et al.*, 2019). Persistence is also a term used to refer to infections that persist in the host without causing disease (Centre for Disease Control and Prevention, 2019) and without reference to antibiotic persistence. Although it has often been speculated that these ‘infection persisters’ are the same kind of cells as antibiotic persisters, this remains to be established. To avoid confusion of terms, Balaban has recently proposed that persisters, meaning a subpopulation of tolerant cells, should, at least initially, be referred to as ‘antibiotic persisters’ (Balaban *et al.*, 2019) to distinguish them from infection persisters. Another distinct subpopulation of cells that can be observed in bacterial culture are viable but non-culturable cells (VBNCs/ sleeper cells) that remain intact and metabolically active after exposure to an antibiotic but, unlike persisters, do not resume growth after removal of the antibiotic (Dong *et al.*, 2019). It has been shown that, if incubated for long enough, some VBNCs of several bacterial species may eventually resume growth (Dong *et al.*, 2019) and could thereby represent a persister population with a very long lag phase. This assumption is supported by transcriptomics, where it has been demonstrated in an innovative study that *E. coli* ‘sleepers’ display similar levels of expression of several persistence-related genes to

persister cells (Bamford *et al.*, 2017). However, for the purposes of this thesis, we will retain the term persisters to cells that both remain viable and eventually regrow after removal of antibiotic. The link between persister formation and persister subclasses within biofilms is another intriguing avenue of research and one which may require further nomenclature changes in the future.

Note that the above persister definition encompasses cells that survive exposure to antibiotic not only *in vitro,* but also during treatment of infections in humans or animal models. The existence of such cells was established as early as 1956 by McCune and Tompset who used a mouse-infection tuberculosis (TB) model to demonstrate that antibiotic-sensitive *M. tuberculosis* bacilli could be cultured from one third of experimental animals 90 days after successful treatment with isoniazid, para-aminosalicylic acid (PAS) and streptomycin (as determined by culture, microscopy, and sub-inoculation) (McCune and Tompset, 1956). A shortened revival time was detected in immuno-compromised mice, suggestive of immune regulation of persistence (McCune *et al.* 1966). Pathogens might survive in a treated host due to lack of penetration of the antibiotic into the persister bacilli or in tissue sites (Ray *et al.*, 2015), cells (Greenwood *et al.*, 2019) or through an inadequate host immune response, as in *in utero* infections of bovine viral diarrhoea virus (Khodakaram-Tafti and Farjanikish, 2017). However, these explanations are unlikely to account for the persistence of the infection in multiple body sites after prolonged treatment, as in the above mouse model. It seems more likely, and thereby it is generally assumed, that the subpopulation of cells that survive prolonged antibiotic treatment in patients or animal models are indeed the same kind of persister cells that survive prolonged antibiotic exposure *in vitro*. This is an important assumption as it justifies the relevance of *in vitro* persistence models to *in vivo* systems and clinical disease, however to our knowledge it remains unproven.

The McCune and Tompset experiments also revealed another important aspect of persistence: it is not the same for all antibiotics. Although persister cells survived 12 weeks of treatment with isoniazid, PAS and streptomycin in the mouse model, no viable bacteria could be recovered from animals treated for the same period with just pyrazinamide and isoniazid. This suggest that pyrazinamide may be more effective at killing TB persisters, however the exact mechanism through which this occurs is currently unknown. The observation that antibiotics differ in their relative efficacy against persisters vs the bulk population of cells demonstrates that persisters are physiologically distinct from the bulk population. This provides the rationale for the long-term aim of identifying novel compounds that target these physiologically distinct antibiotic-recalcitrant cells in order to shorten treatment regimes.

Table 2.1. Terms used commonly in persistence research

antibiotic persistence	A phenotypic feature defining a subpopulation of isogenic bacterial cells which display a greatly reduced killing rate to antibiotic(s) when compared to the entire population; the reduction of the killing rate is largely independent of the antibiotic concentration (i.e., no change in minimum inhibitory concentration (MIC) to the antibiotic is observed); also referred to as **subpopulation tolerance** and **heterotolerance** (Balaban *et al.*, 2019)
antibiotic tolerance	A feature defining an entire population of bacterial cells which display decreased killing rate to antibiotic(s); similarly to persistence the reduction of killing rate is largely independent of the antibiotic concentration (Balaban *et al.*, 2019)
antibiotic/antimicrobial resistance (AMR)	A feature of the entire population of microorganisms which possess a genetic resistance mechanism that allows them to overcome the harmful effect of a given antibiotic; AMR is concentration dependent and characterised by an increase in MIC for a given antibiotic (Canton and Morosini, 2011)
persistent (chronic) infection	Any infection (bacterial/viral/fungal) which persists in the host for a prolonged period (Centre for Disease Control and Prevention, 2019)

2.1.3. What are the evolutionary origins of antibiotic persistence?

Although persistence is non-heritable, the frequency of persister cells in a population is a heritable trait, as has been shown by several studies that demonstrate gene mutations that either increase or decrease that frequency (Moyed and Bertrand, 1983; Wolfson *et al.*, 1990; Hingley-Wilson *et al.*, 2020). Being heritable, the frequency of persisters in the population would be visible to natural selection and likely evolved as a 'bet hedging' strategy. 'Bet hedging' is an evolutionary survival strategy first described in 1974 (Slatkin, 1974). It proposes that in uncertain changing environments it is evolutionarily favourable to introduce phenotypic heterogeneity into an isogenic population to be better prepared for unpredictable environmental perturbations, such as encountering antibiotics (Slatkin, 1974). The theory is supported by mathematical models in which populations generating higher persister cell levels have an increased fitness (capability of surviving the bottleneck event of antibiotic exposure) when repeatedly exposed to bactericidal antibiotics (Johnson and Levin., 2013). It also seems to be supported by recent evidence that laboratory exposure of *E. coli* to repeated dual-antibiotic regimes results in significant enrichment of the persister fraction, through convergent mutations in proteins involved in tRNA synthetases, as well as methionine synthetase MetG (Khare and Tavazoie, 2020). An alternative perspective is that persistence is an inevitable consequence of 'errors' during cell cycle and division that introduce phenotypic heterogeneity, a hypothesis sometimes known under the acronym 'PASH' (persistence as stuff that happens) (Levin *et al.*, 2014). It could be that different persister classes as described below have different evolutionary origins.

2.1.4. Can antibiotic persistence facilitate the emergence of genetic antibiotic resistance?

It has recently been hypothesized that this already clinically relevant subpopulation may be a reservoir for genetic antibiotic resistance. For example, prolonged exposure to DNA-damaging fluoroquinolones and hydroxyl radicals produced as a result of exposure to β-lactams, fluoroquinolones and aminoglycosides (Kochanski *et al.*, 2007) is likely to lead to a degree of DNA damage, and as a result activation of the SOS response. SOS response activation in turn causes induction of expression of error-prone DNA polymerases such as DNA polymerase IV and V which increases rates of adaptive mutation (McKenzie *et al.*, 2000), provided that the cell survives the antibiotic exposure (i.e. is a persister). Indeed, there is an increasing array of evidence suggesting that persistence (and whole population antibiotic tolerance) could accelerate genetic

resistance development (Liu *et al.*, 2020; Mok and Brynildsen, 2018; Vogwill *et al.*, 2016). For example, there is *in vitro* evidence that persistence can be a contributing factor to the emergence of resistant strains of *M. tuberculosis*, possibly as a result of increased levels of mutagenesis-inducing hydroxyl radicals found in *M. tuberculosis* persisters (Sebastian *et al.*, 2017).

Interestingly, persistence to one antibiotic could not only facilitate the emergence of genetic resistance to that antibiotic, but other antibiotics as well. For instance, rifampicin (RIF)-persisters in *M. tuberculosis* which carried elevated levels of hydroxyl radicals were found to carry *de novo* acquired mutations not only associated with RIF-resistance mutations (*rpoB*), but also moxifloxacin-resistant mutations (*gyrA*) (Sebastian *et al.*, 2017). Increased mutagenesis rates were also identified in moxifloxacin persisters of *Mycobacterium smegmatis,* which developed moxifloxacin resistance, as well as resistance to ethambutol and isoniazid (Swaminath *et al.*, 2020). A similar mechanism has also been identified in *S. aureus* where exposure to ciprofloxacin resulted in the induction of error prone DNA polymerases that increased the number of resistant mutants 30-fold when compared to a SOS response or error-prone polymerase deficient knock-out control (Cirz *et al.*, 2007).

Finally, analysis of clinical isolates of MRSA carried out by Liu and colleagues (Liu *et al.*, 2020) has demonstrated that certain combination therapies which are effective in preventing emergence of genetic AMR through a mechanism called ‘suppressive action’ fail to do so if tolerance to the primary (non ‘suppressive’) drug is established prior or during the course of treatment. Suppressive action is a mechanism by which a combination of two drugs is less effective than the single drug alone, for example, as a proof-of-concept in the case of treatment with any β-lactam antibiotic (which most effectively targets dividing cells) and chloramphenicol (which slows down growth) (Jawetz *et al.*, 1951). This paradoxically decreases the survival rate of chloramphenicol resistant mutants and thereby decreases their frequency in the population. Pre-establishment of tolerance to the non-suppressive antibiotic negates its anti-AMR effect, providing *in-vivo* evidence of a direct link between tolerance (and persistence), resistance and clinical treatment failure (Liu *et al.*, 2020). This study suggests that targeting persisters and inhibiting the persistence state could thereby inhibit the development of genetic AMR.

2.1.5. How is antibiotic persistence quantified?

The “gold standard” experimental system used to demonstrate the presence of persisters and estimate their abundance is the antibiotic time-kill experiment, which generates the classic biphasic kill curve from the average killing dynamics (Figure 2.1). Typically, an exponentially-growing population of isogenic bacteria is exposed to antibiotic and samples are taken at regular time points for determination of colony forming units (cfu, on a log scale) as a function of time. If persister cells are present, the kill rate of is made up of two components: a fast initial kill characteristic of the susceptible population and a slower kill characteristic of the persister subpopulation. If the slow killing phase is extrapolated to zero time then where it crosses the y axis provides an estimate of the persister fraction in the initial population (Balaban *et al.*, 2019). Figure 2.1 shows an ‘ideal’ difference in kill curve shapes between susceptible, highly-persistent, genetically-resistant, and tolerant populations. For instance, a typical time-kill curve of *M. tuberculosis* using front-line antibiotics such as isoniazid follows a biphasic curve, as highlighted in this comprehensive review detailing TB persisters (Vilcheze and Jacobs 2019).

It should however be emphasized that kill curves are extraordinarily sensitive to the precise conditions of the experiment and particularly the growth state of the initial population, which can lead to well-known reproducibility issues. This experimental and stochastic variation in each experiment can obscure data from the relatively minute persister subpopulation. Different batches of antibiotic or media, culture age, variation in storage or growth conditions and the presence of resident phages can also influence the shape of kill curves (Harms *et al.*, 2017). Culture conditions can also profoundly influence phenotypic heterogeneity (Smith *et al.*, 2018) which, as we will later discuss, plays a key role in persistence. It also appears that selection and outgrowth may also affect reproducibility where growth regulation is affected, discussed in more detail in chapter 4 of this thesis.

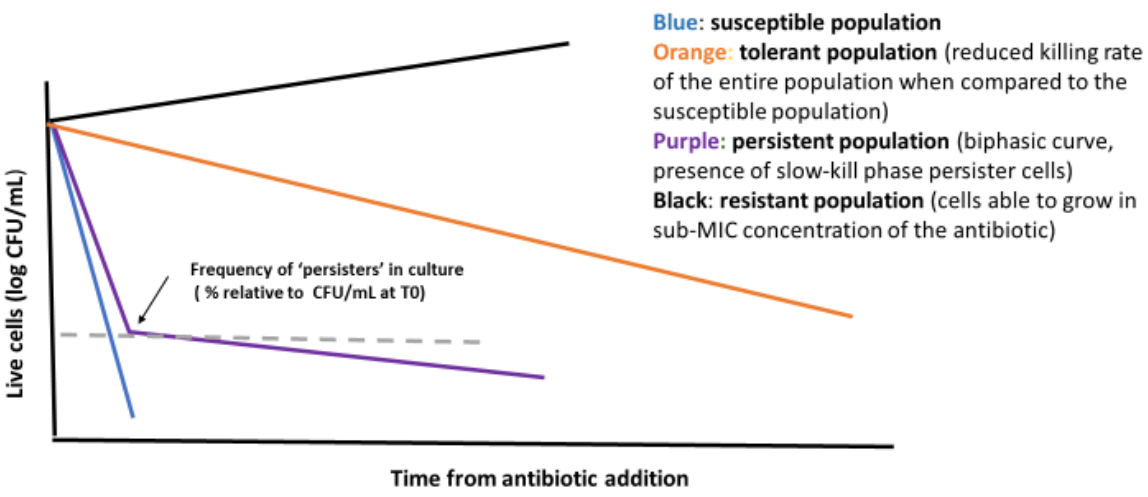

Figure 2.1. The highly heterogenous persister cell can be observed at batch level. *Biphasic killing at batch level: an example time-kill curve shape of resistant, susceptible, high-persister and tolerant cultures. The resistant population is able to grow in sub-inhibitory concentrations of an antibiotic, whereas tolerant and persister cells are eventually killed by the antibiotic, but at a much slower rate. Persistence is quantified as % of live cells following antibiotic exposure relative to the starting population.*

Since, as illustrated by the biphasic kill curve (Figure 2.1), persistence is a property of only a minority of cells, traditional microbiological, cell biological, or molecular biological analysis techniques that examine bulk populations are unsuitable for studying the phenomenon. Two approaches have been most productively applied to study persistence: microbial genetics and single cell microscopy studies.

The majority of antibiotic persistence studies have been performed on the microbial workhorse, *E. coli*, which will be discussed first, particularly with reference to the canonical *hipA7* system from which much of the theory of persistence has been derived. After examining both genetic and single cell studies of this system we will go on to outline a general theory of persistence and then examine how well the theory accounts for the evidence from a variety of systems.

2.2. Antibiotic persistence in *Escherichia coli*

2.2.1. Genetic studies to identify *E. coli* hip mutants

The first significant advance in the study of persisters was the application of mutagenesis and microbial genetic studies in the 1980's to identify 'high-persister' or hip mutant strains of *E. coli* K12 strain, including the intensively-studied HipA7 strain (Moyed and Bertrand, 1983). In this study, an *E. coli* K12 strain was exposed to untargeted chemical mutagenesis in rich media and then subjected to three rounds of enrichment for mutants that survived repeated exposure to 100 µg/mL of ampicillin, the third exposure being for 20h. Hip mutants were identified as strains that showed a higher survival (quantified as % of live cells following antibiotic exposure) after exposure to ampicillin, compared to the wild-type. Mutants that were genetically resistant or unable to grow on minimal media were discarded. It should be noted that mutants with substantially reduced growth of the whole population were also discarded. Note that techniques to examine growth of sub-populations were not yet available. Nonetheless, all the hip mutants identified showed some degree of growth impairment in rich media (Lysogeny broth commonly known as LB), providing a link between mutations increasing persistence and slow growth (Moyed and Bertrand, 1983). However, two mutants, HM7 and HM9-GLUCOSE, grew as rapidly or faster than the parental strain in minimal media yet continued to display 1000-fold higher frequencies of persisters than the wild-type in this media, proving that slow growth of the bulk population is not a requirement of high levels of persistence. The researchers performed batch time-kill assays for wild type and both the HM*7* and HM9-GLUCOSE mutants. Examination of the curves obtained suggested a population of around 0.1% persisters in the wild-type and about ten times this in both mutants. The researchers then went on to utilize classical microbial genetic approaches to map the genetic loci for both HM7 and HM9-GLUCOSE (Moyed and Bertrand, 1983) to the closely-linked loci *hipA7* and *hipA9* (high-persistence locus A7 and A9).

Later studies (Korch *et al.*, 2003) established that the *hipA7* gene encoded the toxin component of one of several of toxin-antitoxin systems present in the *E. coli* genome. To our knowledge the *hipA9* gene remains uncharacterised. Toxin-antitoxin modules are widely distributed in bacteria and consist of genes encoding a stable toxin and an unstable antitoxin (Ezaki *et al.*, 1991). The wild-type *hipA* gene encodes the toxin, HipA, which is neutralized by its antitoxin, HipB, encoded by the adjacent *hipB* gene. If not neutralized, HipA acts as a serine-threonine kinase that inhibits protein synthesis by phosphorylating (and therefore inactivating) glutamyl-tRNA synthetase (GltX),

responsible for attachment of glutamine to tRNA. The protein inhibition results in accumulation of uncharged tRNA which indirectly increases levels of (p)ppGpp (guanosine pentaphosphate) in the cell. (p)ppGpp is an alarmone (*i.e*., a signalling molecule produced in unfavourable conditions) and component of the stringent response in response to amino acid starvation. Downstream effects of its increase include inhibition of RNA synthesis and initiation of growth arrest to induce a state of "dormancy", understood as a reversible state of little-to-no growth and lower metabolic activity (Semanjski *et al.* 2018). ppGpp levels are themselves regulated by proteins collectively referred to as RSH (RelA SpoT homologs) that are upregulated by various stress-related molecules as the aforementioned uncharged tRNA or cAMP. The HipAB system thereby connects with a wide range of cellular physiological systems (Atkinson *et al.*, 2011).

Evidence for HipA toxin-induced growth arrest has been obtained from several systems. For example, Korch and colleagues discovered that over-expression of HipA from a plasmid induces a VBNC-like state in approximately 95% of the population that continued for up to 72hrs with continuous HipA expression. A fraction of cells, from 1.8 to 20%, resumed growth following the 72hrs of continuous induction, decreasing with increasing induction time. Additionally, in cultures overexpressing HipA a significant (10 000-fold) increase in the number of persisters to ampicillin was observed (Korch et al, 2006). It was hypothesized that the much lower fraction of persisters in the wild-type population is accounted for by lower levels of HipA expression, similar to that of the HipB antitoxin.

The *hipA7* high-persistence phenotype is conferred by point mutations at two separate sites in the *hipA* gene (*hipA7* allele), both of which are necessary for the hip phenotype (Moyed and Bertrand 1983). How these mutations lead to high levels of persistence is not fully clear (Figure 2.2A and 2.2B). One appears to render the HipA protein non-toxic since its overexpression only moderately inhibits growth and translation in comparison to wild-type HipA, while the other is required for the observed 'high-persistence' phenotype (Korch *et al.*, 2003). The non-toxicity is thought be a consequence of a reduced ability of the HipA7 protein to phosphorylate targets such as GltX and several other proteins involved in regulation of transcription (Semanjski *et al.*, 2018). It also has a weaker binding affinity to its cognate antitoxin. However, and rather paradoxically, over-expression of the *hipA7* allele causes a 12-fold higher phosphorylation of GltX when compared to the wild-type toxin (Semanjski et al, 2018). A model has been proposed to account for these apparently contradictory findings, in which chromosomally expressed HipA7 exists more abundantly in the unbound form when compared to HipA, allowing phosphorylation of more GltX. This results in the slower growth rate of HipA7 expressing strain (however this phenotype is lost whenever HipA is artificially overexpressed).

Additionally HipA, unlike HipA7, also phosphorylates other targets which are proposed to contribute to its toxicity (Semanjski *et al.*, 2018) and ability to induce the VBNC state (Korch *et al.*, 2003). Interestingly, naturally occurring *hipA7* variants has been identified in urinary tract infections suggesting that the locus may also induce persistence *in vivo* (Schumacher *et al.*, 2015).

It is important to note that although both *hipA* and *hipA7* alleles have primarily been investigated in relation to persistence to ampicillin, there is a evidence that these toxins contribute to multidrug tolerance. For instance, recently identified *E. coli* clinical isolate carrying the *hipA7* allele on the bacterial chromosome has been shown to display up to ~100-fold higher persistence to fluoroquinolone ciprofloxacin when compared to its parental strain (Schumacher *et al.*, 2015). Similar effect has also been observed previously in lab-adapted *E. coli* MG1655 cells induced to overexpress the wild-type HipA from a plasmid (Germain *et al.*, 2013). This observed 'high-persister' phenotype to fluoroquinolones is presumably a result of toxin-induced extended lag phase of *hipA/hipA7* persisters, discussed further in section three of this chapter.

A.

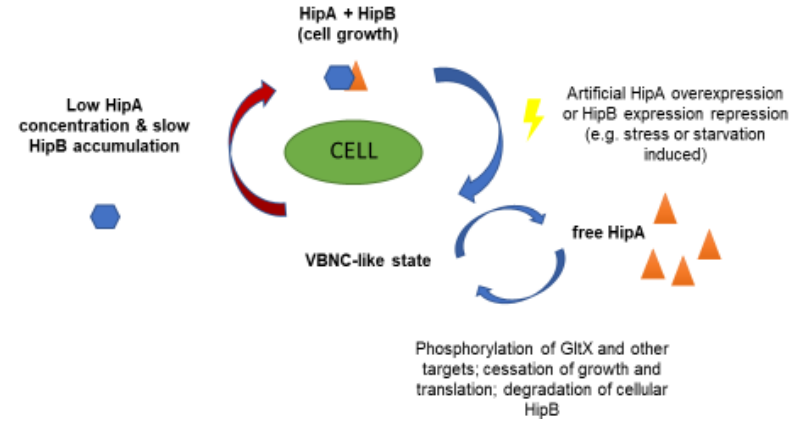

B.

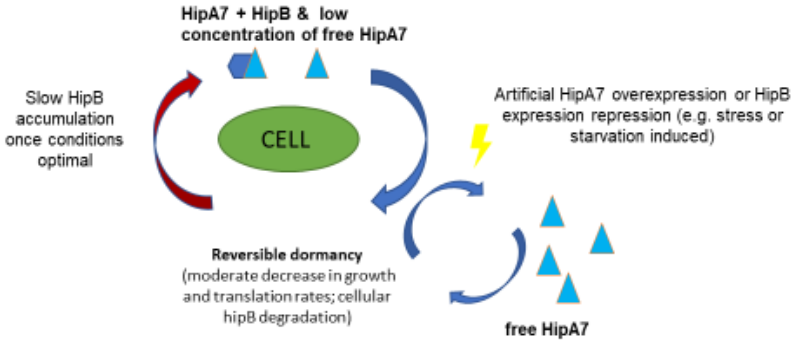

Figure 2.2. Schematic representation of A. HipA and B. HipA7-induced changes in cellular metabolism. *A. HipA phosphorylates GltX, as well as several other proteins involved in growth and translation regulation, inducing a HipA/HipB ratio-dependent VBNC-like state in cells containing unbound HipA. Growth can resume only after HipB binds to and inactivates free HipA. B. The mutant HipA7 protein (lower panel) can exist in the unbound form at higher levels in the cell without inducing a VBNC-like state as it only phosphorylates GltX and with lower efficiency than the wild-type protein. High levels of free HipA7 in the cell induce reversible "dormancy" which is proposed to be responsible for the high-persistence phenotype.*

2.2.2. Single cell studies of the HipA7 mutant

Although characterization of hip mutants provided insights into factors that might increase or decrease the frequency of persistence, the nature of the persister cells remained a matter of conjecture until pioneering studies performed by Balaban and colleagues who developed microfluidic systems to perform live cell imaging of bacterial populations before, during and after antibiotic exposure. The focus of much of their studies was the HipA7 mutant as its characteristic high frequency of persister cells (1000 x more than wild-type frequencies in their studies) made the phenomenon much more experimentally tractable. The character of persistence was found to be associated with cells that, prior to antibiotic exposure, were either slow-growing or non-growing, prompting the hypothesis that persistence is due to pre-existing phenotypic heterogeneity associated with slow growth rate in the starting population (Balaban *et al.*, 2004). The established association between *hipA7* and toxin-antitoxin systems prompted the proposal that stochastically variable levels of expression of the HipA toxin and consequent low or zero growth in a sub-fraction of cells might be a source of the pre-existing variation (Korch *et al.* 2003; Keren *et al.*, 2004) and origin of persistence. Thereafter, many other high-persistent mutants in numerous bacterial strains and species have been described (Torrey *et al.*, 2016, Wilmaerts *et al.*, 2018). Additionally, low persister mutants that have a lower frequency of persisters than wild-type cells have been identified, eg *E. coli* Δ*ybaL* (Hingley-Wilson *et al.*, 2020). Both types of mutants identify genes that influence the frequency of persisters in bacterial populations and thereby provide clues as to the mechanisms of persistence, or, at least, mechanisms involved in the generation of persisters.

Moreover, Balaban observed two distinct types of persister cells: triggered (previously type I) persisters which were non-growing cells in stationary phase that displayed extended lag phase upon inoculation into fresh media (presumably caused by nutrient starvation) and stochastic (previously type II) persisters which were slow-growing or non-growing cells generated during exponential phase of growth seemingly without an environmental trigger (Balaban et al, 2004; Balaban *et al.*, 2019). These persister sub-populations, detected with dual-reporter phages in combination with single cell imaging, were also noted in *M. tuberculosis* following isoniazid treatment (Jain *et al.* 2016). In the aforementioned article, authors fused a fluorescent dTomato reporter to promoters of several genes previously shown to be upregulated in persister cells. These promoter fusions were then introduced into the genome of mycobacterial cells isolated from human sputum samples with the use of bacteriophages constitutively expressing Green

Fluorescent Protein GFP (a positive transduction marker) and analysed with fluorescence microscopy and flow cytometry.

Interestingly, a potential third class of persisters (referred to here as 'specialised persisters') which are not slow-growing prior to antibiotic exposure and often display antibiotic specific persistence mechanisms has also been observed (Goormathigh and Van Melderen, 2019; Wakamoto *et al.*, 2013), as shown in Figure 2.3.

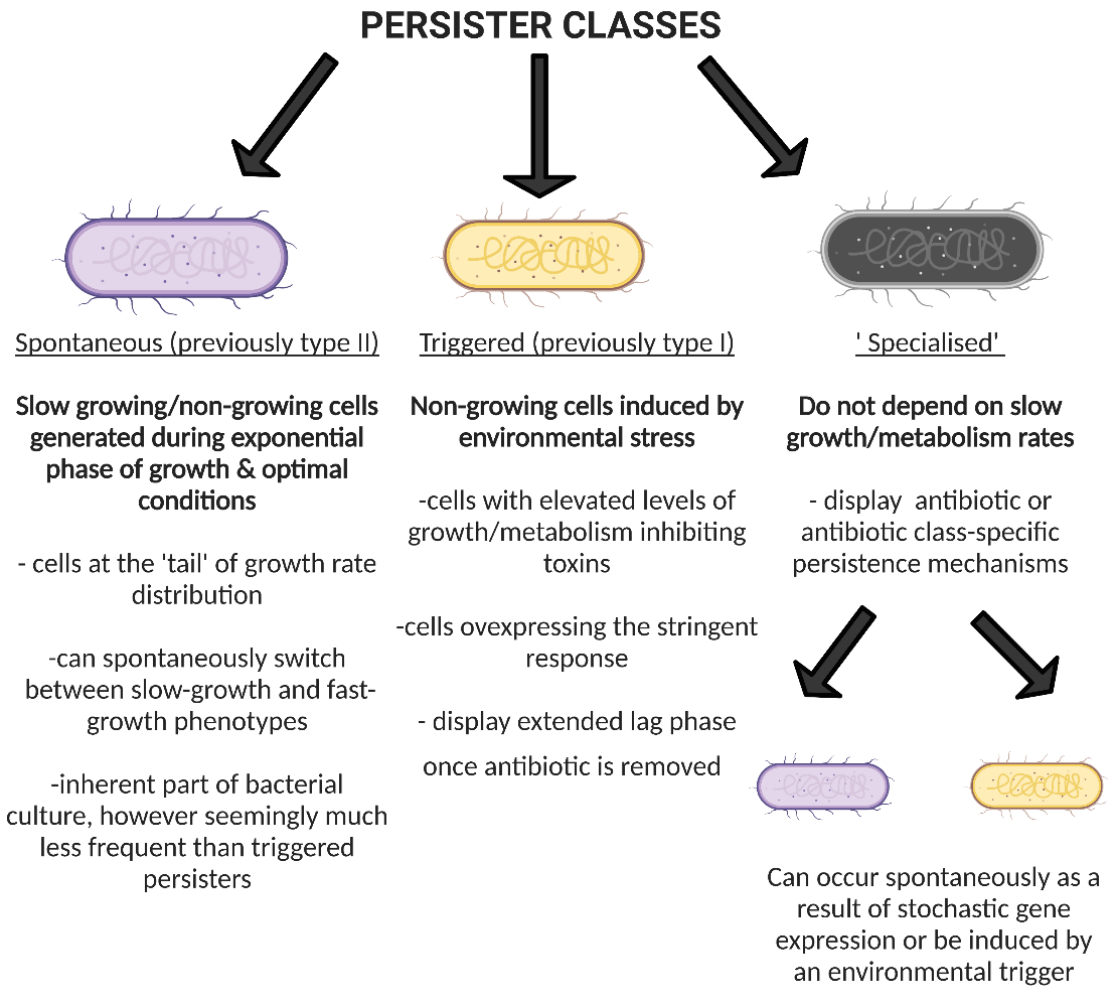

Figure 2.3. Proposed addition of specialised persisters to classification of persister cells (Balaban et al., 2019). *Both spontaneous and triggered persisters are slow/non-growing prior to antibiotic addition and often display a general, rather than antibiotic-specific, persistence phenotype. It is, however, important to note that not all slow/non-growing cells are persisters. In contrast, 'specialised' persisters do not depend on slow growth/metabolic rates to survive antibiotic exposure, but instead display antibiotic-specific persistence mechanisms. They can occur spontaneously, for example,*

in Mycobacteria, through stochastically low levels of expression of the enzyme catalase-peroxidase that activates isoniazid (Wakamoto et al., 2013) or be induced by a stress-signal, for example ciprofloxacin persisters which are induced by exposure of E. coli to this antibiotic (Dorr et al., 2009, Goormaghtigh and van Melderen, 2019).

2.3. Molecular mechanisms involved in persister cell formation

2.3.1. Toxin-antitoxin systems and induction of the stringent response are one of the many pathways leading to persistence

Inspired by the discovery of the HipA system multiple other TA systems have been linked to the establishment of persistence. HokB toxin expression in *E. coli* is upregulated by the Obg GTPase which is involved in stress response as a regulator of cellular energy levels and whose overexpression results in pore formation in the membrane and ATP leakage from the cell (Wilmaerts *et al.*, 2018). TisB toxin, also present in *E. coli,* is involved in a multi-drug tolerance phenotype under the regulation of the SOS response pathway (Dorr *et al.*, 2010). Another well researched toxin-antitoxin module, MazF-MazE, is induced under stressed conditions and disrupts protein synthesis in *M. tuberculosis* leading to degradation of selected mRNA targets and induction of the stress response operons resulting in growth arrest (Tiwari *et al.*, 2015).

However, a fair share of uncertainties surround the effort of developing a unified persistence model based on toxin accumulation, with conflicting results often reported by different research groups. One notable example is a model which aimed to provide a 'blanket' pathway on how persistence is established in a model organism *E. coli.* This neat model proposed that increasing levels of ppGpp as a response to external stress cause accumulation of polyphosphate, activation of Lon protease and Lon-mediated accumulation of toxin components of TA systems which in this model acted as effector molecules inducing persistence (Gerdes and Maissoneuve, 2012). Although discovery of a single 'persistence switch' (in this case Lon-mediated toxin accumulation) would certainly allow for a more systematic approach to persistence research, the 'real-life' scenario is likely more complex. The model proposed by Gerdes and colleagues was based on the observations of a decreasing number of persisters following deletions of 10 subsequent TA modules. Unfortunately, some of the data on which this model was based may have been confounded by the presence of resident prophages whose lytic cycle can be induced by an antibiotic (in this case ciprofloxacin) resulting in cell lysis and

reduced number of surviving cells, irrespective of persistence mechanisms (Harms *et al.*, 2017). This led to the re-evaluation of the role of TA modules in persistence with some groups reporting a link between TA modules and persistence irrespective of ppGpp levels in *E. coli* (Chowdhury *et al.*, 2016) and *M. smegmatis* (Bhaskar *et al.*, 2018) and others reporting no link between persistence levels and TA module deletion *in E. coli* (Goormaghtigh *et al.*, 2018). The role of TA modules in persistence thereby appears to be more complex.

Following Moyed and Bertrand's landmark publication, a significant amount of research has focused on the (p)ppGpp alarmone system. (p)ppGpp levels are upregulated as a result of various environmental stressors such as nutrient starvation, acid stress or heat shock (Abranches *et al.*, 2009), which could act as a trigger in the formation of persister cells, at least in *E. coli* where a link has been established between elevated ppGpp levels in persister cells and nutrient starvation or oxidative stress (Radzikowski *et al.*, 2016; Brown, 2019). Experiments *on P. aeruginosa*, both *in vitro* and in a mouse infection model, have implicated relA/spoT, which synthesize and degrade (p)ppGpp, respectively. A mutant lacking the genes (and therefore incapable of initiation of (p)ppGpp-mediated stringent response) produced 100-fold fewer persisters compared to the wild-type strain (Nguyen *et al.*, 2011). The frequency of persisters to multiple antibiotics was also altered in *Mycobacteria* deletion mutants of sigma factors *sigE* and *sigB* (Pisu *et al.* 2017). SigE regulates the transcription of rel_{Mtb}, which involves synthesis of (p)ppGpp (Avarbock *et al.* 2005). Deletion of rel_{Mtb} resulted in failure of (p)ppGpp synthesis and a decreased persistence of *M. tuberculosis* under stress conditions, such as nutrient starvation or infection (Dahl *et al.* 2003; Atkinson, *et al.*, 2011).

Taken altogether these findings point towards the hypothesis that persistence is a complex phenomenon potentially involving multiple mechanisms (Figure 2.4), both passive (such as growth arrest as a result of toxin accumulation) and active (such as response to oxidative stress). This makes the effort of establishing a comprehensive persistence model a challenging task.

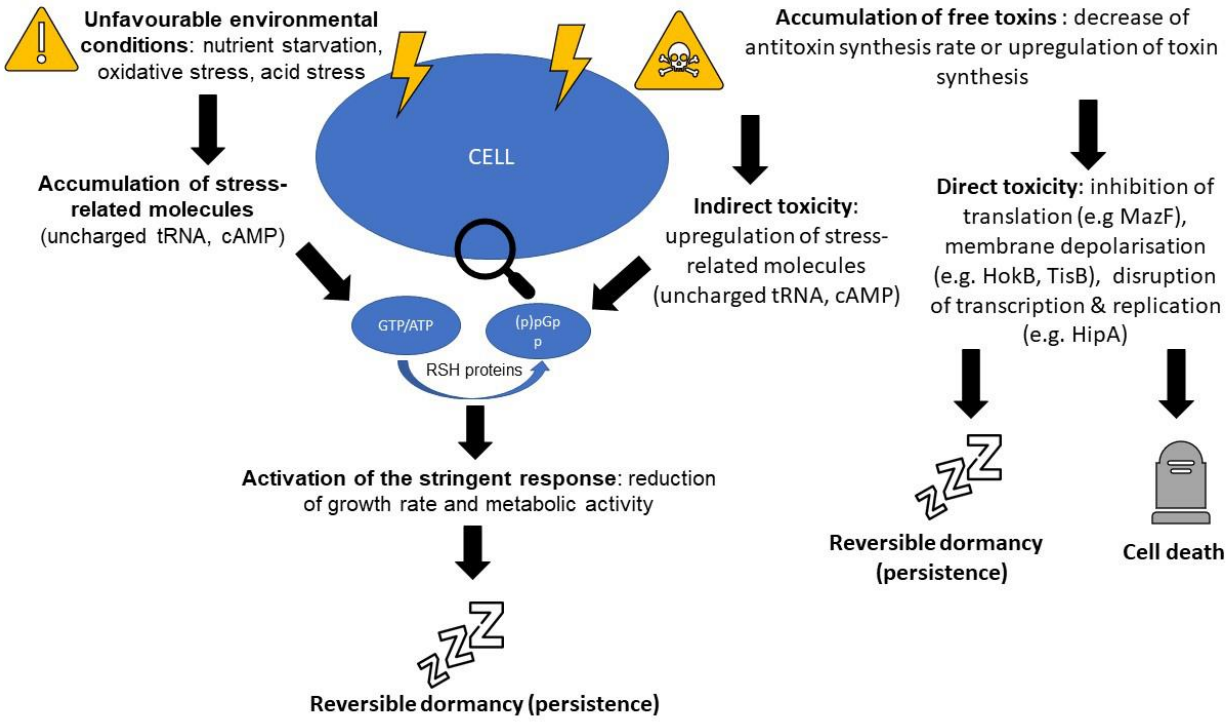

Figure 2.4. Simplified network displaying the role of the TA systems and the stringent response in establishment of persistence. *Cells sense changes in the external environment through receptors such as two-components systems (histidine kinases), thermosensor molecules, pH sensing molecules or GltX inhibition through accumulation of free radicals or phosphorylation by HipA/HipA7. Downstream signaling causes accumulation of stress-related molecules in the cells such as cAMP, uncharged tRNA, heat shock proteins etc. This is sensed by RelA/SpoT proteins which in turn convert ATP/GTP into the (p)ppGpp alarmone. (p)ppGpp affects cellular metabolism directly (by interacting with RNA polymerase) and indirectly (by depleting cellular GTP levels) and has been linked to establishment of the persister state. Toxin components can also directly inhibit crucial metabolic processes such as protein synthesis or replication or affect cellular membrane potential. Depending on the free/bound toxin ratio, this can either result in cell death or temporary growth (persistence).*

2.3.2. Specialised persisters

It seems likely that the phenomenon and mechanisms of persistence are much more varied than toxin-antitoxin systems and ppGpp-induced growth arrest. For example, 'specialised' persister cells are generated during exponential growth, but are not associated with slow individual cell growth, and are specific to a particular antibiotic (Wakamoto *et al.*, 2013; Goormagthigh and van Melderen, 2019 and Figure 2.3). The antibiotic isoniazid is an inactive prodrug, which becomes activated inside the mycobacterial cells through cleavage by the bacterial enzyme KatG (catalase-

peroxidase). Single-cell level observations have shown that, during exposure to isoniazid, the growth/ division rate of a cell does not correlate with persistence i.e., slowly growing cells were as likely to die as fast-growing cells. Instead, intrinsic noise (stochastic variation) in gene expression leads to fluctuations in the level of transcription and translation of all cellular genes resulting in cell-to-cell variation of individual gene expression levels (Raj and van Oudenaarden 2008). In *Mycobacteria*, intrinsic noise in *katG* gene expression gave rise to a pulsing of intracellular enzyme activity that appeared to be associated with persistence specific to isoniazid. Even a small increase in *katG* expression was shown to lead to a huge decrease in the number of persister cells and persister cells tended to express less 'pulsing' of KatG levels than non-persister cells (Wakamoto *et al.*, 2013). Similarly, a single-cell imaging study carried out on *E. coli* has demonstrated that survival to fluoroquinolones requires appropriate timing of the SOS system induction during the recovery and repair phase and hence, prior to growth resumption. This study demonstrated that fluoroquinolone persisters are highly heterogenous and are not always slow-growing or SOS-induced prior to antibiotic addition (Goormaghtigh and Van Melderen, 2019).

2.3.3. Persistence as a result of extended lag phase

Duration of the lag phase can be extended by elevated levels of growth-inhibiting toxin components of the TA systems (such as MazF or HipA) and was found to be an important mechanism for establishment of persistence to fluoroquinolones in *E. coli.* Fluoroquinolones damage the DNA of both actively growing and non-growing cells and therefore, through extension of their lag phase *E. coli* persister cells were able to repair incurred DNA damage prior to growth resumption. This made them much more likely to survive exposure to DNA-damaging antibiotics, such as ciprofloxacin (Mok *et al.*, 2018). A similar effect was observed when *E. coli* cells were exposed to sub-MIC concentrations of ofloxacin, which significantly (1200-fold) increased the number of persisters upon subsequent exposure to a high concentration of this antibiotic, when compared to cultures only exposed to high concentrations of ciprofloxacin. A proposed model behind this involves 'priming' of the SOS response through low-levels of DNA damage, resulting in the overexpression of the TisB toxin and subsequent toxin-induced growth arrest (Dorr *et al.*, 2009). Both MazF and TisB persisters also displayed a multidrug tolerance phenotype and were tolerant to ampicillin, presumably as a result of their arrested growth state (Dorr *et al.*, 2009; Mok *et al.*, 2015). However, there is also supporting evidence that persistence to fluoroquinolones is governed by more than the presence of TA systems and is not only a passive-by product of arrested growth state (Bernier *et al.*,

2013), as described above (Goormagthigh *et al.*, 2019). It is plausible to assume that both types of growth arrested and growth-independent (‘specialist’’) fluoroquinolone persisters could co-exist in an isogenic culture and that their ratio would fluctuate depending on environmental/culture conditions.

2.3.4. Transporter-linked persistence

Increasing intracellular antibiotic uptake has been shown to lead to elimination of persister cells is some systems (Allison *et al.* 2011). Subsequently, it was demonstrated that, when treated with β-lactam antibiotics, *E. coli* persister cells show higher efflux pump activity compared to non-persister cells and accumulate lower levels of drug intracellularly (Pu *et al.*, 2016). Heterogeneity of uptake mechanisms and efflux pumps may thereby be another source of persisters. Indeed, it has been demonstrated that intrinsic heterogeneity of efflux pump distribution amongst daughter cells affects their susceptibility to antibiotics (Bergmiller *et al.,* 2017). Several time-kill studies have also confirmed that increasing efflux pump activity can decrease the number of persisters (de Steenwinkel *et al.* 2010; Caleffi-Ferracioli *et al.*, 2016; Pu *et al.* 2016; Lapinska *et al.,* 2022).

2.3.5. Intrinsic asymmetry of cell division and persistence

Bacteria reproduce asexually through binary fission, during which a ‘mother’ cell first duplicates its genetic material, then moves a copy of the bacterial chromosome to each cell pole and afterwards splits in half into two ‘daughter’ cells by synthesis of new cell wall. This mechanism of cell division results in an intrinsic asymmetry since each daughter cell inherits an ‘old pole’ (from the mother cell) and a ‘new pole’ (synthesized during division). Further fission events will then result in some cells accumulating ‘old poles’ (‘old pole daughters’ of ‘old pole mothers’) (Lapinska *et al.*, 2019). Research on *E. coli* has shown that these old pole cells tend to have lower growth and glucose accumulation rates when compared to their ‘new pole’ sisters and that this effect is cumulative until the ‘old pole’ lineage reaches an apparent asymptote (in other words the change accumulation with subsequent generations reaches near-zero). The underlying mechanism behind this phenomenon is currently unknown but does not appear to simply be caused by an accumulation of old and misfolded protein aggregates at the ‘old pole’, as previously hypothesized (Rang *et al.*, 2011; Lapinska *et al.* 2019). Whatever its origin,

since asymmetric cell division appears to be a source of asymmetry in growth rate, it is potentially a source of persistence.

2.4. Origin of phenotypic heterogeneity of bacterial populations as a source of antibiotic persistence

2.4.1. Noise in gene expression levels leads to phenotypic heterogeneity

It has been apparent since the advent of single cell studies that clonal populations of cells exhibit stochastic variation (noise) in the expression of genes (Elowitz, M. B., *et al.* 2002; Cai, L., *et al.* 2006; Levine, E. and T. Hwa 2007). The causes of this variation are largely unknown but the amount of noise in any system is inversely proportional to the copy number of molecules controlling the system, so very low copy numbers of many cellular components, such as regulatory molecules and structural molecules (Guptasarma, P. 1995), will lead to high noise levels. Random partitioning of low copy number molecules at cell division is also a source of phenotypic variation (Huh, D. and J. Paulsson 2011).

Heterogeneity may be present in any cell phenotype but, given the strong association between growth rate and persistence, phenotypic variation that influences growth rate is highly likely to influence the frequency of persisters in a population.

The source of epigenetic variation in growth rate is currently unknown, but it is well established that a myriad of genes can influence growth rate, as is apparent from the commonplace observation that mutation or induced changes in gene expression very often lead to altered growth rates. It thereby seems likely that stochastic variation in expression of many genes will cause stochastic variation of growth rate. Note also that, in the previously mentioned mutational screen that led to the isolation of the original *E. coli* hip mutants including the HipA7 strain (Moyed and Bertrand 1983), all of the putative hip mutants grew slower than the wild-type in rich media. As already described, the phenotype of the intensively studied *hipA7* mutant is caused by a mutation in a toxin-antitoxin system whose expression depresses growth rate.

The hypothesis that persistence is due to epigenetic variation in growth rate is supported by recent results from our laboratory, which have identified control of epigenetic inheritance as a potential source of persisters (Hingley-Wilson *et al.*, 2020). The research studied the hipQ mutant of *E. coli*, isolated in during mutagenesis screen in 1990, which

displays increased spontaneous persisters when exposed to norfloxacin and ampicillin (Wolfson *et al.*, 1990). Single cell growth studies across several generations established that the high persister phenotype of HipQ is associated with the novel phenotype of *reduced phenotypic inheritance* (RPI), identified as reduced correlation of growth parameters such as division time, size at birth or cell elongation rate, either between mothers and daughter cells, or between sister cells. The results suggested that genes influencing epigenetic inheritance play a role in persister cell formation. The study also identified the locus of the HipQ phenotype as a mutation in a gene, *ydcI*, that encodes a putative transcription factor (Hingley-Wilson *et al.*, 2020).

2.4.2. A hunker theory of persistence

Aforementioned studies tend to argue against a single mechanism of persistence prompting a more general theory of persistence. However, growing slowly, or not at all (dormancy) has been shown to induce whole-population tolerance, particularly to cytotoxic antibiotics. For example, Toumanen and colleagues determined that the rate of killing of *E. coli* cultures exposed β-lactams was directly proportional to their growth rate, with slower growing cultures exhibiting enhanced tolerance (Toumanen *et al.*, 1984).

For antibiotics to reach their target, they need to penetrate the cell and bind to their target. Cells that, for a variety of reasons, *hunker down* by growing more slowly, metabolising more slowly, transporting materials across their cell membranes more slowly or activating antibiotics more slowly, will be killed more slowly leading to a state of persistence.

This hunker theory of persistence is consistent with the finding that persisters are not necessarily slow growing, as in the specialised class of persisters (Figure 2.4). Clearly, not all slow-growing cells are persisters; and not all persisters are slow growing (Omar and Brynildsen, 2013). Slow growth may predispose towards the state of persistence; but it is neither sufficient nor necessary. Just as there are many possible ways of hunkering down to survive a storm (sheltering in the basement, shutting the windows, reinforcing the roof), there may be many ways to survive the onslaught of antibiotics. Indeed, it seems likely that any stochastically-varying factor that varies growth, metabolism, drug penetration or activity in individual cells, is likely to be capable to initiating a persister state and that these may be antibiotic specific (i.e. the SOS response after removal of ofloxacin) (Goormaghtigh and Van Melderen, 2019).

2.5. Is it possible to devise therapies that target the persistence state?

2.5.1. Clinical application of persister-targeting treatment regimes

Up to recently, little attention had been given specifically to the elimination of persisters in the clinical setting, however some antibiotics which were designed to treat drug resistance have also been found to shorten treatment duration, suggesting that the elimination of persisters in clinical infections can play a role in enhancing treatment efficacy. Two new licensed drugs for TB treatment - bedaquiline (BDQ) and delamanid (DLM) which have been used to treat multidrug-resistant *M. tuberculosis* since 2012 and 2014 respectively (Zumla *et al.*, 2014), also showed potential in eliminating persisters in clinical treatment. BDQ binds to the a and c subunits of the F_0 domain of the ATP synthetase, thus inhibiting ATP synthesis and causing cell death in both replicating and metabolically-active non-growing mycobacteria (Goulooze *et al.*, 2015). A BDQ-modified regimen could achieve total organ CFU count clearance in the *M. tuberculosis*-infected mice after 8 weeks, much faster than the standard regimen (rifampicin, isoniazid, pyrazinamide and ethambutol) which takes 14 weeks on average (Hu *et al.*, 2019). DLM inhibits the synthesis of mycolic acids, which disrupts the formation of cell wall and facilitates drug penetration into mycobacterial cells (Liu *et al.*, 2018). DLM also showed bactericidal activity against non-growing cells (although at higher concentrations) and shortened treatment duration of chronic TB disease in the guinea pig model (Chen *et al.*, 2017).

Since discovery of entirely new drugs is notoriously difficult, repurposing antibiotics has been proposed as an alternative strategy to identify effective drugs. Some regimens which are used to treat other diseases have also been shown to be effective in the killing of persisters. Mitomycin C, a former cancer drug, was shown to be effective on both actively growing cells and non-growing cells through spontaneous cross-linking of DNA in bacteria. Mitomycin C is more effective than ciprofloxacin and ampicillin in killing persisters of enterohaemorrhagic *E. coli*, *S. aureus* and *P. aeruginosa* within laboratory culture as well as in the Lubbock chronic wound pathogenic biofilm model, a model which closely represents growth conditions of polymicrobial infections (Kwan *et al.*, 2015). Therefore, mitomycin C could potentially be a broad-spectrum compound used to eliminate persisters in the treatment of recalcitrant infections (Kwan, Chowdhury, and Wood 2015). Unfortunately, like many cancer drugs, mitomycin C treatment can cause multiple side-effects, notably hair loss, nausea and vomiting, leukopenia and thrombocytopenia or in some cases pneumonitis and haemolytic-ureaemic syndrome

(NIHCE, 2020) and therefore development of less 'invasive' persister treatment regimens is still urgently needed. Laboratory screening of existing antibiotic regimens and small molecules using different persistence models, such as stationary-phase culture, biofilm-phase or animal models could help to identify potential compounds that could be used in clinical practice.

Although only a few compounds specifically targeting persisters have been used in a clinical setting, several potential strategies of persister cell elimination have been proposed, including direct killing of persisters, sensitization of persisters to antibiotics and inhibition of persister cells formation (Figure 2.5). Conversely, research into mechanisms and gene mutations responsible for generating low frequency persister strains or cultures may lead to identifying drug targets that reduce persister formation yet is an area that is often overlooked.

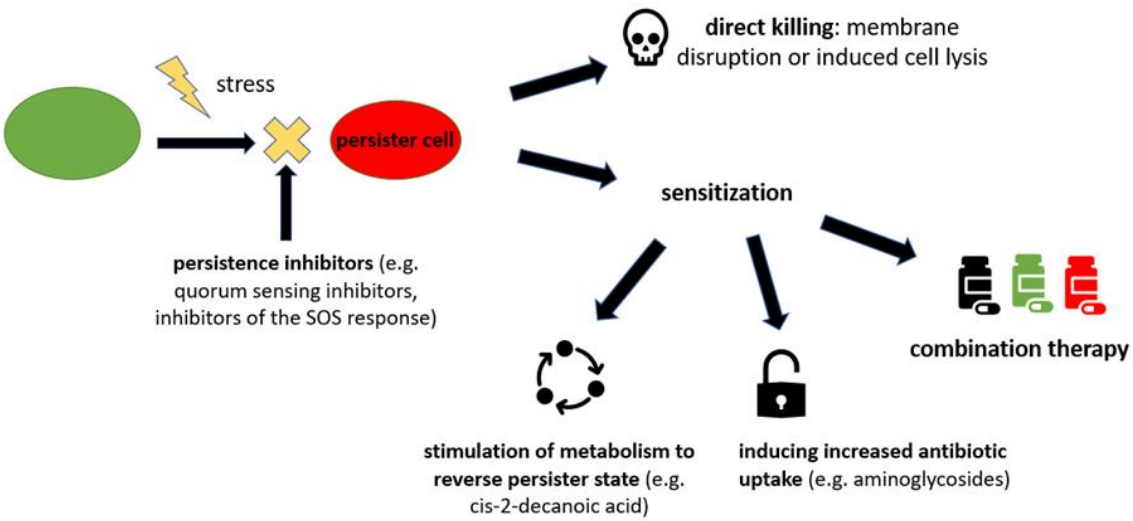

***Figure 2.5. Overview of current strategies tackling the presence of persister cells**. Several strategies are displayed here which have been developed that target persisters specifically through direct killing, sensitization to antibiotics or by prevention of persister cell formation.*

2.5.2. Direct killing of persister cells can be achieved by membrane disruption or induced lysis

Several compounds have been used *in vitro* to kill persisters directly. For example, a quinolone-derived compound HT61 has been found to have a synergistic effect when used with neomycin, gentamycin and chlorhexidine (antiseptic agent) in both MSSA and

MRSA treatment (Hu and Coates, 2013). HT61 depolarises bacterial cell membrane through interaction with the lipid bilayer, resulting in leakage of cytoplasmic proteins and ATP from the cell, thus being effective against both actively growing ('specialised') and and growth-arrested persister cells (spontaneous and triggered) (Hubbard *et al.* 2017). Brilacidin, a type of host defence protein mimetic (a synthetic peptide which mimics natural hosts defence peptides), which is under phase II clinical trial for the treatment of serious skin infection, causes membrane depolarization in both Gram-positive and Gram-negative bacteria, such as *S. aureus* (Mensa *et al.*, 2014) or *E. coli* (Mensa *et al.*, 2011). It also showed bactericidal activity against non-replicating bacteria (Mensa *et al.*, 2014). Phage-derived lysins, such as endolysin LysH5 produced by a *Staphylococcal* bacteriophage phi-SauS-IPLA88, are another source of compounds capable of killing both replicating and non-replicating bacteria (Garcia *et al.*, 2010). Treatment with this endolysin was able to eliminate planktonic *Staphylococcus* persisters *in vitro* remaining after treatment with ciprofloxacin and rifampicin, and so it is a potential adjuvant candidate for those antibiotics (Gutierrez *et al.*, 2014). Another candidate molecule, polycationic glycopolymer (PAAG) induces rapid permeabilization of the cell membrane, causing membrane depolarization and cell death of *P. aeruginosa* persisters, as well as in actively-growing cells (Narayanaswamy *et al.*, 2018). Alternatively, protein pseudocapsids (shell-like structures), which are capable of forming nanopores in bacterial cell membrane upon fusion, have been demonstrated as effective against *E. coli* persister and VBNC cells *in vitro.* However, more research is required *in vivo* to confirm the potential of these effector molecules.

2.5.3. Persistence can be reversed by 'kick-starting' cellular metabolism or increasing antibiotic uptake

Persisters with reduced growth rate and downregulated metabolism significantly increase the time required for many antibiotics to achieve a desired killing effect. Induction of metabolism or growth of persisters can thereby facilitate the action of antibiotics. A fatty acid signalling molecule- cis-2-decenoic (cis-DA) can increase overall metabolic activity of *P. aeruginosa* persisters (measured as respiratory activity) (Marques *et al.*, 2014). Combination of cis-DA with ciprofloxacin resulted in up to a 2-log culturable cell number reduction when compared to treatment with ciprofloxacin alone (Marques *et al.*, 2014).

Alternatively, promotion of antibiotic uptake will increase its intracellular concentration particularly in persisters that display increased efflux activity. Efflux pump inhibitors

(EPIs) could effectively eliminate efflux-dependent persisters (Kvist *et al.*, 2008). Although no EPIs have been put in clinical practice, a great number of EPIs like Carbonyl Cyanide-m-Chlorophenylhydrazone (CCCP) or phenylalanyl arginyl β-naphthylamide (PAβN) showed synergistic effect with antibiotics *in vitro* (Singh *et al.*, 2011; Lamers *et al.*, 2013). Hypoionic shock could also facilitate uptake of aminoglycosides by increasing proton motive force (PMF) of both nutrient shift and nutrient starvation-induced *E. coli* persister cells (Chen *et al.*, 2019). Although hypoionic shock is not feasible in the clinic, developing alternative PMF drug-uptake inducing strategies could be effective against persisters. Indeed, aminoglycoside uptake through PMF has also been demonstrated in persister cells though metabolic stimuli such as mannitol and fructose in *E. coli, P. aeruginosa* and *S. aureus* (Allison and Brynildsen, 2011; Barraud *et al.*, 2013). Finally, pre-treatment with polymyxin B, a pore forming agent, significantly decreased cell-to-cell variability in roxithromycin (macrolide) uptake into *E. coli* cells, and subsequently significantly increased the intracellular antibiotic concentration (Lapinska *et al.,* 2022).

Although most of these compounds are currently only researched in a laboratory setting and might not be practical in a clinical practice, exploration of novel compounds could be the steppingstone for development of new effective regimens.

2.5.4. Combination therapy is an effective tool against non-growing, antibiotic-tolerant subpopulations

Combination therapy is an effective approach that has been used to target persisters as it would enable differential killing of naturally heterogenous persisters and potentially inhibit the generation of genetic AMR from persister cells. For instance, treating *Borellia burgdoferi* (the causative agent of Lyme disease) with a combination of doxycycline (bacteriostatic, active against growing cells), cefoperazone (β-lactam) and daptomycin (which disrupts membrane potential and is active against both growing and dormant cells) was effective in eradicating persister cells which had previously been able to survive the standard doxycycline treatment. Combinations of these three antibiotic classes *in vitro* was more effective against persisters than any of the compounds alone or in combinations of two (Feng *et al.*, 2015). Similarly, by combining erythromycin which is known to inhibit quorum sensing pathways and motility in *P. aeruginosa* with colistin (a membrane pore-forming antibiotic) eliminated persister cells in *P. aeruginosa* biofilms (Chua *et al.*, 2016; Baek *et al.*, 2020).

Notably, active *M. tuberculosis* infection is routinely treated with a combination of isoniazid, rifampicin, pyrazinamide and ethambutol in order to eradicate infection (WHO 2019). Pyrazinamide (PZA) was found to shorten the treatment of TB from 9-12 months down to 6 based on clinical trials and animal studies, indicating that it is likely targeting persister cells. The target of PZA has recently been identified (Sun *et al.*, 2020) as PanD, which is an aspartate decarboxylase involved in the pantothenate biosynthetis (Sun *et al.*, 2020). However, the exact mechanism and whether PZA targeting of PanD reduces mycobacterial persisters remains to be determined.

2.5.5. Inhibition of persister cell formation

Inhibition of signalling pathways involved in the establishment of the persistence state under stressful environmental conditions is another potential strategy of targeting persistence. However, this is a challenging task as persisters can form through numerous often redundant routes. Nevertheless, this approach has shown some promising results. For example, Vitamin C at high concentrations showed inhibitory effect on synthesis of (p)ppGpp *in M. smegmatis*, which could potentially stall long-term infection and persistence in *M. tuberculosis* (Syal *et al.*, 2017). Interestingly, a recent seminal study on vitamin C has determined its capacity to reduce treatment time with front-line drugs including isoniazid or rifampicin *in vivo* in a murine model of tuberculosis

(Vilcheze et al, 2018). This study determined that enhancing *M. tuberculosis* respiration via the addition of Vitamin C or N-acteylcysteine prevented persister formation (Vilcheze *et al.* 2017). Another compound, relacin, a RelA inhibitor capable of reducing (p)ppGpp synthesis, decreased cell viability of *Streptococcus pyogenes in vitro* (Wexselblatt *et al.*, 2013). Although more supporting evidence of *in vivo* efficacy of RelA inhibitors is needed, a recent study utilising a dental root infection model has shown that relacin combined with NaOCl (commonly used in dental practice as disinfectant) was effective at eradicating *Enterococcus faecalis* biofilms without displaying cytotoxicity to human cells (Cai *et al.*, 2018). The study provides a proof of concept of the principle that compounds which inhibit persister cell formation can be effective components of treatment strategies.

2.6. Summary

The phenomenon of antibiotic persistence is intimately linked with phenotypic heterogeneity, which may be critical for survival of microbial populations. Persistence has been linked to treatment failure since its discovery over 70 years ago, and more recently has been suggested to be a 'stepping-stone' for the emergence of genetic resistance. Heterogeneity is also rife in the low frequency persister subclass, which includes spontaneous and triggered growth-dependent, and specialised growth-independent phenotypic variants. However, much remains unclear, such as how different mechanisms involved in the establishment of the persister state are regulated (if at all). Persister cells appear to be generated by a great variety of mechanisms as described here, leading to the hunker theory of persistence in which the phenomenon is associated with stochastic variation of factors influencing growth, drug penetration, metabolism or the SOS and stringent response. Since the acknowledgment of the clinical importance of persisters, multiple treatment strategies have been developed to target persister cells by either inhibiting their formation or 'waking them up' from the persister state; however, the efficacy of these strategies *in vivo* requires validation. This highly heterogenous and clinically relevant subpopulation may require simultaneous approaches to target each class of persisters in order to subvert persistence and hinder the development of genetic resistance.

3. General Methods

Please refer to Methods Appendix for detailed buffer and media composition.

3.1. Growth assays

Bacterial stocks (25% glycerol in Lysogeny Broth (LB)) were kept at -80^{o}C, streaked on fresh LB Miller agar *(Sigma Aldrich)* plates and incubated for 16-24 hrs at 37^{o}C. Afterwards, single colonies were selected and incubated in 3-5mL of LB Miller *(Sigma Aldrich)* or M9-GLUCOSE minimal medium (Harms *et al.*, 2017) at specified pH, in 50mL conical tubes *(Falcon)*, for 18-20 hrs. Incubation was carried out at 37^{o}C, with shaking at 200rpm. Overnight cultures were diluted in LB Miller or M9-GLUCOSE broth to an optical density (OD_{600}) of 0.05 (referred to as starter cultures from now on). Starter cultures (50mL) were incubated in 500mL Erlenmeyer flasks at 37^{o}C with shaking (200-250rpm). OD_{600} measurements in a standard 1cm plastic cuvette, as well as a Miles and Misra (MM) serial dilution series spotted onto oven-dried LB Miller agar plates (Miles, Misra and Irwin, 1938) were performed every hour for 8 hours and afterwards a final measurement was taken at 24hrs. MM dilutions were prepared as 200 µL final volume and 10-20 µL/'spot' were plated with 3 'spots' per replicate. MM series agar plates were incubated at 37^{o}C for 18-24hrs before the colonies were counted using a colony counter.

3.2. Time-kill assays

Starter cultures were prepared as described in section 3.1, and incubated for 2-3hrs at 37^{o}C in specified media, volume and shaking until the cultures reached mid-log phase of growth (OD_{600} of ~ 0.5 in M9-GLUCOSE medium and OD_{600} of ~1 in LB or CFU/mL of $8\text{^}10^{8}$ – $1.5\text{^}10^{9}$, see Figures 4.4 and 4.5). OD_{600} measurements, as well as a MM dilution series on LB Miller agar plates was performed as described in section 3.1 to determine starting CFU/mL values (i.e., time 0, prior to antibiotic addition). Next, antibiotic was added at specified (25-50X MIC) concentration to achieve concentration-independent killing, as outlined by a recent consensus statement (Balaban *et al.*, 2019). Cultures were then returned to the shaking incubator and an MM series was performed at 5 and 24 hours following antibiotic addition. At T_5 and T_{24} antibiotic was removed by washing prior to carrying out the MM series: 100µL sample was removed from the culture at each timepoint and centrifuged at 5000x*g* for 5 minutes. The cell pellet was then resuspended in 100µL of standard phosphate-buffered saline (PBS), pH 7.4 *(Sigma Aldrich)* or fresh media and this suspension was used in the MM dilution series. MM plates were incubated at 37^{o}C for 18-24 24hrs, except for and for the HipQ and KY strains, as it was

determined that the HipQ strain persisters required 48hrs for regrowth on agar plates (see Figure 4.6). Colonies were counted manually with a colony counter.

3.3. Minimum inhibitory concentration (MIC) assays

Five mL starter cultures in 50mL conical flasks *(Falcon)* were prepared as described in section 3.1 in LB Miller broth *(Sigma-Aldrich),* with shaking at 200rpm, and incubated for 2-3hrs at 37^{o}C until the mid-log phase of growth (OD600 ~ 1 or CFU/mL ~ 1x10^{9}, see Figures 4.5 and 4.6). Clear, flat-bottom, tissue culture-treated, 96-well antibiotic plates were prepared: the outside wells of the plate were filled with sterile water and a 2-fold serial dilution of a specified antibiotic in LB Miller broth was performed across the plate, with the starting concentration of 2 times the highest antibiotic concentration screened during the assay and well volume of 50 µL (Figure 3.1). The concentration range was estimated from previously published MIC values for *E. coli* (Tashiro *et al.*, 2017). If multiple plates were prepared at the same time, following incubation culture flasks were kept at 4^{o}C right until the cells were aliquoted into the antibiotic plate in order to slow down further bacterial growth. Prior to inoculation onto the antibiotic plates, cultures were diluted 1:1000 in fresh media to achieve the standard concentration between 10^{5}-10^{6} CFU/mL (Andrews, 2001). Cultures were then added to each antibiotic-containing well and no antibiotic control in 1:1 ratio (to a total well volume of 100 µL). The plate was sealed with tape and incubated statically at 37^{o}C for 24hrs. Following incubation, 10µl of 0.02% w/v filter-sterilised metabolic dye resazurin *(Sigma Aldrich)* was added to the wells to a final concentration of ~ 0.002% (limit of detection ~ 10^{6} viable cells/mL – 5-10 times the starting CFU/mL, determined experimentally) and any colour change was recorded after 4hrs, which was a marker for cellular respiration and therefore viability (Markossian, Grossman and Brimacombe, 2021). The MIC value was determined as the lowest concentration of the antibiotic which inhibited bacterial growth i.e., did not result in colour change following resazurin addition.

	1	2	3	4	5	6	7	8	9	10	11	12
A							H_2O					
B		X	0.5X	0.25X	0.125X	0.0625X	0.03125X	0.01562X	0.00781X	0.00390X	positive	
C		X	0.5X	0.25X	0.125X	0.0625X	0.03125X	0.01562X	0.00781X	0.00390X	control	
D		X	0.5X	0.25X	0.125X	0.0625X	0.03125X	0.01562X	0.00781X	0.00390X	(no antibiotic)	
E		X	0.5X	0.25X	0.125X	0.0625X	0.03125X	0.01562X	0.00781X	0.00390X	negative	
F		X	0.5X	0.25X	0.125X	0.0625X	0.03125X	0.01562X	0.00781X	0.00390X	control	
G		X	0.5X	0.25X	0.125X	0.0625X	0.03125X	0.01562X	0.00781X	0.00390X	(media only)	
H							H_2O					

Figure 3.1. MIC assay plate set up. *X refers to the highest tested concentration of a given antibiotic. Biological repeats are marked by peach and light blue colours (rows B to D and E to G). Antibiotic concentration decreases 2-fold through columns 1-12 and the range tested is estimated for each antibiotic/strain from available literature.*

3.4. DNA extraction

Bacterial stocks (25% glycerol in LB Miller) were stored at -80°C, streaked on LB Miller agar plates *(Sigma Aldrich)* and incubated for 16-24 hrs at 37°C. Afterwards, single colonies were selected and incubated in 3-5mL of LB Miller broth *(Sigma Aldrich)* for ~16hrs at 37°C, with shaking at 200rpm. Genomic DNA was extracted from stationary-phase bacterial cultures using the Monarch genomic DNA extraction kit, according to manufacturer's instructions (*NEB, UK*). Plasmids were extracted from stationary phase-cultures using the Monarch plasmid miniprep kit (*NEB, UK*), according to manufacturer's instructions. DNA yield and purity was assessed using the Nanodrop spectrophotometer, according to manufacturers instructions. 260/280nm absorbance ratio (~1.8) was used to confirm absence of RNA in the sample and 260/230nm absorbance ratio (~2) was used confirm absence of other organic contaminants *(ThermoFisher Scientific)*.

3.5. Polymerase chain reaction (PCR)

PCRs were performed according to the manufacturer's instructions (dependent on the type of DNA polymerase used), either on purified DNA prepared as described in section 3.4 or on single bacterial colonies inoculated directly into the PCR reaction tubes (referred to as 'colony PCR' from now on). Primers were designed in the Eurofins PCR primer design tool *(Eurofins Genomics)* by inputting the target DNA sequence and selecting the primer set with most optimal specificity, size, and GC content. Please refer to respective chapters' appendices for a list of primer sequences and PCR conditions.

3.6. DNA sequencing (Sanger method)

Genomic or plasmid DNA for sequencing was extracted from bacterial cells as described in section 3.4. For chain-termination sequencing method (Sanger and Coulson, 1975) the fragment of interest was first amplified by PCR as described in section 3.5 and afterwards purified with the Monarch PCR and DNA clean up kit, according to manufacturer's instructions *(NEB, UK)*. Subsequent sample preparation and the sequencing reaction was performed by GeneWiz UK. Obtained sequences were analysed using nucleotide BLAST *(NCBI)* by alignment to a reference sequence. The quality of individual fluorescence peaks (corresponding to 'called' DNA bases) was viewed in SnapGene *(GraphPad Software)*.

3.7. Transformation

3.7.1. Chemical transformation

Overnight *E. coli* cultures were prepared as described in section 3.1. The cultures were then diluted 1:200 in super optimal broth (SOB*) (Sigma Aldrich)* or LB Miller and incubated at 37^{o}C (unless otherwise specified) to an OD_{600} of 0.3-0.5 (~3hrs). Next, the cultures were spun at 5000xg for 10 minutes. The supernatant was removed and remaining pellets were concentrated 10 times in transport and storage solution (TSS), placed immediately on ice and left for an hour (chemically competent cells). 100-200ng of DNA to be transformed was diluted to 200 µL in chilled TCM and kept on ice. 200 µL

of prepared as above competent cells was then transferred to tubes containing the TCM-diluted DNA and mixed by pipetting, taking care to not warm up the tubes. The mix was left on ice for an hour. Afterwards the samples were transferred to a heating block set to 45^{o}C for 2 minutes and returned to ice for 5 minutes. Next the samples were diluted with 0.6mL of SOC (SOB medium supplemented with 20mM filter-sterilised glucose) or LB Miller and incubated at 37^{o}C (unless otherwise specified), with shaking at 200rpm, for one hour. 100 µL of the sample was then spread on LB Miller agar plates supplemented with a specified selective antibiotic concentration and incubated at for 24hrs. PUC19 plasmid was used as positive transformation control and non-transformed competent *E. coli* cells were used as the negative control.

3.7.2. Electroporation

Overnight *E. coli* cultures were prepared as described in section 3.1. Next, cultures were diluted 1:100 and incubated in LB Miller (*Sigma Aldrich)* for 2hrs (to OD_{600} = 0.3-0.5), at 37^{o}C, unless otherwise specified, and with 200rpm shaking. Cultures were then placed on ice for 15 minutes. Next, cultures were centrifuged at 5000xg for 5 minutes and the pellet was resuspended in the same volume of 10% ice-cold sterile glycerol. The wash step was repeated 2 more times and the pellet from the final wash was concentrated 20X in sterile ddH_2O. 50 µL of the resulting cell suspension was then mixed with the DNA to be transformed (50-100ng) and transferred to a pre-frozen 0.2cm electroporation cuvette *(VWR).* Electroporation was carried out 200Ω, 25 µF and 2.5kV on a GenePulser X-Cell system *(BioRad)*. LB was added to the cuvette immediately following electroporation (enough volume to fill up the cuvette). Cells were then transferred to an Eppendorf tube and incubated at 37^{o}C, unless otherwise specified, with shaking at 200rpm for 1 hour. Finally, 100 µL of the cell suspension was spread on LB Miller agar plates containing a specified concentration of the selective antibiotic and incubated for 24hrs at 37^{o}C, unless otherwise specified.

3.8. Restriction enzyme cloning

The choice of restriction sites and ‘dry’ cloning was done in SnapGene *(GraphPad Software)*. Vector and insert-containing plasmids were extracted from *E. coli* cultures as described in section 3.4. Alternatively, if a PCR product was the insert it was amplified as described in section 3.5 using primers with restriction enzyme sites added at 5’ and 3’ ends (please refer to respective chapter appendix for the list of primer sequences). Vector and insert were then digested with specified restriction enzymes according to

manufacturer's instructions. Appropriate digestion buffer, temperature and time for the enzyme pair was obtained from NEB cloner website *(NEB).* Digested fragments were then electrophoresed on 1% agarose gel for 1hr at 100V and imaged under UV light. Bands corresponding to expected digested insert/vector (backbone) sizes were cut out from the gel using a surgical scalpel. Next, the DNA was purified from the gel using the QIAquick gel extraction kit *(Qiagen),* according to manufacturer's instructions. DNA concentration and purity was assessed with Nanodrop spectrophotometer *(ThermoFisher Scientific),* as described above. Insert and vector were ligated at 3:1 molar ratio, with 50ng of vector. Ligation was carried out overnight, at 4^{o}C, using the T4 DNA ligase (*Promega),* according to manufacturer's instructions. Afterwards, the ligation mix was heat-inactivated at 65^{o}C for 20 minutes and chemically transformed into competent cells as described in section 3.7.1. Plasmid nucleotide sequence was verified by Sanger sequencing as described in section 3.5.

3.9. Flow cytometry

E. coli starter cultures were prepared as described in section 3.1. The time-kill assay method described in section 3.2 was then followed, with the exception that at T_0 (prior to antibiotic addition) and T_{24} (24hrs post antibiotic addition) sample aliquots were diluted 1:500 in sterile PBS (to 10^6 total cells/mL). Next, cells were live/dead stained with Zombie near-infrared (near-IR) fixable dye (*BioLegend)* (1:1000 or 1 µL/10^6 cells) and incubated for 20 minutes in the dark. For heat-killed control samples, undiluted aliquots (1mL) were incubated at 75^{o}C for 30 minutes and diluted to 10^6 total cells/mL in sterile PBS prior to live/dead staining. Next, cells were loaded onto the LSR Fortessa Cell Analyser *(BD Biosciences)* and forward scatter (FSC), side scatter (SSC) and zombie near-IR fluorescence (650nm excitation, 746nm emission) was recorded. Subsequent data analysis was performed in FlowJo v.10.8 *(BD Biosciences).* First, doublets were excluded based on FSC-A/FSC-H ratio (Cosma, 2020) and then cell population was gated manually based on FSC and SSC values. Live/dead discrimination was performed by applying a bifur gate on histogram plot of zombie near-IR fluorescence, using live cells (mid-exponential cultures, no antibiotic) and heat-killed cells as staining controls. For statistical analysis, data from individual cells was extracted from FCS files and analysed in GraphPad Prism v.8 *(GraphPad).*

4. Investigation of the role of the *ydcI* transcription factor in high-persistence to β-lactams and fluoroquinolones in *E. coli* HipQ

Aims

The aim of this chapter was to determine the molecular mechanisms contributing to increased antibiotic persistence observed in *E. coli* HipQ. Specifically, the role of *YdcI* transcription factor in regulation of persister cell formation was investigated through functional analysis of this protein and its downstream partners.

Hypothesis

A non-synonymous substitution in the ydcI gene of E. coli HipQ affects expression of genes regulated by this transcription factor, and is therefore responsible for increased antibiotic persistence and reduced phenotypic inheritance characteristic of this strain.

4.1. Introduction

4.1.1. Review of current literature on the HipQ strain

As mentioned in the introduction section of this thesis, *E. coli* HipQ is a highly-persistent strain of *E. coli,* first discovered by Wolfson and colleagues during an untargeted mutagenesis screen (Wolfson *et al.*, 1990). This strain was found to generate higher number of persister cells following exposure to β-lactams (ampicillin) and fluoroquinolones (norfloxacin), without significantly reducing the growth rate at batch level when compared to its parental strain, *E. coli* KL16 (KY). Following on from that discovery, Nathalie Balaban and colleagues in their pioneering microfluidic study have demonstrated that HipQ is a spontaneous high-persister strain, where persister cells are generated through stochastic variation in gene expression during exponential phase of growth (Balaban *et al.*, 2004). However, the exact genetic locus (or loci) responsible for this phenotype has remained unknown until a recent publication which mapped it to a mutation in LysR transcription factor, *ydcI.* An additional non-synonymous mutation was also found in the inner membrane protein gene *ybaL*, which has subsequently been linked to a lower frequency of ampicillin persister cells, using a knock-out strain as a

model (Hingley-Wilson *et al.*, 2020). Interestingly, apart from high-persistence, HipQ strain was also found to display 'reduced phenotypic inheritance', or RPI. RPI is defined as a reduced correlation of growth parameters between the cells of the same lineage (sister-sister and mother-daughter). In the case of *E. coli* HipQ, this reduced correlation resulted in an increased number of small, slow-growing cells which were significantly more likely to become persisters following exposure to ampicillin. Therefore the authors proposed a link between reduced phenotypic inheritance, high-persistence and the transcription factor *ydcI* which warrants further investigation.

4.1.2. Review of current literature on the YdcI transcription factor and YbaL membrane protein

4.1.2.1. The ydcI transcription factor

YdcI was first characterized in *Salmonella enterica* serovar typhimurium (*S.* Typhimurium) as a protein involved in acid stress resistance as a part of the *RpoS* regulon (Jennings *et al.*, 2011). *RpoS* is a global regulator controlling expression of genes involved in the stress response, virulence, and nutrient acquisition (Schellhorn, 2020). Moreover, in *S.* Typhimurium *ydcI* has also recently been demonstrated to induce biofilm formation (Romiyo and Wilson, 2020). Both *ydcI* and *rpoS* are widely conserved across *Enterobaceriaceae*, however research has shown that the different genera display significantly different tolerances to its expression levels (Solomon *et al.*, 2014). For instance, *E. coli* is significantly more sensitive to *ydcI* overexpression, with a loss of cell viability observed even at low (physiologically relevant) levels. On the other hand, in S. Typhimurium YdcI overexpression did not result in cell death (Solomon *et al.*, 2014). This suggests that YdcI either regulates expression of different genes in *Salmonella* when compared to *E. coli,* or that S. Typhimurium possesses additional regulatory mechanisms conveying tolerance to high levels of YdcI.

Since YdcI is a transcription factor, in order to understand its role in bacterial metabolism, the genes under its regulatory control need to be investigated. Through protein-DNA interaction modelling and immunoprecipitation assays it has been demonstrated that YdcI binds to the regulatory regions of 16 genes (Table 4.1) (Gao *et al.*, 2018). Furthermore, a recent RNAseq study aimed to investigate genes whose expression is regulated by *ydcI* in *E. coli* and *S.* Typhimurium (Romiyo and Wilson, 2020). Out of the 16 genes initially identified by Gao and colleagues, only one was found to be differentially regulated at the mRNA level in the *E. coli ydcI* knock-out strain. That gene was the

antitoxin *tomB* which in the knock-out strain was found to be 5.5-fold downregulated in stationary phase, when compared to the parental strain. Interestingly, TomB expression has independently been linked to an increased antibiotic persistence to ampicillin in *E. coli* (Kim and Wood, 2009). Therefore, expression of this gene was expected to be upregulated in the *ydcI* knock-out strain used as a model by Romyio *et al.*, as *E. coli ΔydcI* has been demonstrated to generate high frequencies of ampicillin persisters (Hingley-Wilson *et al.*, 2020). However, it is possible that YdcI-induced persisters are formed through TomB-independent mechanism or that TomB expression is upregulated in response antibiotic stress. The remaining 15 genes that Gao and colleagues identified as *ydcI*-regulated were not found to be differently regulated by Romiyo *et al.*, which could be a result of culture conditions used in the RNAseq experiment. Additionally, the authors identified 73 other genes which were either significantly up/down regulated in exponential or stationary phase in the *ydcI* KO strain (Romiyo and Wilson, 2020). This could be a downstream effect of *ydcI* regulation, not directly mediated by *YdcI*-DNA binding. Furthermore, the aforementioned studies were performed in slightly different genetic backgrounds: MG1655 strain by Gao *et al.* and TOP10 strain by Romiyo *et al.* TOP10 is a strain of chemically competent *E. coli*, a derivative of the DH10B strain which was found to carry mutations in 226 genes when compared to MG1655 (Durfee *et al.*, 2008) likely affecting the bacterial metabolic network.

Table 4.1 Genes regulated by *ydcI* transcription factor (Gao *et al.*, 2018; UniProt, 2020).

Gene	Function
tomB	toxin-antitoxin module
gltP	glutamate-aspartate transporter
yicG	ion channel
yobF	component of the stress response
dtpA	peptide transporter
gltA	citrate synthetase (component of the Krebs cycle)
trkG	Potassium transporter
nhaA	Sodium transporter
ydhV	uncharacterised oxidoreductase
ybhL	Calcium transporter
yobA	Copper transporter
apbE (yojL)	flavin transferase
ddlA	alanine ligase
LldP	lactate transporter
srlM (GutM)	transcriptional regulator
wrbA	NADP dehydrogenase

4.1.2.2. The YbaL transporter protein

Based on sequence homology, YbaL is predicted to be a membrane protein belonging to the Kef potassium transporter family (*UniProt*, 2020). In *E. coli,* this protein family is responsible for protection against electrophilic compounds through cytoplasm acidification and is regulated by the glutathione/glutathione-S-conjugate repression/activation system (Healy *et al.*, 2014). To the best of the author's knowledge, the function of this protein in *E. coli* has not been directly investigated, however as previously mentioned, a mutation in the *ybaL* gene has been found in the high-persister strain HipQ. Moreover, time-kill assays performed on *ybaL* KO strain have shown that it generates lower frequencies of persisters compared to its parental strain (Hingley-Wilson *et al.*, 2020). This suggests that it could also potentially play a role in bacterial persistence, however the molecular mechanism responsible for this observed phenotype is currently unknown.

4.1.3. Genetic models used for functional analysis of 'persister' genes

The use of knock-out (KO) strains is a widely accepted model for study of gene function. If a gene is responsible for a given phenotype, deletion of that gene will result in the abolishment of said phenotype and subsequent complementation will restore it, fulfilling molecular Koch's postulates (Falkow, 2004). KO models have been widely used in persistence research (Korch, Henderson and Hill, 2003; Hu *et al.*, 2015; Hingley-Wilson *et al.*, 2020). The use of this type of a study model in *E. coli* has recently been further facilitated by the creation of the KEIO collection, a publicly available library which contains individual gene knock-outs of all non-essential *E. coli* genes (Baba *et al.*, 2006) However, it should be noted that in multiple well-described high-persister strains (e.g., *E. coli* HipA7, *E. coli* HipQ) the mutation(s) responsible for the observed 'high-persister' phenotype are single nucleotide polymorphisms (SNPs) (Korch, Henderson and Hill, 2003; Hingley-Wilson *et al.*, 2020). SNPs can either result in a loss-of-function, which can be investigated further using a knock-out model, or a gain-of-function where a knock-out model will not be accurate if the 'gained' function is independent of said protein's inherent function. Therefore, replication of these SNP(s) in a different genetic background to investigate whether it also replicates the high-persister phenotype should be considered as the 'gold-standard' model for investigation of high-persister strains. Finally, 'noise-quenching' through overexpression has also been applied as a method for functional investigation of persister genes. If stochastic expression levels of a given

gene can induce formation of persister cells (e.g., in the case of toxin-antitoxin induced persistence), overexpression of said gene will ‘shift’ the phenotype of the bulk population to that of the persister subpopulation (or in the case of ‘low-persister’ genes, the resulting frequency of persisters will be significantly lower). However, for genes which generate relatively low noise, ‘quenching’ will not affect the phenotype of the bulk population (Nicolau and Lewis, 2022). Altogether, since persistence is a complex phenomenon brought about by a multitude of often redundant pathways, it is often necessary to adapt multiple approaches in order to avoid drawing false conclusions when investigating potential persistence-related genes.

4.2. Methods

Please refer to chapter 3 for the description of general methods. Please refer to chapter 4 appendix for a list of primer sequences and plasmid maps. Please refer to Methods Appendix for detailed buffer and media composition.

4.2.1. CRISPR/λ red genome editing to introduce HipQ *ydcI* SNP into the parental strain genetic background

4.2.1.1. Method overview

CRISPR genome editing in combination with phage λ red recombineering was performed in order to introduce a SNP in the *ydcI* gene on the *E. coli* KY chromosome identical to the mutation present in the HipQ strain (Hingley-Wilson *et al.*, 2020). This method was first described by Michael Payne and colleagues (Payne *et al.*, 2015).

Briefly, a single guide RNA (sgRNA) was designed to target the wild-type *ydcI* gene. Homologous DNA for recombination (insert DNA), which was the *ydcI* gene containing HipQ strain-specific SNP, as well as a silent mutation in the PAM site (recognition sequence of the Cas9 enzyme), was supplied as a PCR product. *E. coli* KY cultures were then transformed with plasmids expressing Cas9 and λ red recombineering system (a phage system which facilitates recombination) (pCas), sgRNA (psgRNA) and the insert DNA. Those cells which underwent successful recombination were 'saved' from Cas9 cleavage and DNA of non-recombinant cells was consecutively cleaved by the Cas9-sgRNA complex, resulting in marker-free selection of recombinants.

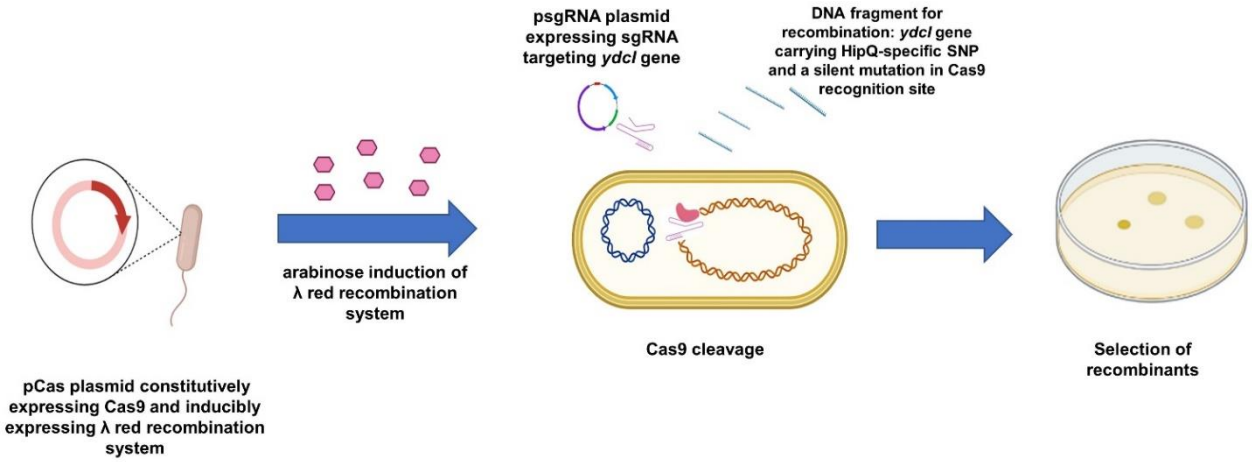

***Figure 4.1. Overview of CRISPR recombineering**. First, E. coli KY cells are transformed with pCas plasmid constitutively expressing Cas9 enzyme and inducibly expressing the λ red phage-derived system which facilitates recombination. Next, cells are induced with L-arabinose and transformed with ydcI-targeting sgRNA and DNA fragment for recombination - HipQ ydcI allele carrying a silent mutation in Cas9 recognition site. Recombinant cells are 'protected' from Cas9 cleavage and, subsequently, cell death. Presumed successful recombinants are selected from agar plates and verified by sequencing. Method adapted from Jiang and colleagues (Jiang et al., 2015).*

4.2.1.2. Preparation of single-guide RNA homologous to wild-type ydcI gene

Guide RNA was designed using Benchling software (Benchling) by inputting the gene sequence of the *E. coli* MG1655 *ydcI* gene (accession number: NC_000913.3 position from 1494148 to 1495071), using the 'guide RNA design' function. The sequence with the highest sensitivity and lowest potential off-target effect scores was selected. Afterwards, the Cas9 binding region and transcription terminator was added at the 3' end of the guide RNA resulting in a complete sgRNA sequence (Figure 4.2). The sgRNA was then converted to the coding DNA sequence by replacing uracils with thymines. Next, a promoter containing the consensus sequence for the *E. coli* sigma70 factor (a constitutive promoter) was added to the 5' end of the coding DNA sequence, and finally recognition sites for *HindIII* (5'end) and *NdeI* (3' end) restriction enzymes were added. Synthesis and subsequent subcloning of the final sequence into the PUC19 plasmid was carried out by NBS biologicals *(Biobasic, UK).*

5'UCGCACAACAAGGAACUUUGGUUUUAGAGCUAGAAAUAGCAAGUUAAAAUAAG
GCUAGUCC GUUAUCAACUUGAAAAAGUGGCACCGAGUCGGUGCUUUUUU3'

Figure 4.2. sgRNA sequence targeting E. coli wild-type ydcI gene. *Target specific homology region of 20 base pairs is highlighted in blue.*

4.2.1.3. Preparation of insert DNA

A silent mutation in the Cas9 recognition site (PAM site) on the *ydcI* gene was introduced through site-directed mutagenesis. Two sets of primers were designed, the first set covering the entire *ydcI* gene (full forward/full reverse) and second set overlapping each other with the Cas9 recognition site in the middle (PAM forward/PAM reverse). The second set of primers contained a mismatch site corresponding to the final nucleotide of the PAM sequence. Two separate PCR reactions using Q5 high-fidelity DNA polymerase *(NEB),* one with full forward and PAM reverse and the second with PAM forward and full reverse primers were performed as described in section 3.5, using a plasmid containing *HipQ ydcI* gene as the template (pET41a;;HipQ_*ydcI*). The resulting amplicons were column-purified, mixed in equal amount and used as a template for the final PCR reaction. This reaction was set up with the full forward/full reverse primers resulting in a full length *ydcI* gene with incorporated silent mutation at the PAM site and the HipQ-

specific SNP. Between subsequent steps 5 µL of each PCR product was electrophoresed on 2% agarose gel (100V, 1-1.5hrs) to confirm amplification specificity. The final sequence was confirmed by Sanger sequencing as described in section 3.6.

4.2.1.4. Cas9/λ red system genome engineering

A pCas plasmid with constitutive caspase 9 expression and arabinose-induced expression of the λ red system was a gift from Sheng Yang (Addgene plasmid # 62225; http://n2t.net/addgene:62225; RRID:Addgene_62225).

E. coli KY was chemically transformed with pCas plasmid as described in section 3.7, with 30 µg/mL of kanamycin used as the selective antibiotic and all incubation steps following heat-shock carried out at 30^{o}C to maintain replication from the temperature-sensitive ORI of pCas. Electroporation of the psgRNA and insert DNA was carried out as described in section 3.7 with following modifications: cells were incubated overnight in SOB with 30 µg/mL kanamycin, and starter cultures were incubated in SOB(AandK) medium (SOB medium with 10mM L-arabinose for the induction of the λ red system and 30 µg/mL kanamycin). All incubation steps were carried out at 30^{o}C. 100ng of psgRNA plasmid was used, together with 400ng of purified insert DNA. Following transformation, all samples were spread onto LB Miller agar plates containing 15 µg/mL kanamycin and 50 µg/mL ampicillin and incubated at 30^{o}C for 48hrs. An additional selection efficiency control which consisted of *E. coli* KY cells transformed with pCas and psgRNA plasmids, but not the insert DNA was also included, as well as a positive control of KY;;pCas transformed with an empty PUC19 vector.

4.2.2. Whole genome sequencing and bioinformatics analysis of E. coli HipQ genome

HipQ genomic DNA was sequenced using the NextSeq platform *(Illumina).* Genomic DNA was extracted as described in section 3.5 and further sample preparation and sequencing was done by MicrobesNG UK. Previous whole-genome sequencing data of HipQ and KY strains (Hingley-Wilson *et al.*, 2020) was downloaded from BioSample, accession numbers SAMN13648605 (HipQ) and SAMN13648604 (KY). Obtained FASTQ sequences (short Illumina reads) were then aligned to the reference sequence of *E. coli KY* downloaded from GenBank (accession no: NZ_CP008801.1) using the Burrows-Wheeler aligner (Li and Durbin, 2009). The reference sequence was then annotated with Prokka (Seemann, 2014). Alignments were viewed with Integrative

Genomics Viewer (Robinson *et al.*, 2011). Variant calling was performed with BCF tools *(Sanger Institute)*, using the mpileup|call pipeline (command: bcftools mpileup -f reference.fa alignments.bam | bcftools call -mv -Ob -o calls.bcf). Called variants were filtered based on quality score of 90 or above, unless otherwise indicated and mapped to the annotated genome.

To assess the potential of a mixed colony having been sequenced in the original sequencing data, nucleotide percentages at highly variable positions were compared between sequencing data from Hingley-Wilson *et al.*, 2020 and HipQ sequencing data obtained during this project. This analysis was done by Dr Huihai Wu at the University of Surrey.

4.3. Results

4.3.1. Growth assays

Culture growth was monitored by optical density (OD) (Figure 4.3a and c) and CFU/mL measurements (Figure 4.3b and d) in order to generate curves portraying population size change over time (growth curves) and to determine whether there was any statistically significant difference in the growth rates of high-persister and parental strain pairs investigated in this chapter (*ΔydcI* and BW25113 and HipQ and KY). As discussed in the introduction, an overall slower growth rate can increase whole population tolerance to antibiotics, and therefore could confound the results of persister assays. Furthermore, undefined culture media, such as LB, can significantly affect reproducibility of time-kill assays which are known to be extremely sensitive to environmental conditions. Therefore, in this thesis bacterial strains were compared in both the 'gold-standard' medium (LB) and a defined culture medium (M9-GLUCOSE), as recommended by Harms and colleagues (Harms *et al., 2017)*.

As can be seen in figure 4.3 and 4.4 , the resulting growth curves demonstrated expected growth phases: adjustment phase (lag phase), although in some cases it was shorter than the timeframe between the first two measurements (1hr), exponential growth (log phase) and cell division/cell death balance (stationary phase) (Ram *et al.*, 2019)

4.3.1.1. At batch level E. coli HipQ shows a transient growth defect in rich but not minimal medium

When growth kinetics of *E. coli* HipQ and its parental strain KY were compared in rich (LB Miller) and minimal (M9-GLUCOSE) media, it was observed that these strains display medium-dependent growth dynamics. When grown in LB, in exponential phase the HipQ strain doubled at half the rate of its parental strain (72 minutes and 36 minutes respectively), and did not reach the same OD_{600} or CFU/mL values in pre-stationary/stationary phase (T_4-T_{24} and T_6-T_{24} respectively). There was also statistically significant difference in both CFU/mL and total biomass (OD_{600}) between T_1 and T_{24}. Moreover, although the starting OD_{600} of both strains was normalised to 0.05, for cells grown in LB starting CFU/mL values differed by approximately 5-fold, with HipQ strain CFU/mL being lower than its parental strain (Figure 4.3a and b). This suggested either a higher proportion of dead and/or VBNC cells in the starting inoculum or a difference in cell size, with HipQ cells being on average larger than KY cells (explaining identical total biomass and lower viable cell counts at T_0). Subsequent single-cell observations in LB

Miller, described in detail in section 4.3.5, confirmed that HipQ cells are bigger than the cells of its parental strain, explaining the observed difference in the starting inoculum in this growth medium. In M9-GLUCOSE medium the doubling time of both strains increased, although the relative increase was greater for the parental strain than the HipQ strain (0.75x LB generation time vs. 0.9x LB generation time respectively). The parental strain also entered the exponential phase of growth later than in LB (T_4 vs. T_1). Furthermore, the difference between strains in both OD_{600} and CFU/mL was not statistically significant at any timepoint in this medium, in contrast to LB.

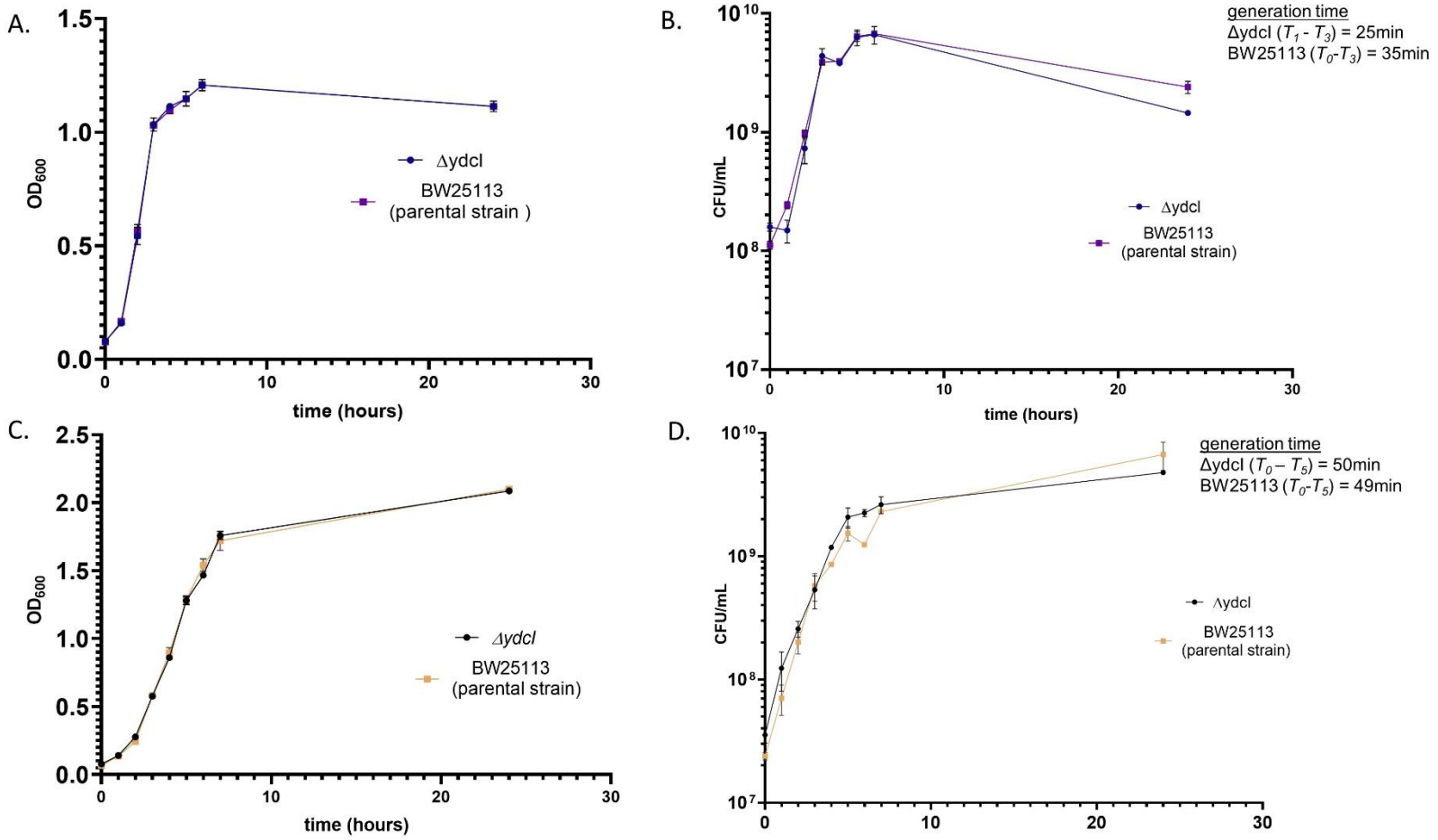

Figure 4.3. Growth kinetics of E. coli HipQ and its parental strain KY in LB Miller (A and B) and M9-GLUCOSE broth (C and D), with 200rpm shaking*. A, C are total biomass measurements by optical density in a standard 1cm cuvette (OD_{600}) and B, D are colony forming unit (CFU/mL) measurements; n=3, error bars are standard deviation; * = p and q < 0.05 by two-way ANOVA (strain vs. time) corrected for multiple comparisons using Benjamini, Kreuger and Yekutieli false discovery control method. Doubling time = duration of log phase (hrs) × ln(2) / ln(CFU/mL at end of log phase / CFU/mL at start of log phase*

Interestingly, when HipQ and KY cultures were passaged at normalised overnight CFU/mL values, at T=2hrs there was no statistically significant difference between HipQ and KY CFU/mL during passage 2, in contrast to passage 1, where the difference was over 10-fold and statistically significant (Figure 4.4). This suggests that the observed growth defect in rich media might be an epigenetic mechanism.

Effect of this growth defect on antibiotic persistence and tolerance is investigated further in section 4.3.2.

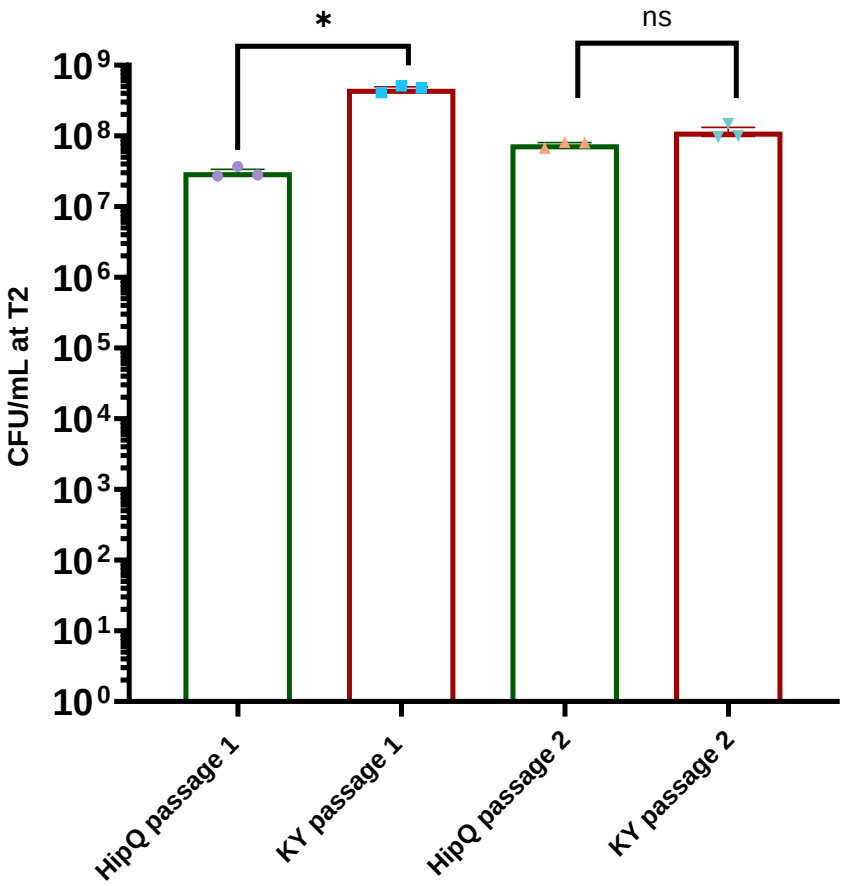

Figure 4.4. E. coli HipQ and KY CFU/mL two hours post starter culture inoculation comparison in subsequent passages (LB Miller). *Overnight CFU/mL were normalised (between 4.5-5.5^10^9 CFU/mL for passage 1 and 7.5-9.5^10^8 CFU/mL for passage 2); n=3 and error bars are SEM; * =p and q <0.05 by repeated measures ANOVA with Geisser-Greenhouse correction and Benjamini, Kreuger and Yekutieli false discovery control method.*

4.3.1.2. E. coli ΔydcI does not show the same growth defect as E. coli HipQ and displays similar growth kinetics to its parental strain in both rich and minimal medium.

Growth kinetics of *E. coli ydcI* knock-out (*ΔydcI*) and its parental strain (BW2113) were monitored through CFU/mL and OD_{600} measurements (Figure 4.5) in both rich (LB Miller) and minimal (M9-GLUCOSE) media. Similarly to HipQ and its parental strain, the doubling time was slower in M9-GLUCOSE (0.5x LB growth for Δydcl and 0.7x LB growth for BW25113). However, there was no statistically significant difference observed for either medium or measurement type, demonstrating that knocking out the *ydcI* gene does not affect growth rate and therefore should not affect whole-population tolerance to antibiotics in assayed conditions. However, since *ΔydcI* has been proposed as a model for HipQ high-persistence (Hingley-Wilson *et al.*, 2020), it was expected that this strain would display similar growth kinetics to *E. coli* HipQ (Figure 4.3). The observation that it does not suggests that the growth defect of *E. coli* HipQ is *ydcI*-independent and therefore its contribution to antibiotic persistence would not be captured using this knock-out model. It is noted that the Δydcl strain has a different genetic background than the HipQ strain, which could also contribute to the observed differences in growth kinetics.

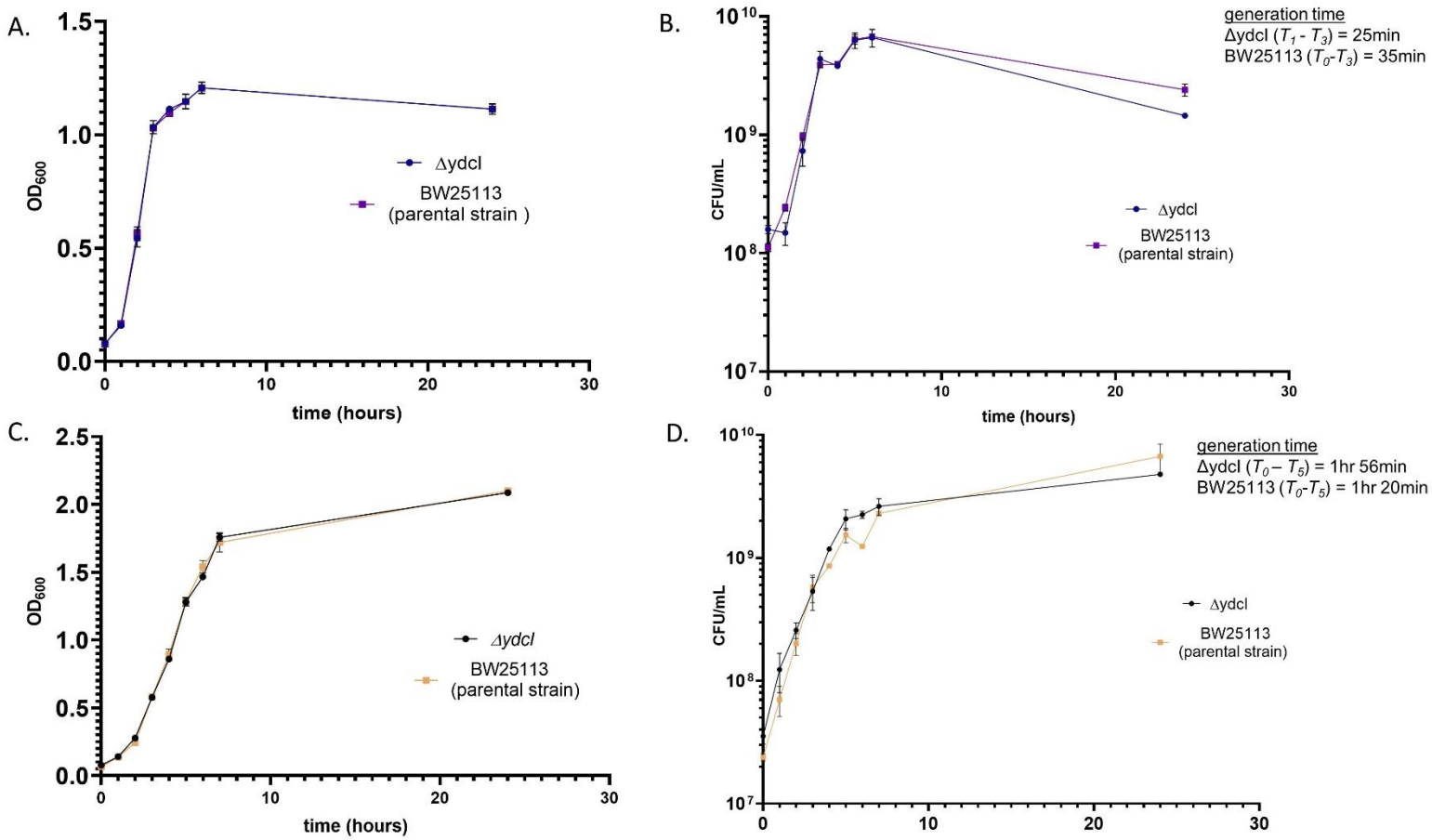

Figure 4.5. Growth kinetics of E. coli Δ*ydcl *and its parental strain BW25113 in LB Miller (A and B) and M9-GLUCOSE (pH 7) broth (C and D), with 200rpm shaking. *A, C are total biomass measurements by optical density in a standard 1cm cuvette (OD_{600}) and B, D are colony forming unit (CFU/mL) measurements; n=3, error bars are SEM; p > 0.05 by two-way ANOVA (strain vs. time) with Geisser-Greenhouse correction and and Benjamini, Kreuger and Yekutieli false discovery control method. Doubling time = duration of log phase (min) × ln(2) / ln(CFU/mL at end of log phase / CFU/mL at start of log phase*

4.3.2. Time-kill and minimum inhibitory concentration assays

Here, ampicillin (100 µg/mL, 20XMIC) and ofloxacin (0.75 ug/mL, 25XMIC) time-kill assays were performed on *E. coli* HipQ and its parental strain KY (Figure 4.6) and *E. coli* ΔydcI and its parental strain BW25113 (Figure 4.7) in order to validate the proposed high-persistence phenotype of *E. coli* HipQ and *ΔydcI*.

4.3.2.1. E. coli HipQ is highly persistent to ampicillin in rich but not minimal medium

Results presented below support the ampicillin high-persistence feature of *E. coli* HipQ; however, it was also observed that the frequency of persisters is media (Figure 4.6a and c) and passage (Figure 4.6a and b) dependent, with statistically significant difference between the HipQ strain and its parental strain only recorded in rich (LB) medium and during the first passage. The media-related difference can be explained by different growth kinetics in either growth medium, as ampicillin's mechanism of action is growth dependent and in M9-GLUCOSE the growth kinetics of both strains were found to not differ significantly (Figure 4.3). However, the fact that overall % survival in M9-GLUCOSE medium was lower for both strains (approximately 10-fold lower for KY and approximately 100-fold lower for HipQ), despite both strains growing slower, suggests presence of additional growth-independent media factors.

The frequency of persisters also differed in-between passages, with up to 1000-fold difference in % survival of *E. coli* HipQ compared to its parental strain during first passage (Figure 4.6a) in contrast to app. 10-fold difference during second passage (Figure 4.6c). This was presumably due to two main factors: faster growth of the HipQ strain during the second passage (as demonstrated in Figure 4.4), as well as accumulation of stress (starvation)-induced persisters in both HipQ and KY cultures 'masking' the difference in stochastic persisters responsible for the high-persistence of HipQ (Balaban *et al.*, 2004). This hypothesis is further supported by a significantly higher overall % survival rate during second, when compared to first, passage (approximately 0.0001% vs 0.5% and 0.05% vs. 0.8% for KY and HipQ strains respectively).

Finally, was observed that HipQ persisters, in contrast to KY persisters require increased regrowth time on agar plates, with additional colonies appearing on HipQ plates after 48hrs of incubation in contrast to KY plates, where all colonies were already grown within 24hrs of inoculation (Figure 4.6d).

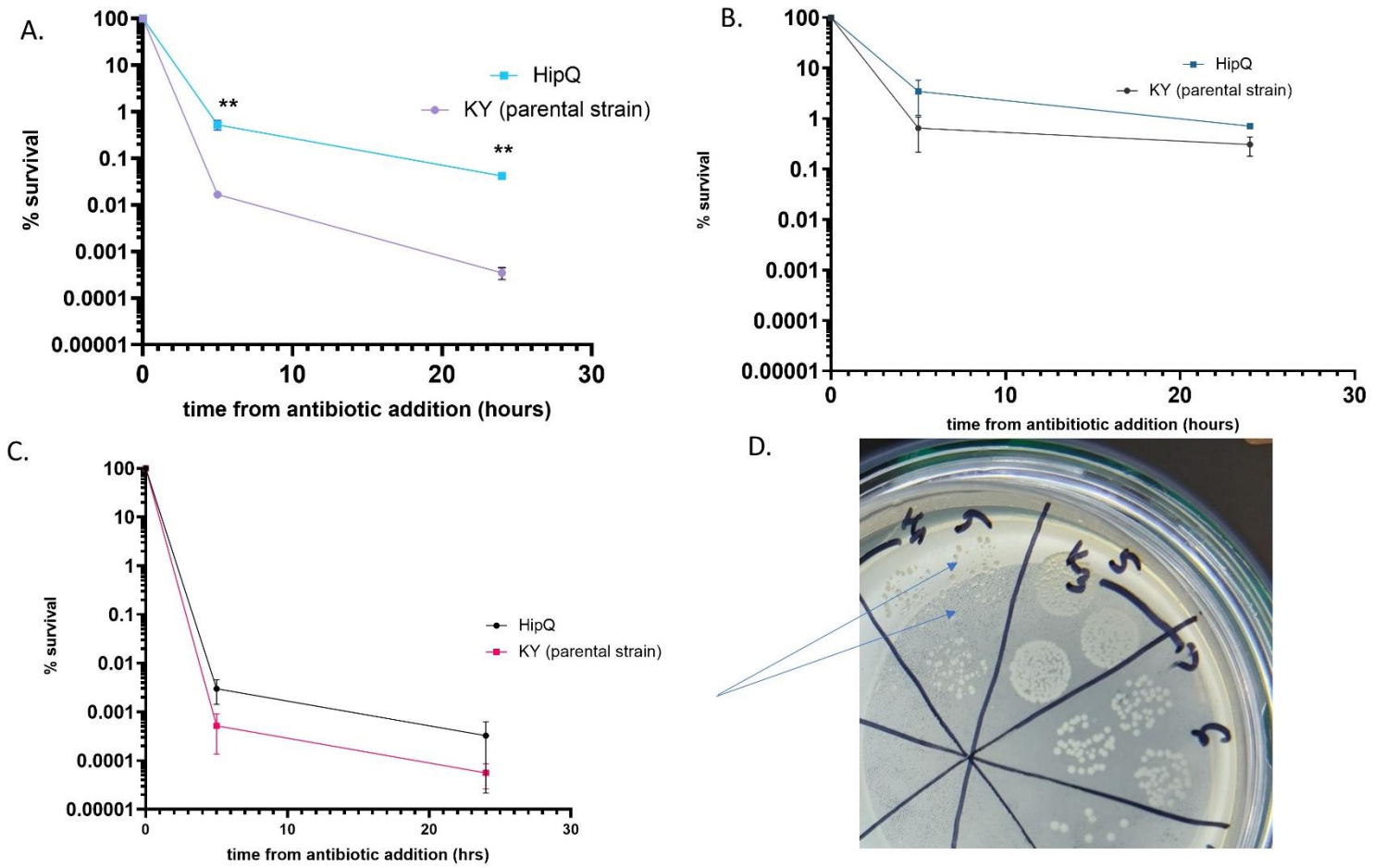

Figure 4.6. Ampicillin (100 µg/mL) time-kill assays of E. coli HipQ and its parental strain KY in LB (A and B) and M9-GLUCOSE (pH7) (C) growth media, with 200rpm shaking*. A. % survival of passage 1 cultures in LB Miller exposed to 20X MIC of ampicillin. B. % survival of passage 2 cultures in LB Miller exposed to 20X MIC ampicillin. C. % survival of passage 1 cultures in M9-GLUCOSE exposed to 20X MIC ampicillin. n=3, error bars are SEM, limit of detection was 500 CFU/mL; * = p and q < 0.05 by two-way ANOVA (strain vs. time) corrected for multiple comparisons with Benjamini, Kreuger and Yekutieli false discovery control method. D. example persister regrowth agar plate; H1 – E. coli HipQ, K1 E. coli – KY; little colonies observed on HipQ plates after 48hrs of incubation are marked by blue arrows.*

*4.3.2.2. E. coli Δ*ydcI *is not highly persistent to ampicillin or ofloxacin in either rich or minimal medium*

Ampicillin time-kill assay results of *E. coli ΔydcI* and its parental strain BW25113 did not demonstrate the previously observed ampicillin high-persistence feature of this strain in neither rich (LB Miller) nor minimal (M9-GLUCOSE) medium (Figure 4.7a and b). Since contamination was excluded as the source of this discrepancy through both molecular (PCR) and biochemical (API strip test, *BioMerieux)* testing (Figure 4.S2), other potential causes were considered. As previously mentioned, time-kill assays are known to be very sensitive to incubation conditions, such as shaking (oxygenation), media pH, media composition or temperature (Harms *et al.*, 2017). However, when culture oxygenation, media pH and starting culture density were screened it was found that none of the tested conditions resulted in a statistically significant difference in frequency of ampicillin persisters between *ΔydcI* and its parental strain (Figure 4.S3).

Following on from these observations, the time-kill assay was also performed with ofloxacin, a fluoroquinolone which *E. coli* HipQ has been previously found to be highly persistent to (Wolfson *et al.*, 1990). Ofloxacin MIC of *E. coli ΔydcI* and BW25113 was determined experimentally prior to time-kill experiments (Figure 4.S4). However, similarly to ampicillin time-kill assay, there was no statistically significant difference in frequency of ofloxacin persisters between *ΔydcI* and its parental strain BW25113 (Figure 4.7c).

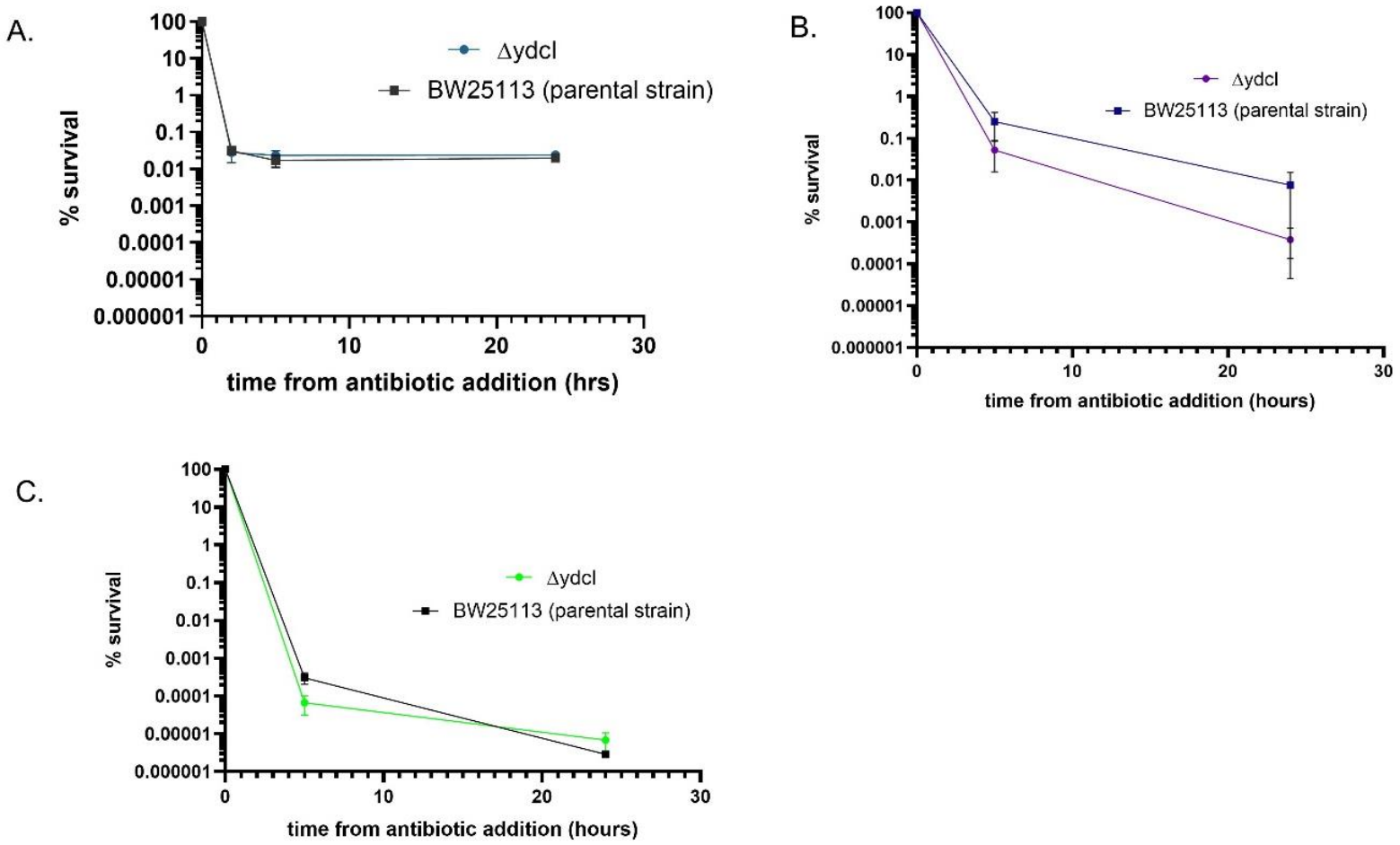

Figure 4.7. Time-kill assays of E. coli ΔydcI and its parental strain BW25113, with 200rpm shaking. *A. % survival of cultures in LB Miller exposed to 20X MIC of ampicillin (blind assay) B. % survival of cultures in M9-GLUCOSE medium exposed to 20X MIC of ampicillin. C. % survival of cultures in LB Miller exposed to 25XMIC ofloxacin. n=3, error bars are SEM, limit of detection was 500 CFU/mL for ampicillin assays and 50 CFU/mL for ofloxacin assays; p and q > 0.05 by two-way ANOVA (strain vs. time) corrected for multiple comparisons with and Benjamini, Kreuger and Yekutieli false discovery control method.*

Since genes whose expression is regulated by YdcI are known (Gao *et al.*, 2018), in order to further investigate the previously proposed link between *ydcI* and persistence independently of *YdcI* expression levels, knock-out models of individual YdcI-regulated genes were investigated next.

4.3.2.3. Genes whose expression is regulated by YdcI do not have a significant influence on resistance or persistence to ampicillin

Both persistence and resistance can be increased with mutation and a widely accepted method of distinguishing those two survival mechanisms are MIC assays (Balaban *et al.*, 2019). In general, antibiotic persisters do not contain specific genes which 'resist' the action of an antibiotic (such as antibiotic-degrading enzymes) and are merely capable of surviving exposure to it for longer time periods. Therefore, high-persister strains should not display a change in MIC when exposed to an antibiotic, whilst simultaneously displaying an increased frequency of persister cells.

4.3.2.4. Minimum inhibitory concentration assays (ampicillin resistance)

In this assay (Figure 4.8), knock-out strains of YdcI-regulated genes (Gao *et al.*, 2018) were obtained from the KEIO collection (Baba *et al.*, 2006). MICs were determined by resazurin viability assay as the lowest concentration of the antibiotic that inhibited bacterial growth. Starting CFU/mL values were lower than the limit of detection of the resazurin assay and therefore bacterial growth, as opposed to survival which is a feature of tolerance and antibiotic persistence was a pre-requisite for a positive result. As can be seen in Figure 4.8, knocking-out any of the 16 genes regulated by YdcI does not significantly decrease the MIC to ampicillin and therefore this transcription factor is not likely to be involved in genetic AMR. Interestingly, for one of the genes, *ddlA*, a deletion of this gene resulted in 2-fold increase of the MIC. This can be explained by the fact that *ddlA* is a ligase involved in peptidoglycan biosynthesis (UniProt, 2020) which is the pathway inhibited by ampicillin. However, MIC of <16 µg/mL is still classified as ampicillin-sensitive (Clinical and Laboratory Standards Institute, 2019). Moreover, in this thesis the concentration of ampicillin used during time-kill assays of *ΔydcI* was 100 µg/mL (20XMIC) and therefore it is unlikely that a 2-fold increase in MIC would have had a significant effect on the frequency of persisters.

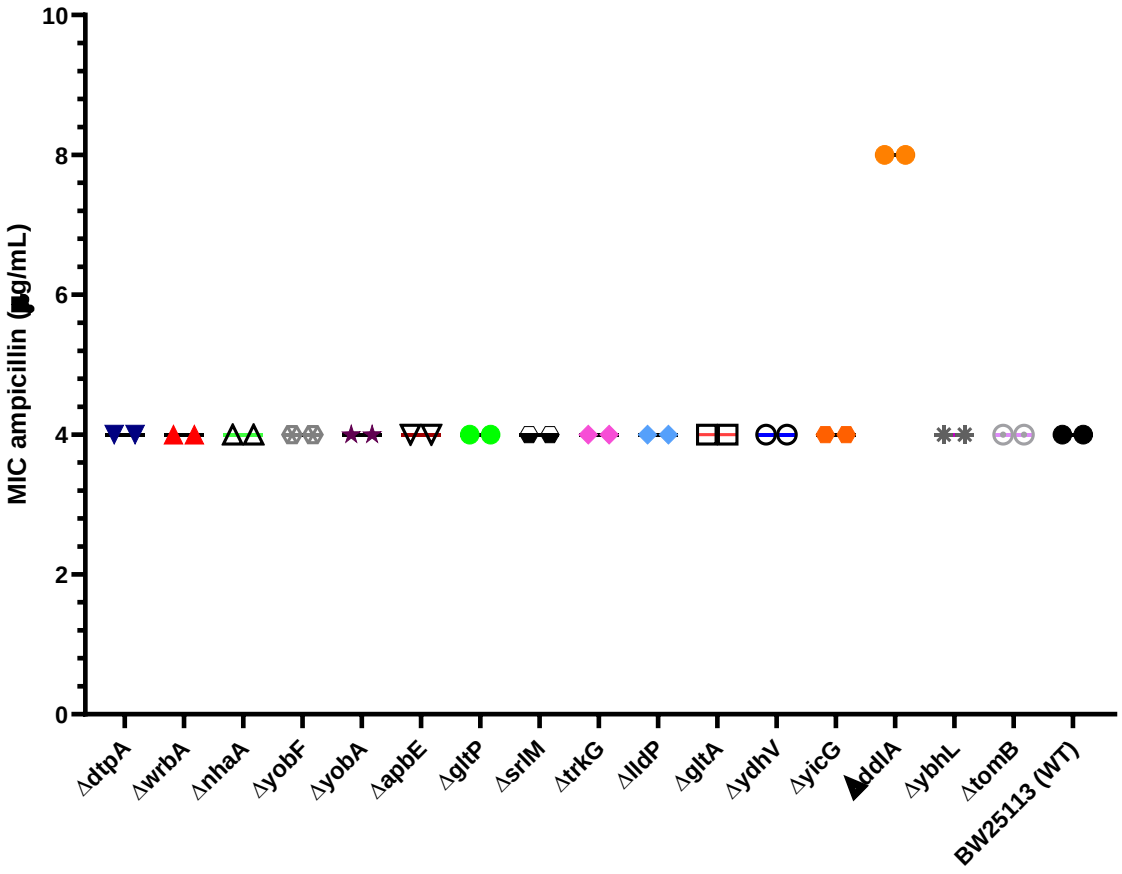

Figure 4.8 Ampicillin minimum inhibitory concentrations of YdcI-regulated genes Kos (LB Miller); *n=2 and each presented data point is an average of 4 technical replicates; MIC value is the lowest concentration of antibiotic that inhibited growth in all technical replicates of a biological replicate (n).*

4.3.2.5. Time-kill assays (ampicillin persistence)

In this experiment, KOs of individual YdcI-regulated genes were exposed to 20x MIC of ampicillin in LB Miller broth and surviving cell frequencies were measured at T=24hrs post antibiotic addition. Since a singular timepoint was measured, this assay was not able to distinguish between persistence and tolerance (as the biphasic kill could not be observed). Therefore, it was used as a preliminary method of evaluating these KOs for further analysis by a multi-timepoint time kill assay. Due to well-known reproducibility issues of persister assays (Harms *et al.*, 2017), each assay included the parental strain (BW25113) as the reference and *ΔydcI* as an additional positive control. Persister frequencies of the KO strains were compared to the parental strain within the assay but not in between assays. Finally, since YdcI could either downregulate a peristence inducer or upregulate a persistence repressor (which in both instances would result in increase of persistence following knocking-out of *ydcI),* knock-out strains with either significantly reduced or increased persister frequencies would be considered as potential 'persister' genes.

As can be seen in Figure 4.9 there was no statistically significant difference in ampicillin persister cell frequencies between any of the 16 KO strains and their parental strain BW25113. Moreover, there was no statistically significant difference between ΔydcI and BW25113 when comparing pooled survival fractions from all assays (p=0.13 by Kolmogorov-Smirnov Z test). However, it was noted that the persister frequencies of the *ΔydcI* strain displayed higher variability (measured as geometric standard deviation) compared to its parental strain. This suggests that knocking-out *ydcI* could significantly affect persistence to ampicillin if unknown and specific requirements are met, but not generally or consistently in the same incubation conditions, as expected from a highly persistent strain such as *E. coli HipQ* (Figure 4.6).

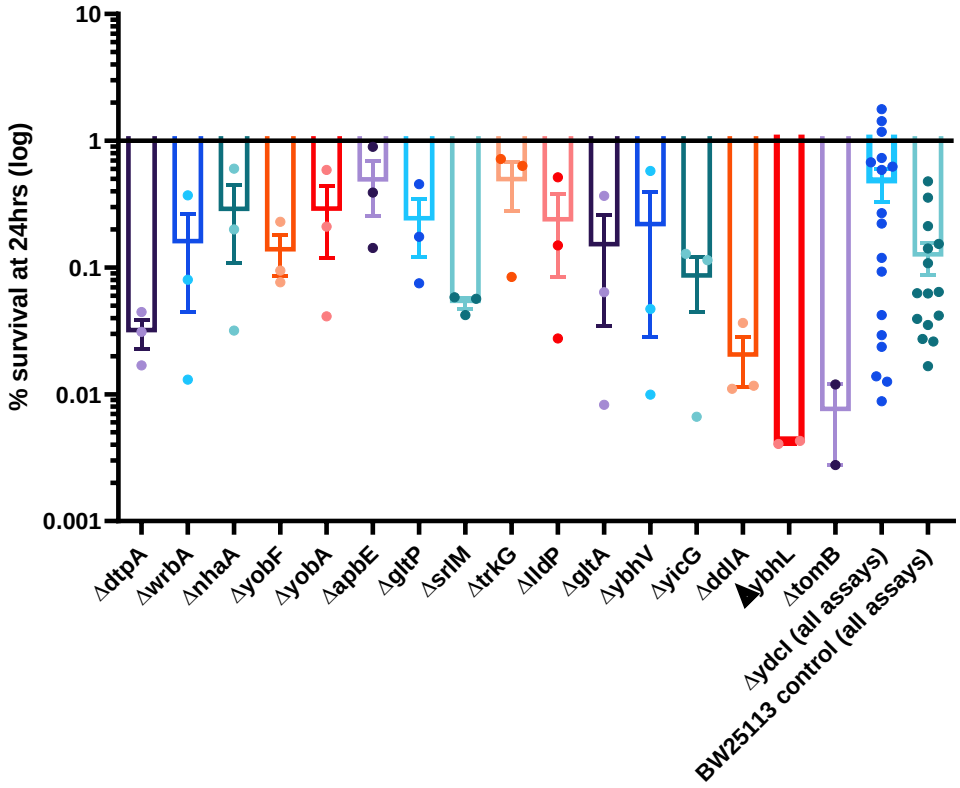

Figure 4.9. Endpoint 20X MIC ampicillin persister frequencies of E. coli cultures exposed to 20x MIC ampicillin in LB Miller, 200rpm shaking.*; n=3 per assay, except ΔtomB and ΔybhL where one repeat was excluded from analysis due to a technical issue; error bars are SEM; % survival of each KO strain was compared to the parental strain (BW25113) control from the same assay by Kruskal-Wallis test with Benjamini, Krieger and Yekuteli method for false discovery control ; Δydcl and parental strain % survival from all assays was compared by Kolmogorov-Smirnov Z test; p and q > 0.05 for all aforementioned comparisons.*

Taken altogether (Figures 4.8 and 4.9), these results suggest that loss of function of the *ydcI* transcription factor, either directly through knocking-out of the *ydcI* gene or indirectly through knocking-out YdcI-regulated genes does not significantly affect susceptibility to ampicillin, at least in the conditions assayed. Next, potential effect of *YdcI* gain-of-function on antibiotic persistence was investigated.

4.3.3. Introduction of HipQ-specific SNP into the *ydcI* gene of *E. coli* KY with CRISPR genome engineering

As explained in the introduction to this chapter, knock-out models are not representative of gain-of-function mutations affecting antibiotic persistence. Therefore, to investigate a potential gain-of-function of the HipQ-specific *ydcI* allele in the same genetic background, and subsequently fulfil Koch's molecular postulates for genotype-phenotype correlation (Falkow, 2004), CRISPR genetic engineering was implemented to introduce the HipQ *ydcI* allele into HipQ parental strain KY. If similar antibiotic persistence levels were observed in the KY;;*HipQydcI* strain as in the HipQ strain, but not the parental strain, it would be concluded that this polymorphism is responsible for the high-persister phenotype.

CRISPR recombineering, a type of CRISPR-mediated genetic engineering, utilises bacterial caspase (Cas9) in combination with sequence-specific guide RNAs as a method of marker-free recombination (Pyne *et al.*, 2015). Please refer to the methods section (Figure 4.1) for detailed overview of CRISPR recombineering technology.

4.3.3.1. Insert DNA (recombination fragment) preparation

A silent mutation in the Cas9 recognition site was introduced into PCR-amplified HipQ *ydcI* allele (recombination fragment) through site-directed mutagenesis, and verified by Sanger sequencing (Figure 4.10a). Therefore, successful recombinants would be protected from Cas9 cleavage since an NGG sequence immediately downstream of the gRNA-corresponding sequence is a pre-requisite for Cas9-mediated cleavage (Pyne *et al.*, 2015) (Figure 4.10b).

A.

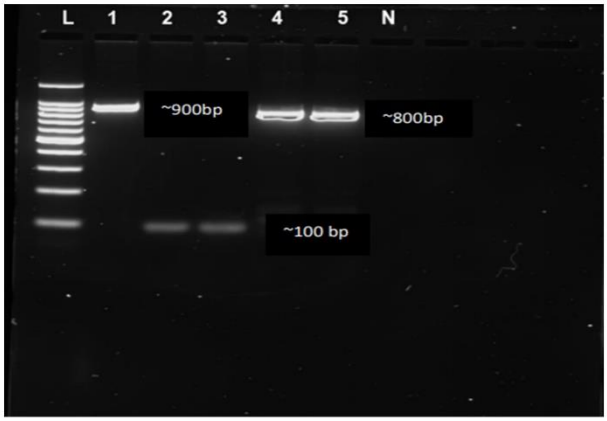

B.

5′**ATGGAAAAAAATAGTC**TGTTTAGTCAGCGCATCCGTTTGCGCCACCTTCATACATTCGTAGCTG**TCGC**
ACAACAAGGAACTTTGGG**A**C**GCGCGG**CTGAAACCCTTAATTTGAGTCAACCTGCGCTCTCTAAGACATTG
AATGAACTGGAGCAGCTGACTGGCGCTCGCTTGTTTGAGCGTGGTCGTCAGGGGGCGCAACTTACCTTAC
CCGGCGAACAATTTTTAACGCATGCAGTCAGAGTTCTTGAC**GC**CATCAACACTGCCGGACGGTCGCTTCA
TCGTAAAGAAGGTCTTAATAATGATGTCGTCAGGGTTGGTGCACTACCTACT**GAG**GCACTGGGGATATTA
CCTTCGGTTATAGGTCAGTTTCATCAGCAACAAAAAGAGACGACCTTGCAAGTTGCGACAATGAGTAACC
CTATGATTCTGGCGGGTTTAAAAACCGGGGAAATCGATATCGGCATTGGTCGGATGTCAGATCCTGAACT
GATGACCGGGCTTAATTACGAACTGCTGTTTCTTGAATCGTTGAAGCTGGTTGTCCGCCCTAATCACCCG
CTACTTCAGGAGAACGTAACGCTAAGCCGGGTGCTGGAATGGCCGGTCGTTGTATCACCAGAAGGCACTG
CGCCACGCCAGCATTCAGATGCATTAGTGCAGAGCCAGGGCTGTAAAATTCCTTCGGGTTGTATCGAAAC
GCTGTCTGCTTCGCTATCTCGTCAACTTACGGTTGAATACGATTACGTGTGGTTTGTCCCTTCTGGCGCT
GTAAAAGACGACCTGCGTCATGCCACGCTGGTGGCCCTGCCTGTTCCGGGACATGGTGCAGGCGAACCGA
TTGGAATACTGACCCGCGTAGATGCGACGTTCTCTTCTGGTTGCCAGTTGATGATTAACGCTATTCGAAA
ATCAATGCCGTTCTGA**3'**

Figure 4.10. Insert DNA preparation*. A. 2% agarose gel electrophoresis of site directed mutagenesis amplicons. From left to right: L-100bp DNA ladder (Promega), 1 – final product: HipQ ydcI allele containing a silent mutation in the Cas recognition site (924bp), 2,3 - upstream fragment (94bp), 4,5- downstream fragment (847bp), negative control (MQ water template). Upstream and downstream fragments were amplified using HipQ ydcI allele as the template and contained a mismatch in the final nucleotide of the Cas9 recognition site in their respective reverse and forward primers; B. ydcI gene of E. coli HipQ. In red is the guide RNA-corresponding sequence. Cas9 recognition site is in blue, and the green box marks the silent mutation site (GGA>GGG, glycine). Blue box highlights the HipQ-specific SNP site (A>C, alanine>glutamic acid).*

4.3.3.2. psgRNA and pCas design and preparation

sgRNA was designed in Benchling and subcloned into the PUC19 backbone by NBS biologicals *(Biobasic, UK)* (psgRNA). pCas plasmid was a kind gift from Sheng Yang.

4.3.3.3. HipQ ydcI allele introduction into E. coli KY suggests that it could be toxic

E. coli KY (HipQ parental strain) was successfully transformed with pCas plasmid. Next, *E. coli* KY;;pCas were induced with L-arabinose to express the λ red recombination system and successfully transformed with psgRNA, as well as the insert DNA. However, no successful recombinants were observed in multiple rounds of cleavage and selection, regardless of the method of target DNA introduction (chemical transformation or electroporation). Since transforming *E. coli* KY;;pCas with empty PUC19 vector (positive control) was successful, this suggested that either *ydcI*-sgRNA had unpredicted off-target cleavage site(s) or that the HipQ-specific *ydcI* allele had a negative impact on cell growth, resulting in recombinants being unable to form colonies on agar plates.

The latter initially seemed unlikely since the HipQ strain carrying this mutation, despite showing a growth defect in LB Miller broth (Figure 4.3), is able to form colonies on LB agar plates. However, whole genome re-sequencing of *E. coli* HipQ, described below, demonstrated that this strain does not carry the previously reported SNP in the *ydcI* gene, making both aforementioned explanations possible.

4.3.4. Whole-genome sequencing of *E. coli* HipQ

Taken altogether, results of *ΔydcI* strain time-kill assays (Figure 4.6) and the challenge of introducing the HipQ-specific *ydcI* SNP into *E. coli* KY genome (section 4.3.3) shed doubt on the *ydcI*'s involvement in HipQ persistence. Therefore, the original glycerol stock of the HipQ strain, prepared in 2012 from an agar stab kindly gifted by Nathalie Balaban (see Balaban *et al.,* 2004), was whole genome sequenced and the compared to previously published sequencing data on this strain obtained from BioSample (accession numbers: SAMN13648605 (HipQ) and SAMN13648604 (KY)).

4.3.4.1. HipQ genome contains over 100 SNPs when compared to its parental strain but no polymorphisms in either ydcI or ybaL genes

Obtained illumina reads were first aligned to the parental strain reference sequence downloaded from GenBank (accession no: NZ_CP008801), annotated using Prokka software, and SNPs were called using workflow described in detail in section 4.2.2.

Sequencing data revealed that the HipQ strain contains 61 non-silent mutations compared to the reference KL16 genome, 54 of which are found in the coding sequences of known genes (table 4.2, peach-coloured rows). Three of these 54 genes have been previously described as antibiotic persistence regulators (table 4.2, blue-coloured rows) (Moyed and Bertrand, 1983; Ngan *et al.*, 2020; Sulaiman and Lam, 2020) and further seven are predicted to affect antibiotic persistence and/or resistance (table 4.2, yellow-coloured rows) as they either encode a toxin (rhsD, ydbD), antibiotic transporter (ompF, ydiM), are involved in biofilm formation (cdgI), or are involved in regulation of the stress response (rseB) (Sanchez-Torres, Hu and Wood, 2011; Koskiniemi *et al.*, 2013; Wang *et al.*, 2015; Masuda, Awano and Inouye, 2016; *STRING*, 2022).

It is also interesting to note that the HipQ genome contains a significantly higher proportion of C-T mutations (72/164 or 44%), compared to any other substitutions. Cytosine is the most unstable of DNA bases and this type of substitution is frequently caused by cytosine deamination, as a result of UV or chemically induced damage, which converts this base to uracil. If not repaired, this will result in cytosine-thymine substitution during subsequent rounds of replication (since uracil is not a canonical DNA component). (Beletskii and Bhagwat, 1996). Furthermore, the ratio of non-synonymous to synonymous mutations was app. 3:1 which is around 10 times higher than previously reported for *E. coli* (Martincorena and Luscombe, 2013). This suggests strong positive selection of mutated alleles. Given that *E. coli* HipQ was created by random chemical mutagenesis and isolated following repeated rounds of antibiotic exposure (bottleneck events) (Wolfson *et al.*, 1990) both of the aforementioned observations were not unexpected.

Table 4.2. Polymorphisms found in the genome of E. coli HipQ*. Reads were aligned to the reference sequence obtained from GenBank (accession no: NZ_CP008801) and the quality filter was set to 90%. Protein function was obtained from the STRING database of protein interactions (STRING, 2022) unless otherwise indicated. Peach-coloured columns indicate mutations in coding sequences. Blue-coloured columns indicate genes that have previously been shown to be persistence regulators and yellow-coloured columns indicate putative persistence regulators.*

POSITION ON REFERENCE GENOME	MUTATION TYPE	REFERENCE	VARIANT	EFFECT	GENE	FUNCTION	REF
526423	missense	C	T	L1378->F	rhsD	toxin involved in intercellular competition	Koskiniemi et al., 2013
985448	deletion	CGT	C	frame shift AR188	ompF	porin; drug transport	STRING database
1039859	missense	C	A	P71->Q	appA	phytate hydrolisis	STRING database
1153729	missense	G	A	R196->H	yceG	murein transglycosylase	STRING database
1403249	missense	T	G	N254->H	IS5 transposase	prophage transposon	UniProt
1403263	missense	T	C	K249->R	IS5 transposase	prophage transposon	UniProt
1411958	missense	C	T	G73->D	IS5 transposase	prophage transposon	UniProt
1413550	missense	C	T	M839->I	IS5 transposase	prophage transposon	UniProt
1431481	missense	C	T	T92->I	paaD	phenylacetyl-CoA epoxidase	STRING database
1446498	missense	C	T	T234->I	hypothetical protein	unknown	N/A
1448802	missense	C	T	A1002->V	hypothetical protein	unknown	N/A
1451152	missense	C	T	P243->S	ydbD	prohage toxin	Masuda et al., 2016
1455618	missense	C	T	A400->V	ynbC	unknown	STRING database
1458790	missense	C	T	P150->S	hrpA	ATP-dependent RNA helicase HrpA	STRING database
1465929	missense	C	T	V23->I	gap	glyceraldehyde-3-phosphate dehydrogenase	STRING database
1498997	missense	G	A	E137->K	yncE	unknown	N/A
1515463	missense	G	A	P804->S	narZ	respiratory nitrate reductase	Sulaiman and Lam, 2020
1525539	missense	G	A	V953->I	fdnG	formate dehydrogenase-	STRING database
1549152	missense	C	T	E441->K	pqqL	putative zinc protease	STRING database
1556995	missense	G	A	T271->I	ydeN	putative ser-type periplasmic non-aryl sulfatase	STRING database
1566734	missense	G	A	A242->V	hipA	toxin component of TA system	Moyed and Bertrand, 1983
1680791	missense	C	T	P87->L	ydgK	membrane protein	STRING database
1686093	missense	C	T	A203->V	rsxG	Na+-translocating ferredoxin	STRING database
1696762	missense	C	T	L73->F	ydhJ	membrane protein	STRING database
1726260	missense	C	T	M12->I	ydhX	putative 4fe-4s ferredoxin-type protein	STRING database
1727302	missense	C	T	R604->H	ydhV	putative oxidoreductase	STRING database
1739497	missense	C	T	D58->N	sufA	iron-sulfur protein biogenesis	Vinella et al., 2009
1745380	missense	C	T	A342->V	ydiK	membrane protein	STRING database
1747224	missense	C	T	T291->I	ydiM	efflux pump; isoprenol tolerance	Wang et al., 2015
1756452	missense	C	T	T257->M	ydiR	putative electron transfer flavoprotein	STRING database
1789293	missense	C	T	P49->S	katE	catalase	STRING database
1846805	missense	G	A	G380->D	cdgI (Yieal)	biofilm formation	Sanches-Torres et al., 2011
1939536	missense	C	G	G266->A	flhA	flagella formation	STRING database
2685084	missense	G	A	L65->F	rseB	Sigma-e factor negative regulatory protein	STRING database
4043531	missense	C	T	R87->C	rho	transcription termination factor Rho	STRING database
4218018	missense	C	T	E354->K	ptsP	phosphoenolpyruvate-dependent phosphotransferase system	STRING database
4259126	missense	T	A	D342->E	rpoB	DNA-directed RNA polymerase subunit beta	STRING database
4269134	missense	C	T	V120->I	thiG	thiazole synthase	STRING database
4269148	missense	G	T	A115->D	thiG	thiazole synthase	STRING database
4290175	missense	C	T	A29->V	hypothetical protein	unknown	N/A
4292659	missense	C	T	A109->V	aceB	malate synthase	STRING database
4305536	missense	C	T	P317->L	yjbB	unknown	N/A
4310897	missense	C	T	A95->V	pgi	phosphogluconase isomerase	Fraenkel and Levsohn, 1967
4358084	missense	C	T	P417->S	yjcE	unknown	N/A
4465971	addition	A	AT	frame shift Q86	mscM	mechanosensitive channel protein	STRING database
4468533	missense	G	A	R24->H	orn	oligoribonuclease	STRING database
4470239	missense	C	T	A230->T	queG	epoxyqueuosine reductase	STRING database
4475310	missense	C	T	A347->V	mutL	DNA mismatch repair	STRING database
4477855	missense	G	A	D109->N	hflX	unknown; involved in hypoxia induced persistence	Ngan et al., 2020
4509777	missense	G	A	P47->S	ytfF	membrane protein	STRING database
4519517	missense	G	A	A159->T	tamA	autotransporter assembly complex	STRING database
4520323	nonsense	G	A	D296-> STOP	tamA	autotransporter assembly complex	STRING database
4522217	missense	T	C	V416->A	tamB	autotransporter assembly complex	STRING database
4524518	missense	G	A	G1183->D	tamB	autotransporter assembly complex	STRING database
4528391	missense	G	A	A159->T	ytfR	galactofuranose transporter	STRING database
4541814	missense	G	A	A409->V	treB	trehalose-specific pts enzyme	STRING database
4545123	missense	G	A	G214->S	mgtA	magnesium transport	STRING database
4566723	missense	G	A	A67->V	yjgR	unknown	N/A
4582183	missense	G	A	G13->D	nanY	unknown	N/A
4589748	missense	G	A	A174->V	fecC	ferric citrate transporter	STRING database

4.3.4.2. Previously reported SNP in the ydcI gene of E. coli HipQ might be a result of HipQ not being isolated as a pure strain

As mentioned throughout this chapter, *E. coli* HipQ was previously reported to contain a mutation in the *ydcI* transcription factor and this mutation has been linked to both high-persistence and reduced phenotypic inheritance features of this strain, (Hingley-Wilson *et al.*, 2020), serving as a basis for the work presented here. Therefore, Sanger sequencing of the *ydcI* gene, PCR-amplified from pure colonies across three glycerol stocks prepared at different times (including the original HipQ glycerol stock), was performed in order to further validate next-generation sequencing results presented in section 4.3d. As can be seen in Figure 4.11, the presence of the *ydcI* gene of expected size (924 base pairs) and sequence in agreement with next-generation sequencing data from this work (332C, wild-type allele) was confirmed for all glycerol stocks screened.

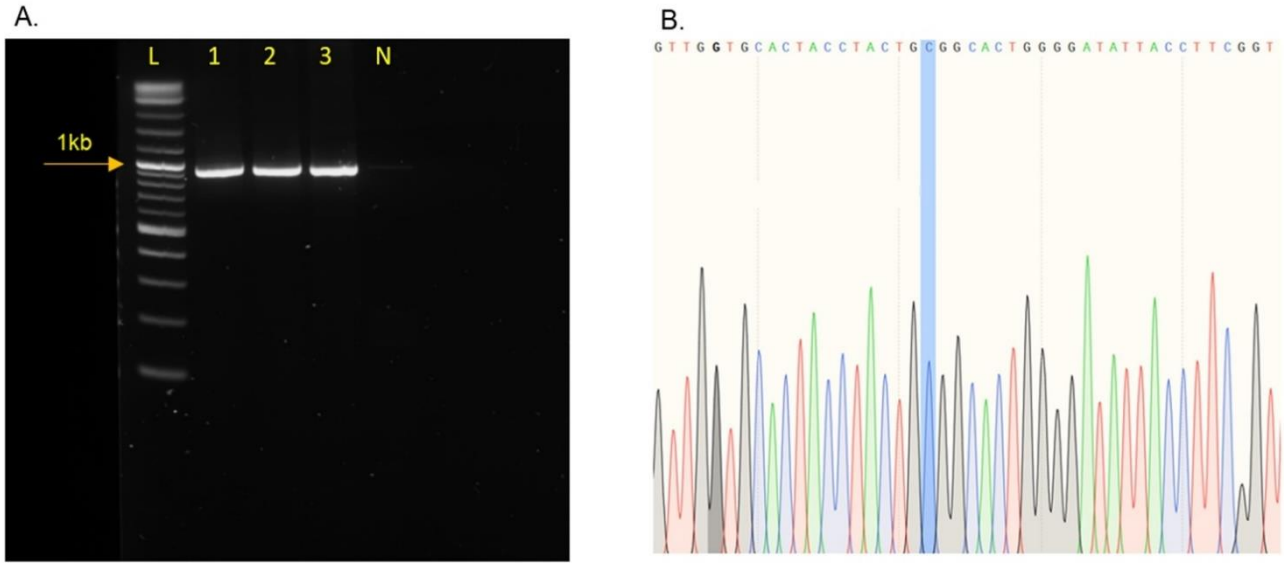

Figure 4.11. Validation of E. coli HipQ next-generation sequencing data with Sanger sequencing. *A. 1% agarose gel electrophoresis of PCR-amplified HipQ ydcI gene; from left to right: L-1kb plus DNA ladder (NEB), 1,2,3 – E. coli HipQ glycerol stocks 1-3, N- no template control; expected band size (full ydcI gene) was 924 base pairs; B. representative Sanger sequencing fluorescence peaks of HipQ ydcI gene. The site of previously reported HipQ-specific SNP (332A>C) is highlighted in blue.*

Next, previous sequencing data of *E. coli* HipQ and its parental strain KY, accessed from BioSample, was re-analysed and variants were called using the same pipeline as described in section 4.2.3 to exclude the possibility that differences in analysis pipelines caused the discrepancy in results. Polymorphisms found in the re-analysis of previous sequencing data agreed with what had been previously reported (Hingley-Wilson *et al.*, 2020) i.e. the presence of *ydcI* and *ybaL* alleles was confirmed, although the polymorphism in the *ybaL* gene was below the originally set quality cut-off score (<10%). Furthermore, the previously described 61 non-silent SNPs (table 4.2) in the HipQ genome discovered as a part of this thesis were not found in the re-analysis of previous sequencing data. Therefore, it was concluded that the discrepancy in sequencing results of the HipQ strain was not due to a different assembly or analysis frameworks.

Finally, the possibility of the HipQ strain being a mixture of two strains was investigated. The 'mixed colony' hypothesis posed that the previously reported genotype was dominant at the time this strain was first sequenced and was afterwards outcompeted by the current genotype during outgrowth and selection. It was reasoned that if this was true, when looking at individual reads of the previous sequencing data, currently established variants would be found at low frequencies. This analysis was kindly provided by Dr. Huihai Wu at the University of Surrey and demonstrated no evidence of currently established variants in the previous sequencing data (table 4.S2).

4.3.5. Single-cell observations with flow cytometry confirm HipQ high persistence to fluoroquinolones and indirectly support previous observations of reduced phenotypic inheritance (RPI) feature of this strain

Since it has been confirmed that the HipQ genotype investigated in this work displays the previously reported high-persistence to ampicillin (see Figure 4.6), it was next investigated if it also displays previously reported high-persistence to fluoroquinolones and reduced phenotypic inheritance (Wolfson *et al.*, 1990; Hingley-Wilson *et al.*, 2020). Flow cytometry, unlike a microfluidics system where HipQ RPI was first observed, is not able to track cell lineages. However, using this method it is possible to determine relative cell sizes based on FSC/SSC values (Cosma, 2020). The HipQ strain has previously been shown to generate a higher frequency of small persister cells than its parental strain KY (Hingley-Wilson *et al.*, 2020). It was therefore hypothesised that the aforementioned small cell size subpopulation should be observable as an increased number of cells at the 'tail-end' of the forward scatter distribution in *E. coli* HipQ, when compared to its parental strain, as FSC is relative to cell diameter (Cosma, 2022).

Interestingly, as can be seen on Figure 4.12c, the average cell size is significantly higher for HipQ cells. This agrees with previous observations from this work (Figure 4.3) where normalising OD values (total biomass) for HipQ and its parental strain resulted in approximately 5-fold difference in CFU/mL counts. Furthermore, an increased frequency of the cells at the low tail-end of FSC values (small cell size) can be seen for the HipQ strain (app. 2.2% vs. app. 0.6-0.9% in the KY strain), however whether these cells are persisters could not be determined here.

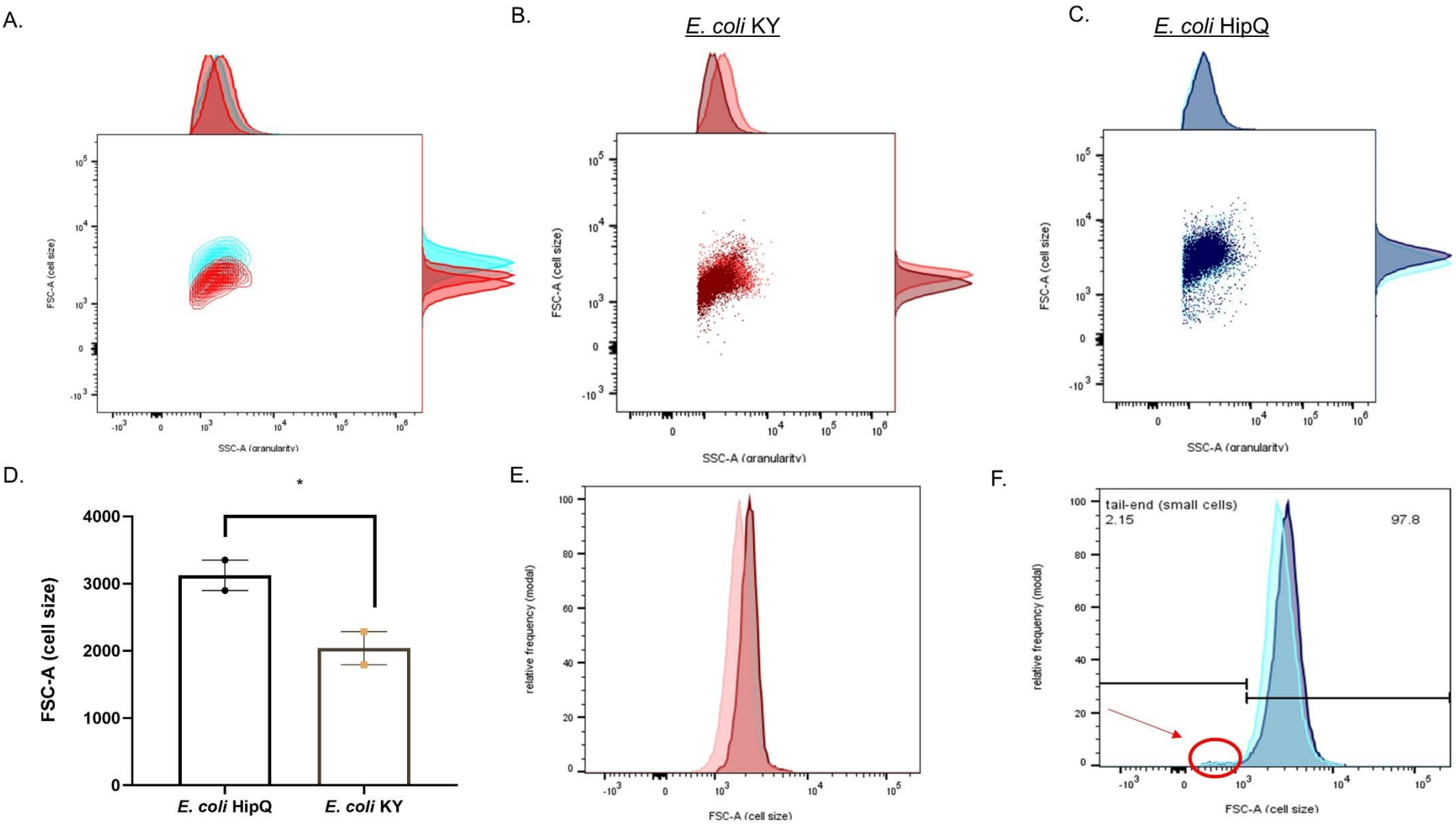

Figure 4.12. E. coli HipQ and KY cell size comparison (LB Miller). *Top panel: relative cell size of A. combined E. coli KY (red) and HipQ (blue) B. E. coli KY, C. E. coli HipQ Bottom panel: Histograms of cell size distributions of D. E. coli KY and E. E. coli HipQ; n=2 from two independent experiments*; biological repeats are represented with colour shades*; error bars are SEM; 100000 events/sample were collected; * = p < 0.05 by paired t-test on averaged FSC values, 'tail-end' of cell diameter consisting of HipQ 'small cells' is marked by red circle.*

Next, persistence of *E. coli* HipQ to fluoroquinolones was investigated both on batch level with time-kill assays (Figure II2.13e) and on single cell level with flow cytometry (Figure 4.13d). *E. coli* HipQ and KY cultures were exposed to 25x MIC of ciprofloxacin (0.4 µg/mL) (Zeiler, 1985) for 24hrs and viable cells were quantified by CFU/mL plating (persister subpopulation) and live/dead staining (persister and VBNC subpopulations). Interestingly, the total fraction of 'live' cells (Figure 4.13b and c) (persisters and VBNCs), was several orders of magnitude higher than the fraction of persisters i.e. cells capable of regrowth on agar plates (Figure 4.13e).

The mean of surviving ('live') cells was 61% and 56% for HipQ and KY strains respectively ($p > 0.99$ by paired t-test). The live/dead staining method applied in this study was initially verified on heat-killed and live (mid-exponential phase) cells (Figure 4.13a, black and green populations respectively) where clear increase in zombie nearIR fluorescence can be observed in the heat-killed (dead cell) samples. It is important to note that the live/dead cell discrimination is based on membrane integrity, with cells with intact membranes staining as 'live', regardless of metabolic activity. It is noted that for non-lytic antibiotics, such as ciprofloxacin, it could lead to an overestimation of the 'live' (persister and VBNC) subpopulation. However, this staining method was subsequently verified in chapter 5 of this work with the use of a respiration marker.

The mean percentage of persisters was 3.2% for the HipQ strain and 0.05% for the KY strain (64-fold difference, ranging from 100-fold to 5-fold between independent experiments). This observed difference in was not statistically significant ($p=0.25$ by Wilcoxon matched-pairs signed rank test) however, a significant variability of persister cell frequencies in-between independent experiments was noted in *E. coli* HipQ.

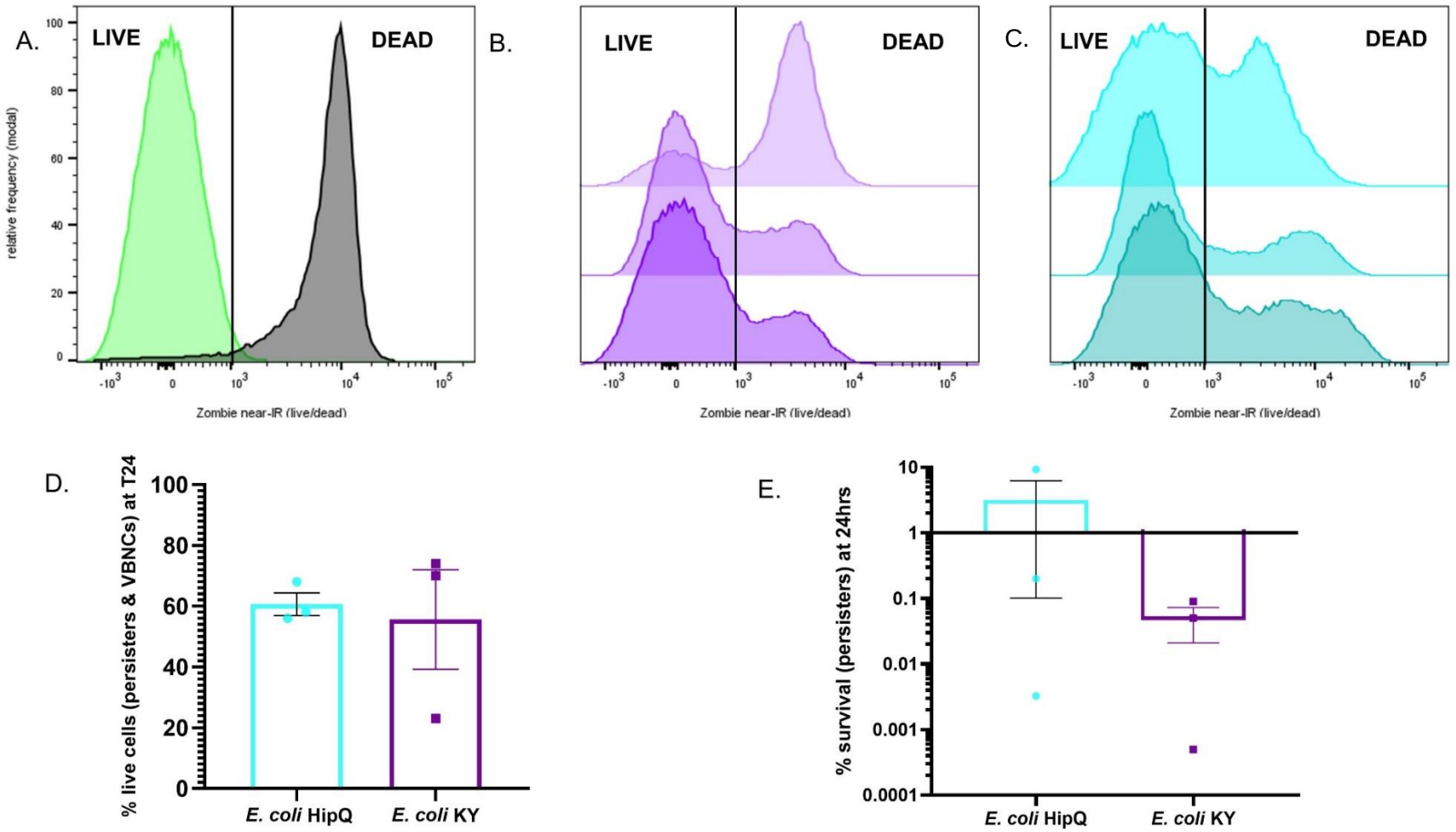

Figure 4.13. E. coli HipQ and KY peristence to ciprofloxacin (LB Miller). *Top panel: live/dead staining of A. heat-killed (black) and live (green) E. coli cells. B. live dead staining of B. E. coli KY and C. E. coli HipQ cultures exposed to 50XMIC ciprofloxacin for 24hrs and; n=3 independent experiments, 100000 events were collected per sample. Bottom panel: D. log % of persisters and VBNCs based on live/dead staining (panels B and C) and E. % of persisters based on CFU/mL plating following exposure to 25X MIC ciprofloxacin for 24hrs, n=3 independent experiments, error bars are SEM, p > 0.05.*

4.4. Discussion

4.4.1. Summary of findings presented in this chapter

The scope of this chapter was to investigate the role of the *ydcI* transcription factor as antibiotic persistence regulator in *E. coli.* Contrary to previous findings (Hingley-Wilson *et al.*, 2020) we did not observe the *ΔydcI* strain to be highly-persistent to ampicillin in any of the multiple conditions tested. Furthermore, KO strains of individual genes regulated by YdcI (as proposed by Gao *et al.*, 2018) were also found to not have a significantly different frequency of ampicillin antibiotic persisters. This disproves the hypothesis that native (i.e., not considering potential gain-of-function mutations) *ydcI* regulates antibiotic persistence through downstream metabolic remodelling.

Moreover, we did not observe the Δ*ydcI* strain to be highly persistent to ofloxacin, a fluoroquinolone which the HipQ strain is highly persistent to (Wolfson *et al.*, 1990). Since *ΔydcI* strain was originally proposed as a model for HipQ's high persistence it was expected to display a similar persistence profile. However, in this work we demonstrated that the HipQ genome carries multiple non-synonymous mutations when compared to its parental strain, yet we were not able to confirm the presence of the previously reported SNP in the *ydcI* transcription factor (Hingley-Wilson *et al.*, 2020). This suggests that the high-persistence feature of this strain is independent of *ydcI.* Finally, when we attempted to introduce the aforementioned SNP to the HipQ parental strain background, we were not able to rescue any recombinants, which points towards potential toxicity of this allele.

On the other hand, we were able to confirm the previously reported high-persistence of *E. coli* HipQ to β-lactams (ampicillin) and fluoroquinolones (ciprofloxacin) (Wolfson et al, 1990). Furthermore, despite the difference in genotype compared to previously published whole-genome sequencing data (Hingley-Wilson *et al.*, 2020), we found supporting evidence of reduced phenotypic inheritance in the HipQ strain investigated in this study. This suggests that RPI in *E. coli* HipQ is independent of *ydcI,* disproving our initial hypothesis.

4.4.2. *ydcI* transcription factor and its role in regulating antibiotic persistence

Although time-kill assays (kill curves) are currently considered the 'gold standard' of antibiotic persistence assays they notorious for their weak reproducibility (Harms *et al.*, 2017). Since persistence is a phenotypic trait, it is possible that a small difference in incubation conditions affected reproducibility of kill curves of the *ΔydcI* strain done as part of this work, when compared to previous observations (Hingley-Wilson *et al.*, 2020). Therefore, as discussed previously, quantitative data obtained from batch-level experiments should ideally be followed up by single-cell observations. Although time-kill assays on the *ΔydcI* strain have not been done in a microfluidics system previously or as a part of this work, it has been independently reported that the *E. coli* Δ*ydcI* is not highly-persistent to ampicillin (Cañas-Duarte *et al.*, 2020) which further validates results presented here.

Based on our initial findings from Δ*ydcI* strain time-kill assays, loss-of-function in the YdcI gene seemed unlikely as cause for *E. coli* HipQ high persistence. Therefore we sought to develop a more accurate model by incorporating the previously reported HipQ-specific *ydcI* allele (Hingley-Wilson *et al.*, 2020) into the HipQ parental strain genetic background. We hypothesised that rather than a loss-of-function, a gain-of-function mutation in this transcription factor could affect persistence to antibiotics. However, we were unable to isolate any viable recombinants carrying this SNP following multiple rounds of selection. Although this could possibly be a result of an unknown off-target activity of the sgRNA, the possibility of this mutation being detrimental (to the point of inhibiting growth of recombinants) could not be excluded. This was initially surprising, as the HipQ strain is able to form colonies on LB agar plates. However, following re-sequencing of our original HipQ stock we found that it did not carry the previously reported mutation in the *ydcI* gene (Hingley-Wilson *et al.*, 2020), which would explain other observations presented in this chapter.

Nevertheless, the strain investigated as part of this work did show increased persistence to ampicillin and ciprofloxacin, as well as increased frequency of small cells as has been previously reported for *E. coli* HipQ (Wolfson *et al.*, 1990; Hingley-Wilson *et al.*, 2020) which suggested that the discrepancy in sequencing data was not a result of contamination. Sequencing results presented in this work have also been independently verified by another research group working with this strain (Cañas-Duarte *et al.*, 2020). Therefore, we conclude that the *ydcI* gene is not mutated in *E. coli* HipQ and is not responsible for the high persistence feature of this strain. As mentioned previously, the

HipQ strain was isolated during a random mutagenesis screen (Wolfson *et al.*, 1990), prior to the advent of next-generation sequencing. Therefore it is not unreasonable to assume that it originally contained a mixture of different mutants with varying growth rates, with the fastest-growing mutant eventually outcompeting other isolates, but perhaps not completely eradicating them, resulting in the observed discrepancy in sequencing data.

Interestingly, our results suggest that both high-persistence and RPI features of *E. coli* HipQ are *ydcI*-independent, in contrast to previous observations (Hingley-Wilson *et al.*, 2020). However, it is important to note that the Δ*ydcI* strain has been shown to display reduced phenotypic inheritance similar to the one displayed by *E. coli* HipQ, on a single-cell level (Hingley-Wilson *et al.*, 2020), despite our results showing that the HipQ strain does not carry a defective *ydcI* allele. We therefore hypothesise that multiple genes can affect heritability of growth parameters in a similar manner.

4.4.3. Molecular mechanisms responsible for HipQ high persistence

In this work we demonstrated that *E. coli* HipQ displays growth defect when grown in rich, as opposed to minimal medium. A growth defect of the HipQ strain in rich media has been previously described (Wolfson *et al.*, 1990). The authors of the aforementioned study noted that this defect was only transient and growth rates of both strains equalized after an additional passage of both cultures, which agrees with observations presented here. Interestingly, we did not observe this difference in growth kinetics in minimal medium. However, it is important to note that both HipQ and the parental strain grow slower in this medium, which could 'mask' the difference between these two strains through increased whole population tolerance to cell-wall synthesis inhibitors, such as ampicillin. Taken altogether, this suggests that HipQ growth defect in rich medium is either phenotypic or epigenetic. As such, it is likely to influence persister cell frequency and could contribute to the 'high-persister' feature of the HipQ strain. Interestingly, previous batch-level assays on the HipQ strain did not take into account this growth defect (Wolfson *et al.*, 1990; Hingley-Wilson *et al.*, 2020), however it has been noted that HipQ produces an increased frequency of stochastic persisters which are slow-growing and slow-dividing cells (Balaban *et al.*, 2004; Hingley-Wilson *et al.*, 2020).

As mentioned previously, *E. coli* HipQ is reported to be highly persistent to ampicillin, however the quantitative measurements differed between publications: up to 100-fold increase of persistence was originally reported by Wolfson *et al.* (Wolfson *et al.*, 1990), although at lower antibiotic concentration than used in this study (10x vs 20x MIC) and

10-fold increase in the number of persisters was previously reported by Hingley-Wilson *et al.* at 20X the MIC (Hingley-Wilson *et al.*, 2020). Our results support the ampicillin high-persistence feature of this strain and show a statistically significant difference in the number of surviving cells between HipQ and its parental strain when the cultures were in the 'slow-kill' phase of the assay, indicating presence of persisters (Balaban *et al.*, 2019). However, we found this difference to be limited to growth in rich media (LB Miller broth). To the best of authors knowledge, time-kill assays in minimal medium on the HipQ strain have not been done previously and here we present that in M9-GLUCOSE medium there is no significant difference in the frequency of ampicillin persisters between HipQ and its parental strain. Moreover, we demonstrate that HipQ displays a higher frequency of ciprofloxacin persisters. This agrees with previous observations by Wolfson and colleagues where an increase in the frequency of norfloxacin persisters (a closely-related quinolone) was reported to be between 15-fold and 1000-fold in this strain (Wolfson *et al.*, 1990). However, it should be noted that there was no statistical analysis included in the original publication on fluoroquinolone persistence of the HipQ strain and subsequent research on this strain focused on its high persistence to ampicillin (Balaban *et al.*, 2004; Hingley-Wilson *et al.*, 2020)

Furthermore, we found that *E. coli* HipQ genome, when compared to its parental strain, carries multiple non-synonymous mutations, including in several previously characterized persistence regulators: toxin *hipA*, respiratory nitrate reductase *narZ* and *hjfx,* encoding a protein of unknown function involved in hypoxia-induced persistence (Moyed and Bertrand, 1983; Ngan *et al.*, 2020; Sulaiman and Lam, 2020). However, as discussed above our sequencing data did not validate the presence of the previously reported SNP in the *ydcI* transcription factor (Hingley-Wilson *et al.*, 2020).

Nevertheless, the mutated *ydcI* allele has been previously isolated from HipQ gDNA (Hingley-Wilson *et al.*, 2020) or following PCR-amplification of the *ydcI* gene from a plasmid template (section 4.3.4). Since *E. coli* HipQ was isolated during a random mutagenesis screen we hypothesise that 'HipQ' is not a pure strain and contains a mixture of genotypes, which are subsequently lost during selection and outgrowth as new stocks are prepared from isogenic single colonies.

Bases on our observations, we hypothesise that the multidrug-persistence phenotype of this strain could stem from multiple of the aforementioned polymorphisms having an effect on the frequency of antibiotic persisters, dependent on different environmental conditions and/or the antibiotic's mechanism of action. Since we could not find evidence

in support of the previously reported link between *ydcI* transcription factor and HipQ high persistence, in chapter 5 of this work we will focus on *ydcI*-independent mechanisms.

5. Characterization of the redox environment of *E. coli* persister and viable but non-culturable cells on a single-cell level

Aims

The aim of this chapter was to investigate the relationship between intracellular redox environment and antibiotic persistence. Specifically, intracellular abundance of ubiquitous redox co-factor NADH was used as a proxy to measure cellular respiration rate and redox activity. RelativeNADH/NAD+ ratio of individual cells was measured prior/post antibiotic exposure with the fluorescent biosensor Peredox and compared between four *E. coli* strains with varying persister cell frequencies.

Hypothesis

Due to their downregulated overall metabolic activity, the antibiotic-tolerant subpopulation will on average display a lower respiration rate and redox activity than the bulk population. However significant heterogeneity will be observed on a single-cell level due to the presence of VBNC cells and different persister classes.

5.1. Introduction

5.1.1. Intracellular redox environment and persistence to antibiotics

Cellular redox environment can be broadly defined as the balance between oxidants: reactive oxygen species (ROS), reactive nitrogen species (NOS) and hydrogen peroxide, and antioxidants - ROS/NOS-degrading enzymes e.g. superoxide dismutase which breaks down superoxide ions (Reniere 2018). During infection, ROS produced by phagocytic cells have been shown to contribute to pathogen clearance (Li *et al.*, 2021). Furthermore, bactericidal action of multiple antibiotic classes has been linked to ROS-mediated damage (Dwyer *et al.* 2014; Kohanski *et al.* 2007). Therefore, it is not unreasonable to assume that differential regulation of redox pathways would also be involved in persistence to antibiotics, with persister cells being able to ‘evade’ damaging

action of antibiotic and/or phagocyte-generated ROS as a result of their transient metabolic state. Indeed, Orman and colleagues have demonstrated that *E. coli* ampicillin and ofloxacin persisters differ in their reductase activities from antibiotic-sensitive cells. However, the reductase activity of persister cells was seemingly dependent on the culture growth phase. In exponentially-growing cultures cells which displayed low reductase activity were significantly more likely to be persisters than the bulk population (Orman and Brynildsen 2013a). In contrast, stationary phase persisters were found to have significantly higher reductase activity than the bulk population (Orman and Brynildsen 2015). The authors hypothesized that in stationary phase, where the majority of persister cells are stress/starvation-induced, high reductase activity results in self-digestion of cellular proteins and RNA, resulting in depletion of antibiotic targets (Orman and Brynildsen 2015). Since to the best of authors knowledge reductase activity of exponential and stationary phase cultures was not compared, it is not known whether exponential phase persisters demonstrate lower reductase activity overall, or just relatively to exponentially growing cells.

Finally, it has also recently been demonstrated that reducing reductase activity of ampicillin and ofloxacin stationary phase persisters with chlorpromazine (CPZ), an FDA approved antipsychotic drug, resulted in 1000-fold reduction of the persister fraction (Mohiuddin *et al.* 2020), suggesting that compounds affecting bacterial reductase activity could be effective as anti-persister drugs.

5.1.2. Characterization of intracellular redox environment on single-cell level

Arguably, the greatest challenge in investigating persister physiology is the inter-experiment variability and issues with reproducibility (Harms *et al.* 2017), as has also been demonstrated in chapter 4 of this work. The subpopulation of persisters is in standard conditions both small and itself heterogenous (Van den Bergh, Fauvart, and Michiels 2017). Therefore, the valuable information on the phenotype of individual persister cells can be lost through averaging of data on the persister subpopulation as a whole. Fortunately, the continued advancement of single-cell techniques, such as microfluidics or flow cytometry has allowed researchers to overcome this issue and led to multiple novel insights into the mechanisms regulating antibiotic persistence (Balaban *et al.* 2004; Goode *et al.* 2021; Hingley-Wilson *et al.* 2020; Orman and Brynildsen 2013a).

Single-cell reductase activity of individual *E. coli* cells has been previously characterized using a commercial reductase activity probe, RSG (RedoxSensorGreen) *(ThermoFisher)* (Mohiuddin *et al.* 2020; Orman and Brynildsen 2013a, 2015). However, it should be noted

that many commercial kits do not disclose the specifics of assay components or reactions due to patenting rights, which can make it difficult to determine specific enzyme(s) whose activity is altered in the persister state. Alternatively, NADH/NAD+ ratio detection system can be used as a proxy to estimate the intracellular redox environment. Nicotinamide adenine dinucleotide (NAD) is a ubiquitous molecule which in its oxidized form (NAD+) functions as an electron acceptor and in its reduced form (NADH) as an electron donor. It acts as a co-factor in hundreds of intracellular redox reactions, including oxidative respiration (a major ROS-producing pathway) (Massudi *et al.* 2012), warranting further investigation of its use as a biomarker for antibiotic persistence.

NADH abundance can be measured biochemically, either indirectly e.g., with a resazurin assay (Davis *et al.*, 2016), or directly with commercially available probes e.g., AAT Bioquest's Cell Meter^{TM}. However, these methods often fail to distinguish between NADH and its phosphorylated form NAD(P)H which carry out vastly different functions in the cell (Blacker *et al.* 2014). Alternatively, a fluorescent biosensor, where a sensor protein is designed to fluoresce upon NADH binding can be used to quantify intracellular NADH. The first such biosensor, Peredox, was developed by Hung and colleagues (Hung *et al.*, 2011) and consists of a circularly permutated and pH-stable T-Sapphire protein, flanked by NADH-binding protein Rex. Upon binding of NADH, the biosensor changes its conformation, resulting in concentration-dependent increase in T-Sapphire fluorescence. Peredox can also bind NAD+ (although at lower affinity), without increase in fluorescence, and therefore this biosensor reports relative (([NADH] partially compensated for [NAD+]) cytosolic NADH/NAD+ ratio (Hung *et al.* 2011). Although originally designed for eukaryotic expression, Peredox has since been used to investigate NADH/NAD+ homeostasis in *Mycobacteria spp.* *Methylococcus capsulatus* and *Ralstonia eutropha* (Bhat, Iqbal, and Kumar 2016; Ishikawa *et al.* 2017; Tejwani *et al.* 2017).

5.1.3. Current evidence of the link between *E. coli* HipQ and *E. coli* Δ*ydcI* antibiotic persistence and the intracellular redox environment

In chapter 4 of this work we demonstrated that *E. coli* HipQ carries non-synonymous mutations in several redox enzymes (table 4.2), which could influence the intracellular redox environment and subsequently affect the frequency of antibiotic persister cells. Specifically, *E. coli* HipQ carries a SNP in the glyceraldehyde-3-phosphate dehydrogenase (*gap*) gene. *gap* encodes a conserved enzyme of the glycolytic pathway, where it catalyses conversion of glyceraldehyde 3-phosphate to glycerate-1, 3-

biphosphate, a process which subsequently requires NAD+ being reduced to NADH (Wang *et al.* 2020). Therefore, better characterisation of the NADH/NAD+ homeostasis of *E. coli* HipQ persisters would lead to a better understanding of *gap*'s involvement in stochastic antibiotic persistence which is significantly increased in this strain (Wolfson *et al.*, 1990).

Furthermore, in chapter 4 of this work we demonstrated that *E. coli* Δ*ydcI* is not highly persistent to ampicillin or ofloxacin (section 4.3.2). However, *ydcI* transcription factor is known to regulate expression of two genes influenced by the NADH/NAD+ homeostasis: *gltA* and *wrbA* (Gao *et al.* 2018). *gltA* encodes a citrate synthetase, a component of the Krebs cycle (oxidative respiration pathway), and this enzyme is inhibited by NADH (Quandt *et al.* 2015). *wrbA* encodes a dehydrogenase which requires NADH as the electron donor and enhances tryptophan operon repression (Patridge and Ferry 2006). Both aforementioned metabolic pathways have previously been linked to antibiotic persistence in *E. coli: gltA* was found to be downregulated in ciprofloxacin persisters (Manuse *et al.* 2021) and *wrbA*-regulated tryptophan is a precursor for indole synthesis which has been shown to either induce persistence to fluoroquinolones (Zarkan *et al.* 2020) or reduce persistence to fluroquinolones and β-lactams (Hu *et al.* 2015), depending on its concentration. Therefore, comparing NADH homeostasis of *E. coli ΔydcI* and its parental strain persisters could provide an answer to whether the aforementioned persister formation pathways are dependent upon *YdcI* expression.

5.2. Methods

Please refer to chapter 3 for the description of general methods. Please refer to chapter 5 appendix for a list of primer sequences and plasmid maps. Please refer to Methods Appendix for detailed buffer and media composition.

5.2.1. Peredox biosensor transformation into *E. coli*

Chemical transformation of pRSETB-Peredox was performed as described in section 3.7. 100 µg/mL of ampicillin was used as the selective agent for successful transformants.

5.2.2. Peredox expression assay

25% glycerol in LB Miller broth bacterial stocks were stored at -80^{o}C, streaked on LB Miller (*Sigma Aldrich)* agar plates or LB Miller agar plates containing 100 µg/mL of ampicillin for pRSETB-Peredox transformed strains. Pates were incubated at 37^{o}C overnight. Next, single colonies were inoculated into 1mL of LB Miller broth or LB Miller broth with 100 µg/mL ampicillin added for plasmid retention. Cultures were incubated at 37^{o}C overnight, with shaking at 200rpm. Overnight cultures were then transferred to a black, clear-bottom, 96-well plate *(ThermoFisher Scientific)* (200 µL/well). Total biomass (OD_{600}) and fluorescence intensity measurements were performed in the CLARIOstar plate reader (*BMG LabTech)*. Fluorescence intensity was recorded at 575nm excitation, 610nm emission for mCherry (plasmid copy number) (table 5.1), in precise mode, sequential well scan and automatic gain adjustment. Fluorescence intensity was normalised to OD values and compared between pRSET-Peredox-transformed and untransformed samples in GraphPad Prism *(GraphPad).*

Table 5.1. Excitation/emission spectra of fluorescent agents used in this chapter. *% refers to percentage of maximal excitation/emission at given wavelength (FPbase, 2022).*

	Excitation (nm)	**Emission (nm)**
T-sapphire (Hung *et al.* 2011)	405 (93%)	520 (100%)
mCherry (Hung *et al.* 2011)	561 (70%) 575 (85%)	610 (100%)
Zombie near-IR live/dead fixable dye *(BioLegend)*	650 (40%)	746 (100%)

5.2.3. PCR for T7 polymerase gene

Genomic DNA was extracted from *E. coli* cultures as described in section 3.4. PCR reaction was set up according to manufacturer's instructions *(New England Biolabs)*. 10 µL of the final reaction product was electrophoresed on 1% agarose gel stained with SyBrSafe *(ThermoFisher Scientific),* at 100V for 45 minutes and imaged under UV light.

5.2.4. Relative NADH abundance measurements with flow cytometry

Flow cytometry method described in section 3.9 was followed. Additionally, T-sapphire fluorescence intensity ([NADH]) was recorded at 405nm excitation and 520nm emission and mCherry fluorescence intensity (plasmid copy number) was recorded at 561nm excitation and 610nm emission wavelengths (table 5.1). Laser power was kept consistent throughout the independent experiments, and compensation was not applied as excitation/emission spectra did not overlap. Single cell subpopulation was gated around manually based on linear FSC-A/FSC-H ratios (Cosma, 2020) and live/dead subpopulations were discriminated as described in section 3.9. Next, the singlet subpopulation was split into NADH biosensor expressing (mCherry positive) and non-

expressing subpopulations (mCherry negative) with a bifur gate, using untransformed cells as the negative control. Untransformed cells were also used to quantify autofluorescence for both aforementioned fluorophores. To quantify relative NADH abundance of individual cells, T-sapphire fluorescence intensity was plotted against mCherry fluorescence intensity. Gating and plotting of all events was done in FlowJo v.10 *(BD Biosciences).* For statistical analysis, fluorescence intensity values of T-sapphire and mCherry of individual events were exported into excel, T-sapphire fluorescence was normalized to mCherry fluorescence and values were averaged within biological replicates.

5.2.5. Ciprofloxacin time-kill assays

Time-kill assays were performed as described in section 3.2. 12.5-25X MIC ciprofloxacin (0.4 µg/mL) was used (Zeiler, 1985; Goswami *et al.*, 2016) and the assays were carried out in LB Lennox broth. For direct comparison, time-kill assays and relative NADH abundance measurements (section 5.3.4) were carried out on the same bacterial cultures, simultaneously.

5.2.6. T-Sapphire and mCherry intracellular stability assay

Overnight cultures were prepared as described in section 5.2.2. Next, cultures were diluted 1:50 into LB Miller broth or LB Miller broth containing 100 µg/mL of ampicillin for pRSETB-Peredox retention. Cultures were then grown to mid-exponential phase, at 37^{o}C, with shaking at 200rpm (~3hrs of incubation, OD=1). Ampicillin was removed by centrifuging the samples at 5000xg
g for 5min and resuspending cell pellets in fresh, antibiotic-free LB Miller broth. Next, 8 µg/mL of chloramphenicol (Tashiro *et al.* 2017) was added to half of each sample to inhibit protein expression. Samples were transferred to a 96-well, black, clear-bottom, flat-bottom, lidded plate *(ThermoFisher).* Total biomass (OD_{600}) and fluorescence intensity (T-sapphire: 405nm excitation, 520nm emission and mCherry 575nm excitation, 610nm emission, and compensation was not applied as excitation/emission spectra did not overlap) measurements were taken every 30 minutes for 24hrs on CLARIOstar plate reader *(BMG LabTech)*. Measurements were taken in precise mode with subsequent well scan and automatic gain adjustment. In between readings the plate was shaking at 300rpm (double orbital mode), and the incubation temperature was set to 37^{o}C. Data

analysis was performed in GraphPad software *(GraphPad).* Untransformed cultures were used as the background fluorescence control.

5.3. Results

pRSETB-Peredox (also referred to as NADH biosensor) was successfully transformed into *E. coli* HipQ and its parental strain KY, as well as *E. coli* Δ*ydcI* and its parental strain BW25113, confirmed by growth on ampicillin (pRSETB selection marker) agar plates. The biosensor consists of T-sapphire whose fluorescence intensity correlates with relative intracellular [NADH/NAD+], as well as constitutively expressed mCherry which can be used to normalise T-sapphire fluorescence. Normalisation is applied to plasmid copy number and biosensor expression level, which can be influenced by factors such as cell age or metabolic state (Hung *et al.*, 2011 and Figure 5.S1).

5.3.1. NADH biosensor is expressed in *E. coli* in the absence of T7 polymerase

Since NADH biosensor expression it driven by the viral T7 promoter (Figure 5.S1), initially no expression was expected without a subsequent transformation of *E. coli* strains with a T7 polymerase-expressing vector (Tabor, 2001). However, pRSETB-Peredox transformants formed red-tinted colonies on agar plates, and it was subsequently confirmed by fluorescence measurements that those cells expressed mCherry, confirming expression from the T7 operon (Figure 5.1). Consequently, it was demonstrated that none of the *E. coli* strains investigated as a part of this study were infected with the T7 phage, unknowingly resulting in T7 polymerase expression (Figure 5.S2). It is hypothesised that the observed NADH biosensor expression is a result of a 'leaky' expression from the T7 promoter and therefore this biosensor can be used in T7 polymerase negative strains without further genetic modification.

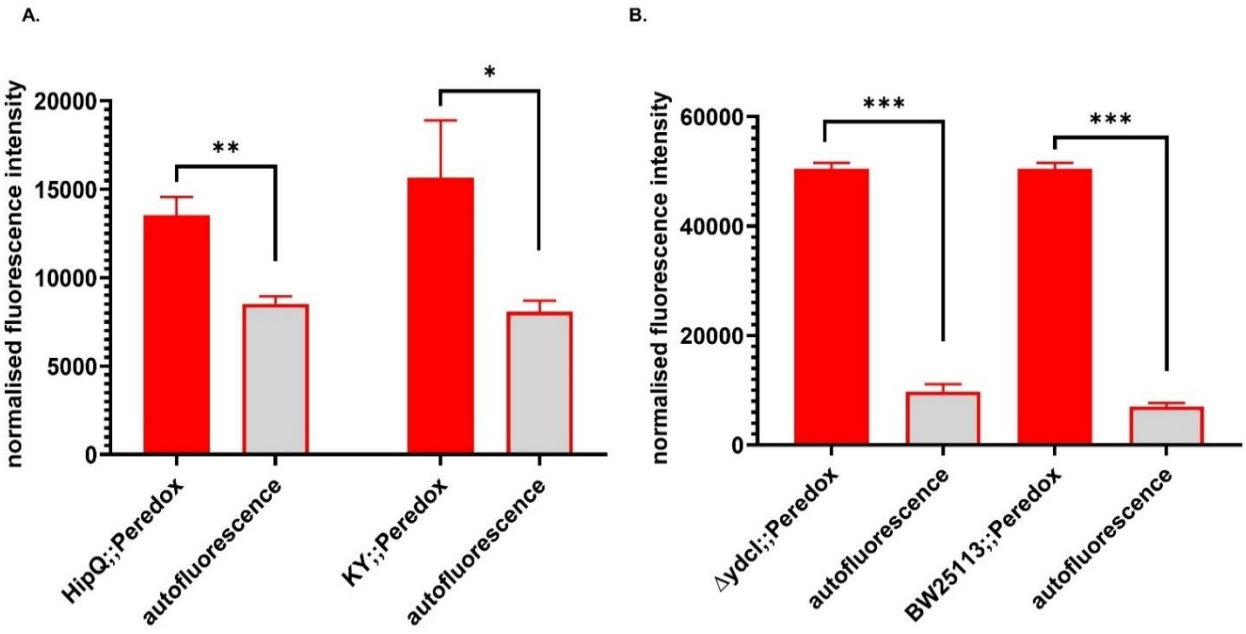

Figure 5.1. NADH biosensor expression in A. E. coli HipQ and its paretnal strain KY and B. E. coli ΔydcI and its parental strain BW25513*. mCherry fluorescence (biosensor copy number) was measured at 575nm excitation, 610nm emission (575/610). Autofluorescence is based on fluorescence intensity of untransformed cultures and fluorescence intensity was normalised to sample biomass. n=3, error bars are SD, * = p < 0.05, ** = p < 0.01 and *** = p < 0.001, and q < 0.05, by repeated measures ANOVA with Geisser-Greenhouse correction and Benjamini, Kreuger and Yekutieli false discovery control method.*

5.3.2. Effect of NADH biosensor expression on growth rate and frequency of ciprofloxacin persister and viable but non culturable (VBNC) cells

Once expression of the NADH biosensor was confirmed in *E. coli*, the next step was to investigate how it affects antibiotic persistence. It was hypothesised that expression of T-Sapphire and mCherry (biosensor components), especially at high levels, could increase the frequency of persisters by slowing down cell growth and/or inducing the stress response due to the presence of protein aggregates (Schramm, Schroeder, and Jonas 2020; Goode *et al.,* 2021b). When growth rates were measured by optical density over 24hrs, a significant difference was observed in growth rates of *E. coli* HipQ;;Peredox, KY;;Peredox, BW25113;;Peredox and their respective untransformed controls (Figure 5.S2). However, as can be seen in Figure 5.4a, no statistically significant difference in CFU/mL was observed between NADH sensor-expressing and untransformed cultures at 3hrs past starter culture inoculation, which was the starting timepoint of the time-kill assays presented in this chapter. Therefore, for this purpose

biosensor-expressing and untransformed cultures were assumed to be in the same growth phase.

Next, ciprofloxacin persister frequencies of biosensor-expressing and untransformed cultures were compared. Ciprofloxacin was chosen as it is non-lytic (LeBel, 1988), meaning that the biosensor would be retained in the cells following antibiotic exposure, and because the HipQ strain is known to be highly persistent to fluoroquinolones (Wolfson *et al.*, 1990). As can be seen in Figure 5.2b there was no statistically significant difference in the % survival (persister subpopulation) of biosensor-expressing and untransformed cultures following 24 hours of antibiotic exposure. There was also no statistically significant difference in the frequency of ciprofloxacin persisters between *E. coli* HipQ and its parental strain KY and Δ*ydcI* and its parental strain BW25113. However, it is noted that there was a significant variability in between biological replicates which decreased the statistical power of this assay. It was hypothesised that the non-lytic mechanism of action of ciprofloxacin could have resulted in a high frequency of damaged, VBNC-like cells whose regrowth was extremely sensitive to environmental conditions. This was further validated by viability staining (Figure 5.3)

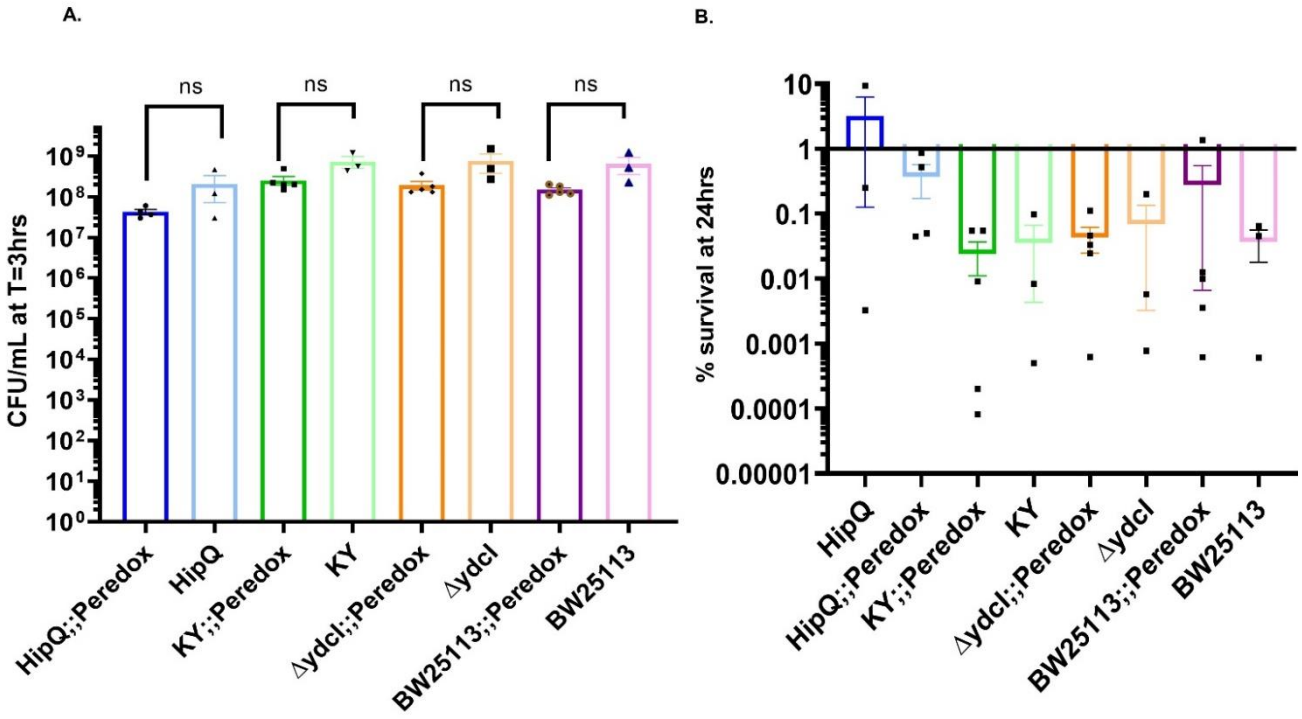

Figure 5.2 A. CFU/mL at time-kill assays starting point (3hrs post-inoculation) and B. ciprofloxacin persister frequency of untransformed and NADH biosensor (Peredox)-expressing E. coli (LB Miller). *n=5 for Peredox-expressing and n=3 for untransformed strains, from 3 independent experiments; error bars are SEM. p and q >0.05 by one-way ANOVA with Benjamini, Kreuger and Yekutieli false discovery control method. 0.4 µg/mL of ciprofloxacin was used in the time-kill assay*

Similarly to persistence, there was no statistically significant difference in the average of live cells (persisters and VBNCs) following 24hrs of ciprofloxacin exposure between biosensor-expressing and untransformed *E. coli* (Figure 5.3; see Figure 5.S4 for histograms), or between HipQ and Δ*ydcI* and their respective parental strains.

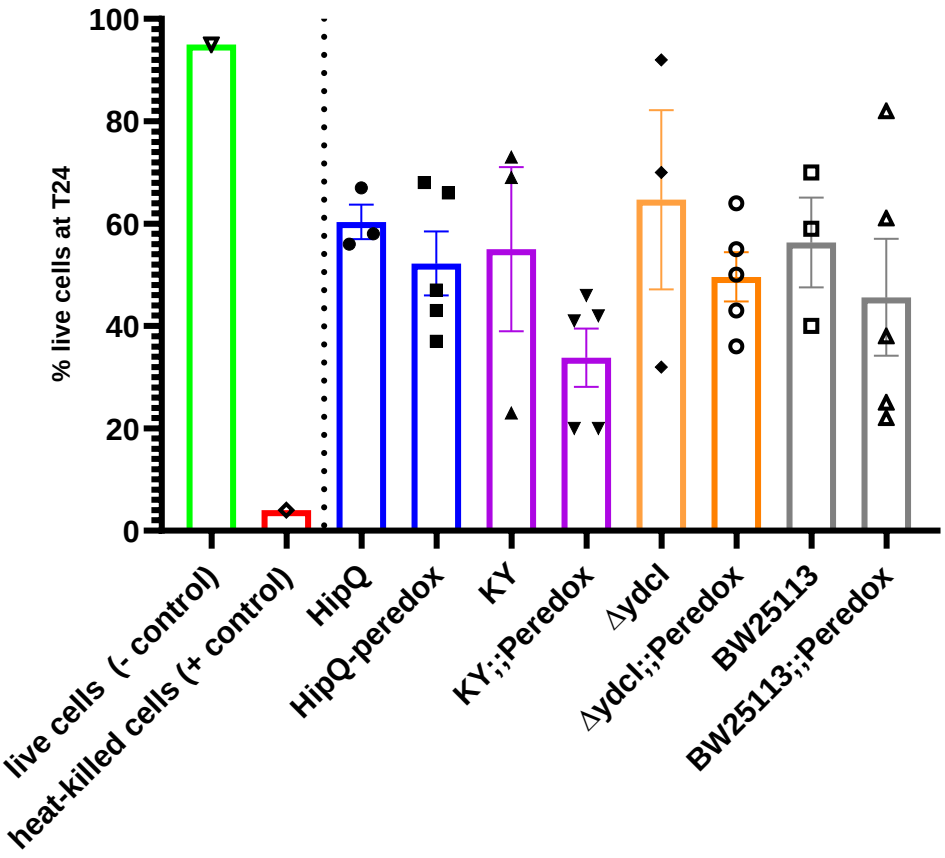

Figure 5.3. % surviving cells (persisters and VBNCs) following 24hr exposure to 25X MIC of ciprofloxacin (LB Miller). *Each point represents an average of 100 000 cells from a biological replicate (n); n=5 for biosensor expressing and n=3 for untransformed E. coli from three independent experiments; p>0.05 by one-way ANOVA with and Benjamini, Kreuger and Yekutieli false discovery control method.*

Interestingly, the frequency of persisters in a biological replicate did not significantly correlate with the frequency of VBNCs i.e., a higher % of live cells did not consistently equal to a higher number of persisters (Figure 5.4). This suggests that ciprofloxacin persister and VBNC formation is potentially influenced by different mechanisms, or in other words that likelihood of regrowth is independent of likelihood of antibiotic exposure survival. It is noted, as previously mentioned in chapter 4, that the live/dead discrimination method was based on cellular membrane integrity and therefore could have led to an overestimation of 'live' cells, given the fact that ciprofloxacin is a non-lytic antibiotic (LeBel 1988). However, it was subsequently demonstrated, that 'live' cells undergo respiration at higher rates than 'dead' cells (see section 5.3.4), suggesting that this subpopulation consists of metabolically active cells.

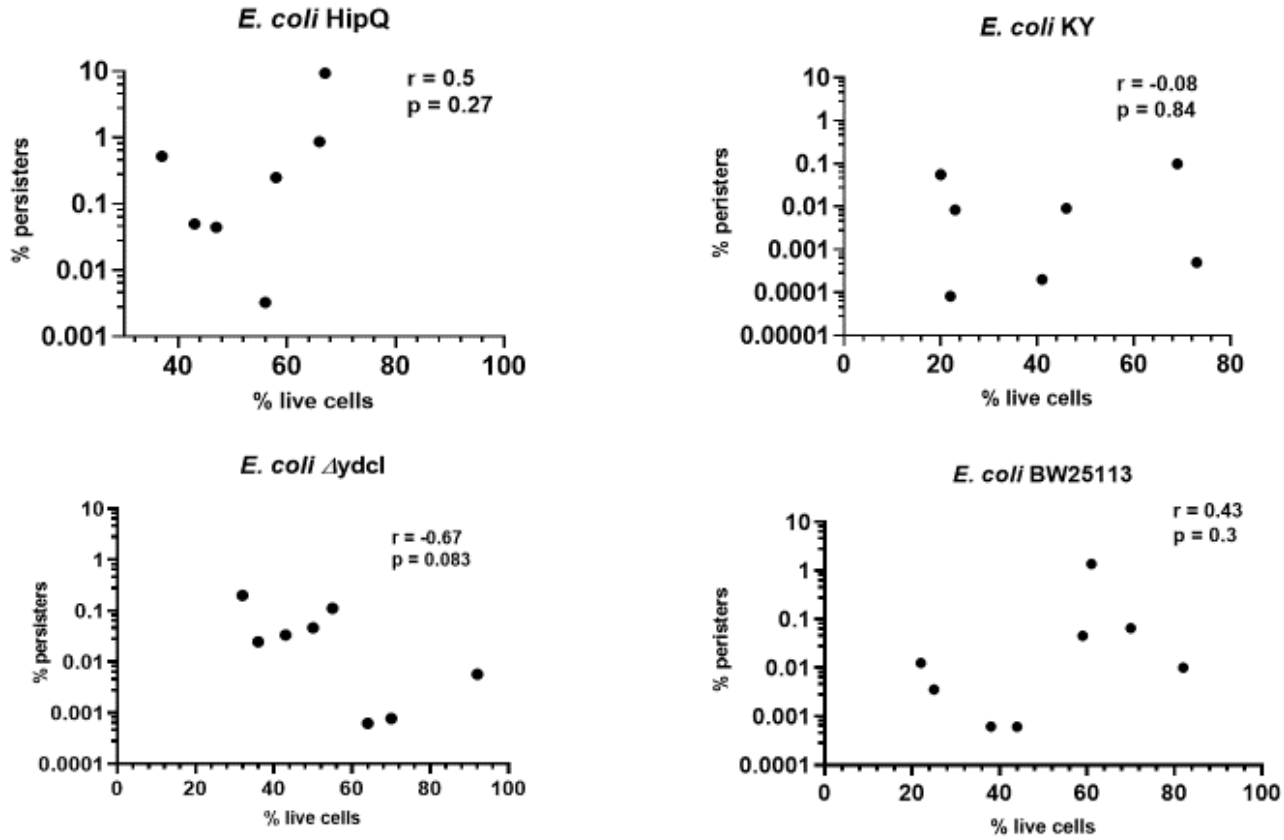

Figure 5.4. Spearman correlation (r) between % of live cells and % of persisters following 24hr exposure to 25xMIC ciprofloxacin*. n=8 from 3 independent experiments; % of persisters is relative to the starting population and % of live cells is relative to the number of intact cells at t=24hrs of antibiotic exposure.*

5.3.3. Intracellular biosensor stability

Upon antibiotic exposure, expression of the NADH biosensor components (T-Sapphire and mCherry proteins) was expected decrease significantly due to upregulation of stress response operons and damage to the cell transcription and translation machinery. Using the biosensor, relative intracellular NADH abundance is quantified by normalising T-Sapphire ([NADH]) fluorescence intensity to the fluorescence intensity of mCherry (plasmid copy number) since both aforementioned proteins constitute a single operon. Therefore, to compare NADH homeostasis at different growth states (prior/post antibiotic exposure), intracellular stability of both proteins needed to be confirmed.

In this assay, *E. coli* cultures were exposed to a bacteriostatic concentration of chloramphenicol, an antibiotic which non-specifically inhibits protein synthesis (Scholar 2007 and Figure 5.5a). Fluorescence intensity of T-sapphire and mCherry was then monitored over 24hrs, which was the period of antibiotic exposure during time-kill assays presented in this chapter. Following exposure to chloramphenicol, biosensor expression (i.e., increase in mCherry fluorescence intensity) continued for approximately 2hrs at a decreasing rate. Afterwards, mCherry fluorescence intensity remained stable up to 24hrs, confirming stability of this protein (Figure 5.5b, Spearman's r of time vs. fluorescence intensity = 0.27; $p = 0.065$). On the other hand in chloramphenicol-free, biosensor-expressing cultures, there was a strong correlation between time and fluorescence intensity (Spearman's $r = 0.99$; $p < 0.0001$). Interestingly, there was also strong correlation between time and fluorescence intensity in untransformed cultures for both fluorophores and therefore fluorescence intensity of biosensor-expressing samples was baseline-corrected for each timepoint to respective untransformed controls. This was likely an effect of accumulation of stress-related proteins in the cells, as previously reported (Surre *et al., 2018)*.

T-sapphire fluorescence intensity of biosensor-expressing cultures increased in the first 6hrs of the assay, regardless of chloramphenicol presence in the media, although as expected it was higher in uninhibited samples (Figure 5.5b). Afterwards it began to decrease, with fluorescence intensity of chloramphenicol-free cultures decreasing by app. 2-fold by t=24hrs. Since T-sapphire fluorescence intensity is relative to NADH concentration, this likely reflected a decrease in intracellular NADH abundance (i.e. respiration rate) as the cultures entered stationary phase. In chloramphenicol-inhibited cultures, however, the decrease in T-Sapphire fluorescence intensity was significantly greater, with T-Sapphire fluorescence intensity equalling autofluorescence from t=17hrs. However, in this assay it was impossible to determine if this was caused by T-Sapphire

degradation or a decrease in intracellular NADH/NAD+ abundance (cellular respiration) caused by bacteriostatic action of chloramphenicol. Moreover, there was a significant increase of autofluorescence in chloramphenicol-inhibited untransformed cultures (Figure 5.S5). It is known that stress, such as exposure to chloramphenicol, increases green autofluorescence in *E. coli* (Surre *et al.*, 2018), explaining this observation.

A.

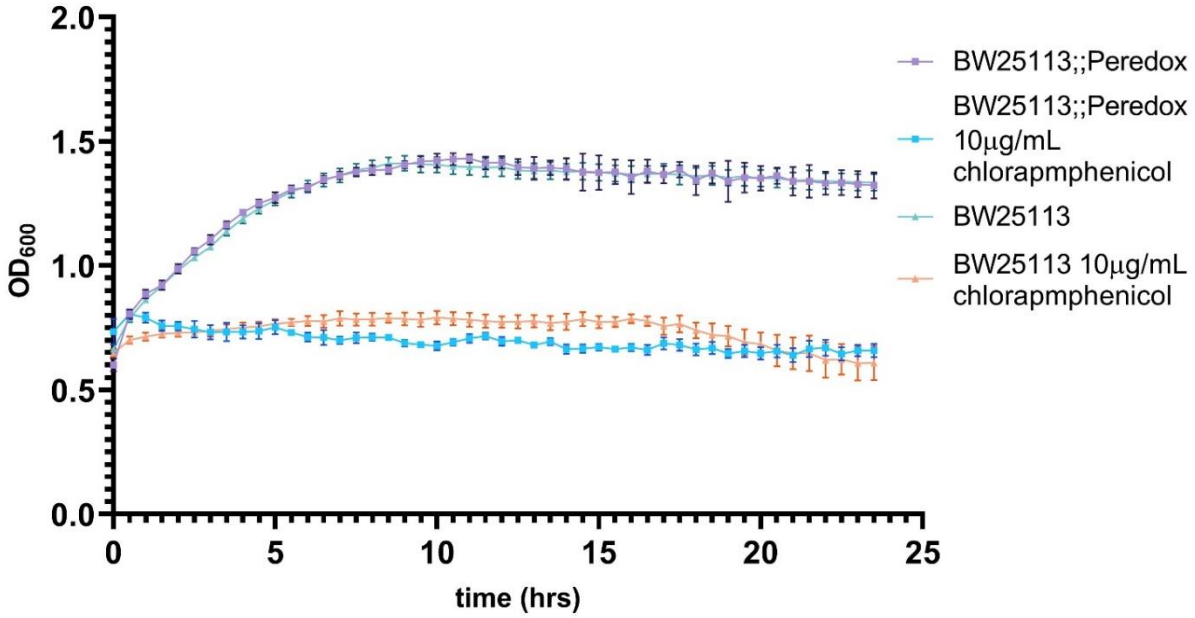

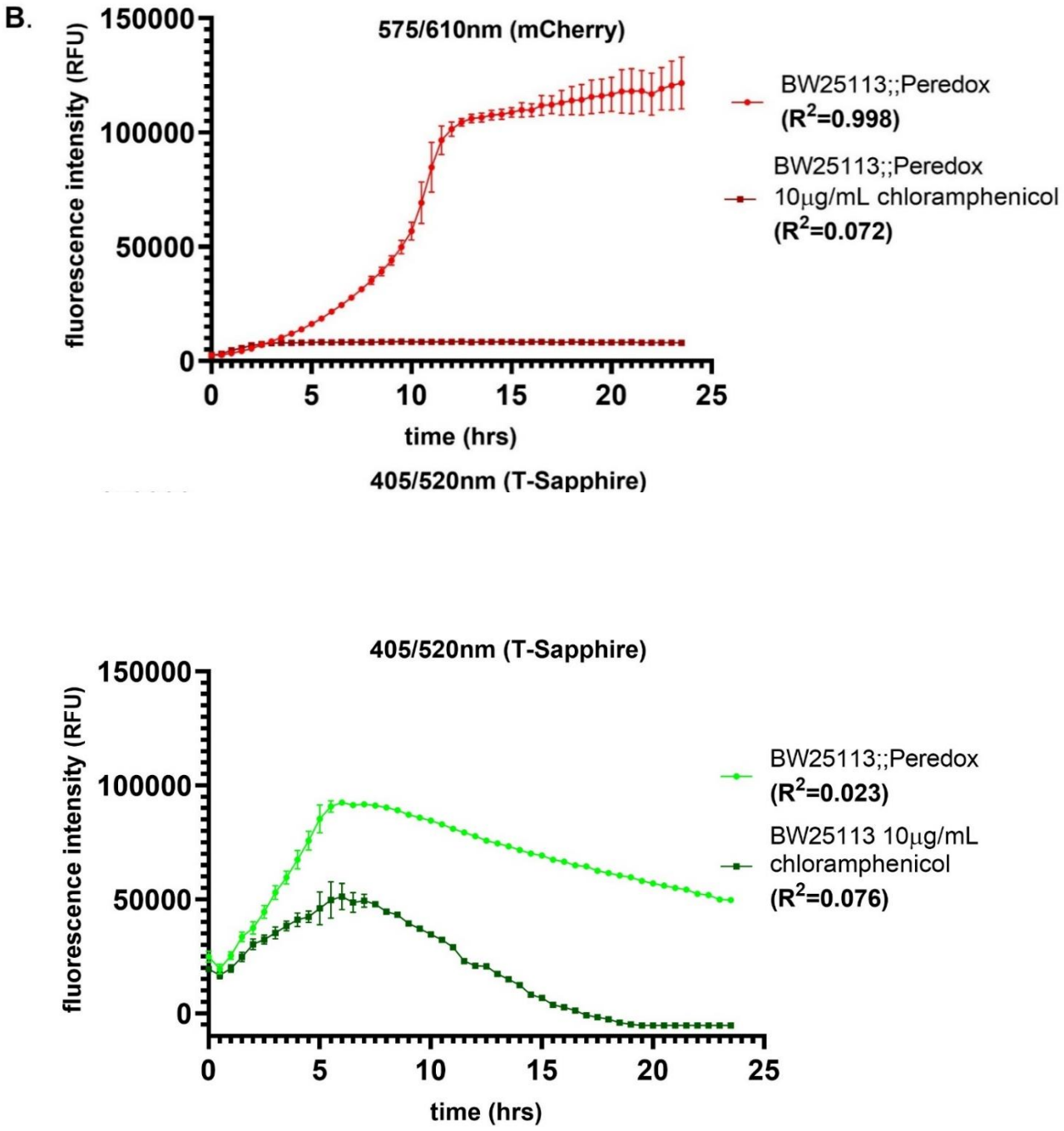

Figure 5.5. NADH biosensor intracellular stability. *A. Bacteriostatic action of 10 µg/mL chloramphenicol on E. coli BW25113, measured as total biomass (OD_{600}) change over time. B. mCherry and C. T-Sapphire protein stability following exposure to bacteriostatic concentration of chloramphenicol. Data points are an average of 6 technical replicates, error bars are SD; R is the Spearman correlation of time vs. fluorescence intensity.*

5.3.4. NADH/NAD+ homeostasis of ciprofloxacin persisters and viable but non culturable cells

In this assay exponentially growing cultures were exposed to 25XMIC of ciprofloxacin and [NADH:NAD+] and viability of individual cells was measured with a flow cytometer. As mentioned previously, ciprofloxacin is a non-lytic antibiotic and therefore it was reasoned that the majority of ciprofloxacin-exposed cells will retain their protein content (including the biosensor), regardless of their viability status.

5.3.4.1. Persisters and VBNCs are metabolically active following antibiotic exposure

First, the relative intracellular [NADH] was compared between 'live' and 'dead' subpopulations. As discussed in section 3b, the discriminating factor between live and dead cells was membrane integrity, and therefore there was a possibility of overestimating the 'live' subpopulation. However, it was hypothesised that live cells, whether persisters or VBNCs, would still undergo respiration and therefore should have higher NADH:NAD+ than dead cells. Since it was confirmed that there was no significant difference between autofluorescence of live and dead cells at t=24hrs (Figure 5.S6), these subpopulations were compared directly. When mCherry fluorescence intensity (plasmid copy number) was originally plotted against T-Sapphire fluorescence intensity, in 1 out of 3 independent experiments (n=2 replicates) there was a subpopulation of 'live' cells which expressed mCherry at low levels, lower than the majority of 'dead' cells, yet higher than autofluorescence at this wavelength (Figure 5.S7). Consequently, the T-Sapphire fluorescence intensity of this subpopulation ([NADH]) was comparable to autofluorescence of untransformed cultures. This subpopulation was not observed in the other two independent repeats of this assay (n=3). It is hypothesised that these cells could have been carrying a very low copy number of the NADH biosensor, since it has been previously demonstrated (section 5.3.3) that mCherry protein is stable up to 24hrs post expression inhibition. Alternatively, these cells could have been 'dormant' (not metabolically active) prior to ciprofloxacin exposure resulting in low levels of biosensor expression, however if that was the case, they were functionally indistinct from dead cells. Due to its unique characteristics, this subpopulation was analysed separately and is referred to below as the 'zombie subpopulation'. Interestingly, no 'zombie cells' were observed in *E. coli* HipQ (Figure 5.S7).

As can be seen in Figure 5.6 there is a statistically significant difference between average intracellular [NADH:NAD+] between live (excluding the zombie subpopulation) and dead cells following exposure to ciprofloxacin. This indicates that VBNCs and persisters are actively undergoing respiration resulting in NAD+ reduction during glycolysis and the Krebs cycle (Massudi *et al.*, 2012). The understanding of NAD(H) stability under physiological conditions is limited, however the biosensor reports NADH:NAD+ relative abundance which accounts for degradation of this co-factor following cell death. Moreover, these observations validate membrane integrity as a live/dead discrimination method for persisters and VBNCs.

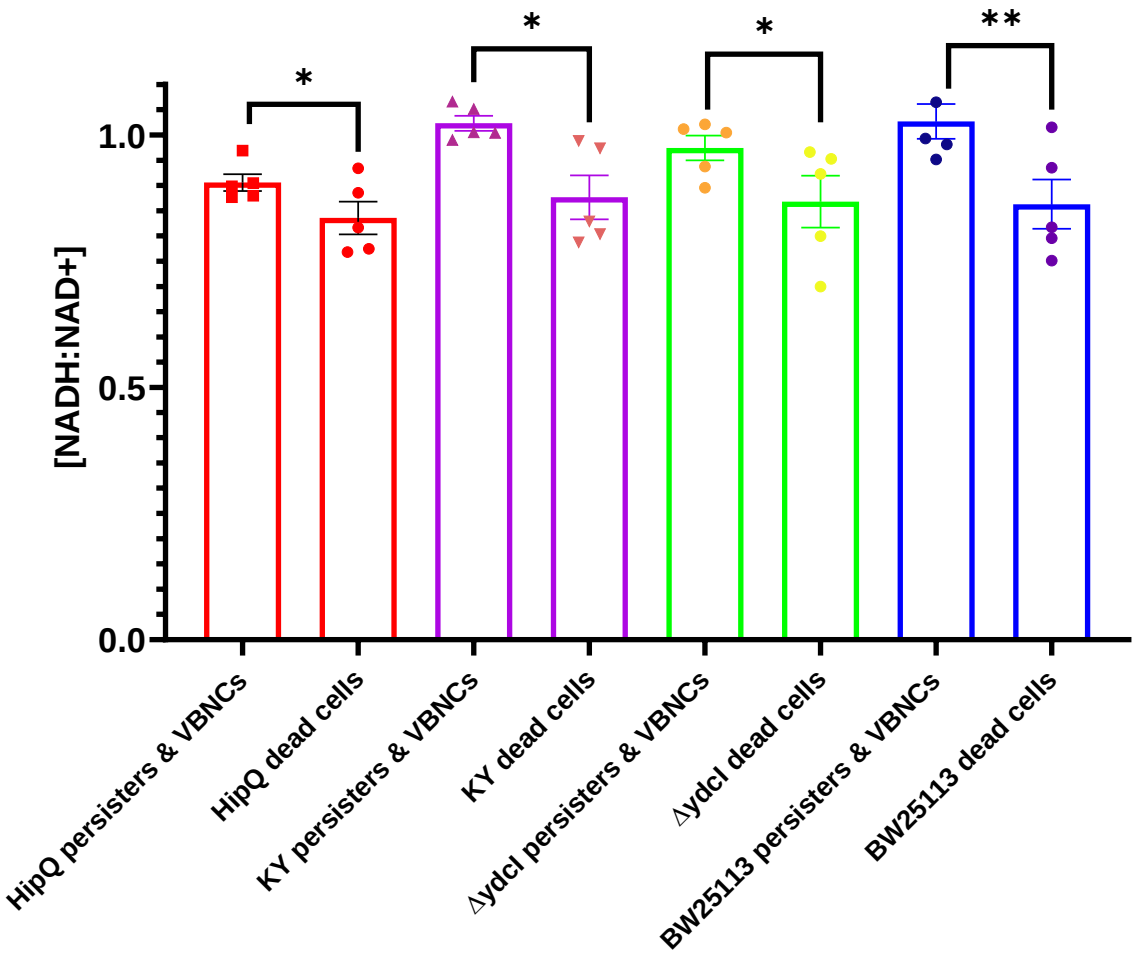

Figure 5.6. Relative intracellular [NADH:NAD+] of 'live' and 'dead' subpopulations following 24hr exposure to 25XMIC ciprofloxacin. *n=5, from 3 independent experiments, 100 000 events per sample (n); error bars are SEM. * = p<0.05, ** = p<0.01 and q <0.05 by RM ANOVA with Benjamini, Kreuger and Yekutieli false discovery control method.*

5.3.4.2. Persisters and VBNCs have a lower [NADH: NAD+] than the bulk population

Next, [NADH:NAD+] was compared between persisters and VBNCs (excluding the zombie subpopulation) and the bulk population prior to antibiotic exposure. As can be seen in Figure 5.7, there is a statistically significant difference in relative [NADH] between live cells at t=24hrs post antibiotic exposure and live cells prior to antibiotic addition, with antibiotic-exposed cells showing lower NADH/NAD+ ratio (respiration rates). The 405/520nm (T-Sapphire) autofluorescence of live cells at t=24hrs vs. t=0hrs was significantly higher, except for *E. coli* KY (Figure 5.S6). Despite the increased autofluorescence at this wavelength, T-Sapphire fluorescence intensity was significantly lower for biosensor-expressing Δ*ydcI* cultures post antibiotic exposure.

Moreover, *E. coli* HipQ persisters and VBNCs showed a significantly lower [NADH:NAD+] than persisters and VBNCs of its parental strain KY, despite no statistically significant difference at bulk population level prior to antibiotic exposure. This supports the hypothesis that perturbed NADH homeostasis contributes to the high-persistence of this strain. However, it is important to note that the ciprofloxacin-tolerant subpopulation was itself heterogenous on a single cell level (Figure 5.S8) with a subpopulation of antibiotic-tolerant cells having a higher NADH:NAD+ than the average for the bulk population prior to antibiotic exposure.

It is noted that in this assay the reported relative NADH/NAD+ abundance is representative in majority of the VBNC subpopulation, since VBNC frequencies were several orders of magnitude higher that the frequencies of persister cells (Figures 5.2 and 5.3).

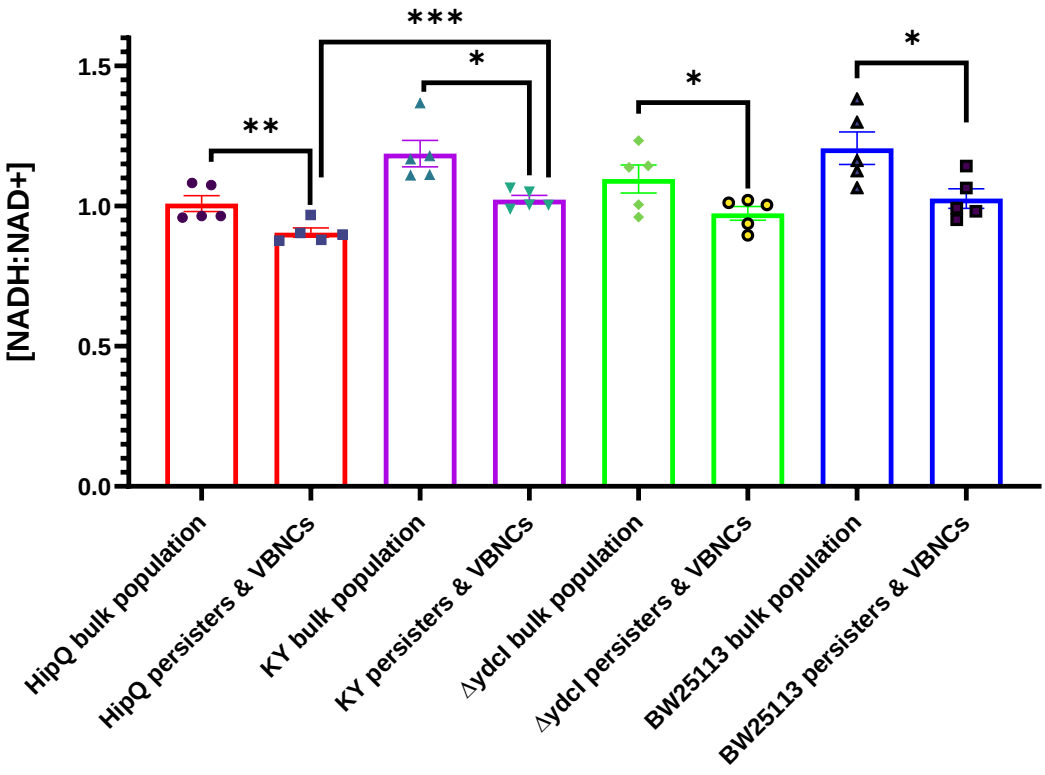

Figure 5.7. Relative Intracellular [NADH:NAD+] of live cells prior (bulk population) and following 24hr exposure to 25XMIC ciprofloxacin (persisters and VBNCs). *n=5, from 3 independent experiments, 100 000 events per sample (n); error bars are SEM. * = p<0.05, ** = p<0.01 and *** p<0.001 and q < 0.05 RM ANOVA with Benjamini, Kreuger and Yekutieli false discovery control method.*

5.4. Discussion

5.4.1. Summary of findings presented in this chapter

The scope of this chapter was to investigate the intracellular NADH homeostasis of *E. coli* ciprofloxacin-susceptible and ciprofloxacin-tolerant cells with the use of an [NADH:NAD+] biosensor, Peredox (Hung *et al.*, 2011). As explained in more detail in the introduction to this chapter, strains selected for this study differ in their ciprofloxacin persister cell frequencies and furthermore were expected to differ in their NADH homeostasis, as a result of mutations in genes encoding NADH co-factored enzymes. However, to the best of our knowledge the link between relative intracellular [NADH] and antibiotic persistence had not been previously investigated.

In this chapter we first validated the use of the NADH biosensor Peredox as a method for measuring intracellular [NADH] in persisters and VBNCs to non-lytic antibiotics. Since NAD+ reduction to NADH occurs during both glycolysis and the Krebs cycle (Masuddi *et al.*, 2012), its relative abundance was used as a proxy for measuring cellular respiration rates. We note that NAD(H) is a co-factor in numerous other metabolic reactions, however NAD+ to NADH reduction has previously been shown to correlate with cellular respiration (Pinzon et al, 2011; Ricciardi 2014; Braissant *et al.*, 2020).

Consequently, we determined that the ciprofloxacin-tolerant subpopulation is comprised of predominantly of VBNC cells, whose frequency was several orders of magnitude higher than persisters. Furthermore, we demonstrated that ciprofloxacin-tolerant cells are actively undergoing respiration, although at a significantly lower rate than the bulk population prior to antibiotic exposure. This supported our initial hypothesis that these cells ‘hunker down’ from antibiotic-induced damage by downregulating respiration and subsequently ROS production. Finally, we showed that the highly-persistent *E. coli* HipQ ciprofloxacin-tolerant cells have a significantly lower NADH:NAD+ than antibiotic-tolerant cells of its parental strain KY, suggesting that dysregulation of NADH homeostasis contributes to the high-persistence of this strain.

5.4.2. The vast majority of ciprofloxacin-tolerant cells are in the VBNC state

Previous research has demonstrated that ciprofloxacin exposure induces a high number of VBNC cells (up to 90% of the population) (Mason *et al.*, 1995; Zhang *et al.,* 2023) which is consistent with observations presented in this chapter. This is likely a consequence of mechanism of action of this antibiotic since ciprofloxacin inhibits DNA gyrase, impairing DNA replication and repair without causing cell lysis (LeBel, 1988). However, VBNC cells have also been observed in response to lytic antibiotics, such as ampicillin, although at a much lower frequency (Mohiuddin *et al.*, 2020b; Goode *et al.*, 2021a).

There has been an ongoing debate in the field whether the VBNC state is separate phenomenon to persistence, with some research groups reporting a distinct phenotypic state associated with VBNC cells (Goode *et al.*, 2021a), and others suggesting that VBNCs are simply 'aged' persisters (Kim *et al.*, 2018; Ayrapetyan, Williams, and Oliver 2018) . Regardless of classification, VBNCs are a clinically relevant subpopulation and pathogens such as enteropathogenic *E. coli, Vibrio cholerae* (Senoh *et al.* 2012) and *M. tuberculosis* (McCune *et al.* 1966) VBNC cells have been shown to be resuscitated in *in vivo* (or *in vivo* mimicking) conditions, which could contribute to infection. Therefore, better understanding of the VBNC state would aid in design of improved antibiotic treatment regimens, effective against heterogenous antibiotic-tolerant subpopulations.

It is important to note that the definition of 'viability' regarding the viable but non culturable state differs and can be based either on transcriptional/translational activity and membrane integrity (e.g. Goode *et al.*, 2021a) or on membrane integrity alone (e.g. Kim *et al.*, 2018; Ayrapetyan, Williams, and Oliver 2018; Zhang *et al.,* 2023) . However, recent findings suggest that membrane integrity is not a sufficient determinant of viability and that there are cell-like particles, filled with protein aggregates or lacking cytosolic contents altogether, which maintain intact membranes (Song and Wood, 2021). The authors suggest that these 'shells' could have been mistakenly classified as VBNCs in previous research. Therefore, in this chapter we based our live/dead cell discrimination on both membrane integrity and metabolic activity, demonstrating that ciprofloxacin VBNCs are not dead 'shells' as they actively undergo respiration. However, it is possible that the 'zombie' subpopulation we observed, which consisted of 'live' cells (i.e., cells with intact membranes) with a very low level of biosensor fluorescence were these cell-like particles described by Song and colleagues.

5.4.3. NADH homeostasis of persister cells

Next, we sought to investigate the redox environment of ciprofloxacin-tolerant cells. Previous research by Orman and colleagues has demonstrated that in exponentially growing *E. coli* cultures, ofloxacin persisters were more likely to have a lower reductase activity than the bulk population (Orman and Brynildsen, 2013a). We validated these results with a closely related quinolone, ciprofloxacin. We note that reductase activity measured by Orman *et al.* is not specific to [NAD(H)], as there are NAD(H) independent redox reactions occurring within cells, such as NADP(H) or ATP mediated reactions (Gowda, 2018). However, to the best of our knowledge the enzyme(s) involved in RSG dye redox reaction, used by the authors, are not specified. Here we demonstrated that tolerance to ciprofloxacin in *E. coli* is associated with a lower intracellular [NADH] and subsequently, lower cellular respiration (Pinzon et al., 2011). Respiration-inducing drugs have been previously reported to be active against ciprofloxacin persisters (Marques *et al.*, 2014), and our work suggests that those could also be effective against VBNCs. However, we also found that cells that survive prolonged antibiotic exposure consisted of two subpopulations: those whose NADH:NAD+ was lower than the bulk population prior to antibiotic exposure and a smaller subpopulation with a higher NADH:NAD+ than the bulk population. This is further evidence that the antibiotic-tolerant subpopulation is itself heterogenous and suggests a combination therapy approach might be necessary for its eradication, as described in more detail in chapter 2.

5.4.4. NADH homeostasis is affected in the highly-persistent *E. coli* HipQ but not *E. coli* Δ*ydcI*

It has been previously shown that *E. coli* HipQ generates 15-100 fold more ofloxacin persisters than its parental strain KY (Wolfson *et al.* 1990). This agrees with ciprofloxacin persister cell frequencies presented here, since ofloxacin is a closely related quinolone. To the best of our knowledge, persistence to fluoroquinolones of *E. coli* Δ*ydcI* had not been previously investigated, however in chapter 4 we demonstrated that this strain is not highly persistent to ofloxacin (section 4.3.2), similarly to ciprofloxacin observations from this chapter.

Subsequently, we showed that *E. coli* HipQ antibiotic-tolerant cells have a lower [NADH:NAD+] than those of its parental strain KY. This suggests that respiration occurs at a lower rate in these cells. *E. coli* HipQ has previously been shown to generate an increased number of stochastic persisters i.e., cells at the 'tail-end' of growth/division

rate distribution (Balaban *et al.*, 2004; Hingley-Wilson *et al.*, 2020). Our observations point towards a link between stochastic persistence and respiration rate, with cells at the 'tail-end' of respiration rate distribution being more likely to survive antibiotic exposure. This hypothesis is further supported by the observation that *E. coli* HipQ carries a mutation in *gap* (glyceraldehyde-3-phosphate dehydrogenase)-encoding gene (section 4.3.5), which is a component of the glycolysis pathway (Wang *et al.* 2020). Interestingly, we found no significant difference between intracellular NADH in *E. coli* Δ*ydcI* and BW25113 antibiotic-tolerant cells, suggesting that this transcription factor is not involved in regulation of NADH homeostasis. However, we note that the observations presented in this chapter were not able to distinguish between persisters and VBNCs and that the antibiotic-tolerant subpopulation was heterogenous. Therefore, we cannot conclude whether persisters survive antibiotic exposure through the same mechanisms as VBNC cells, as persisters could have constituted a distinct subpopulation of antibiotic-tolerant cells.

6. Antibiotic persistence in the clinical setting: Comparative analysis of uropathogenic *Escherichia coli* isolates

Aims

The aim of this chapter was to characterise a panel of uropathogenic *E. coli* (UPEC) collected from hospital patients from United Kingdom and Australia. Specifically, the correlation between multidrug resistance, antibiotic persistence to critically important antibiotics, as well as biofilm formation of these isolates was investigated.

Hypothesis

Substantial antibiotic consumption in both United Kingdom and Australia has resulted in high-levels of both multidrug resistance and antibiotic persistence amongst UPEC, including persistence to 'last-resort' antibiotics meropenem and colistin. Biofilm formation capability of UPEC isolates is largely dependent on attachment surface.

6.1. Introduction

6.1.1. Public health burden of urinary tract infections

Urinary tract infections (UTIs) are common, and are in majority caused by uropathogenic *E. coli* (UPEC) (80%), followed by *Klebsiella pneumoniae*, *Proteus mirabilis*, *Enterococcus faecalis* and *Staphylococcus saprophyticus* (Flores-Mireles *et al.* 2015). Comprehensive epidemiological data on global UTI incidence and prevalence is lacking, with public health organisations in different countries applying different diagnostic and/or reporting criteria. However, the Global Burden of Disease (GBD) report provides valuable insights into the global burden of UTIs. GBD is a tool used by policymakers to inform public health focus areas (IHME, 2020). Data from the 2019 report shows a high incidence of UTIs, with 404.61 million cases, as well as mortality, with 236790 deaths reported worldwide. Furthermore, the GBD data demonstrates a significant geographical variation in both incidence and AMR profile of urinary tract pathogens (Yang *et al.* 2022). For relevance and clarity, the focus of this chapter will be on epidemiological data from United Kingdom and Australia.

In the most recent report from the Australian Commission on Safety and Quality in Health Care (ACSQH), in 2017, 281 per 100,000 Australians were hospitalised with a UTI and/or kidney infection (pyelonephritis). Furthermore, there was a significant geographical and socioeconomic disproportion, with people living in remote areas and/or areas of high socioeconomic disadvantage, as well Indigenous Australians being twice as likely to be hospitalised (ACSQH, 2018). The general consensus is that almost all kidney infections are sequelae of untreated/improperly treated UTIs and are caused by bacteria migrating from the bladder to the kidneys, which subsequently makes them largely preventable (Fulop, 2012). To the best of authors knowledge, corresponding in-depth analysis of hospital admissions from the United Kingdom is not publicly available, however according to the GBD 3,721,623 infections (5,536 per 100 000 people) and approximately 7.5 thousand deaths were reported as UTI or pyelonephritis in 2019 (IHME, 2020). Furthermore, in 2013 UTI-related hospital admissions were the most common cause of emergency hospital ambulatory care admissions (16%) (Blunt, 2013). Taken altogether, this demonstrates the significant burden of UTIs and UTI sequelae on public health systems in both Australia and the UK.

6.1.2. Challenges to successful treatment: the role resistance, persistence, and biofilm formation

UTIs disproportionately affect women, caused by the shorter length of the female urethra, and the elderly where those are predominantly associated with catheter use (CAUTIs). It is estimated that in the United Kingdom one in two of women will be treated for a UTI in their lifetime, resulting in significant consumption of antibiotics (NIHCE, 2021). The risk of contracting a UTI also increases with age, with the yearly risk increasing from 3% to 10 for men aged 65-74 and over 85 respectively, and from 10% to 20% for women in the same age groups (Ahmed *et al.* 2018).

6.1.2.1. Antibiotic resistance

The majority of urinary tract infections require antibiotic treatment in order to relieve symptoms and decrease the risk of pyelonephritis (Jarvis, Chan and Gottlieb 2014). In the United Kingdom, the most commonly prescribed antibiotics are nitrofurantoin and trimethoprim-sulfamethoxazole (Bactrim), followed by amoxicillin-clavulanic acid (Augmentin), pivmecillinam, fosfomycin, cephalexin, and ciprofloxacin (NIHCE, 2018). In Australia, the first-line antibiotics are trimethoprim, cephalexin, and amoxicillin-clavulanic acid, followed nitrofurantoin and norfloxacin/ciprofloxacin. Worryingly, increasing rates

of antibiotic resistance are being reported. Based on the SURF (Susceptibility and Resistance to Fosfomycin and Other Antimicrobial Agents among Pathogens Causing Lower Urinary Tract Infections) report, in the UK approximately one in three of UPEC isolates is resistant to trimethoprim, one in four is resistant to amoxicillin-clavulanic acid, one in seven is resistant to ciprofloxacin and one in ten is resistant to either mecillinam or cephalexin (Tutone *et al.* 2022). Similarly, the 2021 Australian Report on Antimicrobial Use and Resistance in Human Health (AURA) reported one in five UPEC isolates to be resistant to trimethoprim, one in eight to be resistant to ciprofloxacin, and one in ten to be resistant to either cephalexin or amoxicillin-clavulanic acid (ACSQH, 2021). In contrast, resistance to fosfomycin (UK) and nitrofurantoin remained relatively low (<3%) (ASQH, 2021; Tutone *et al.* 2022). Collectively, this highlights the need for antimicrobial stewardship, as well as better implementation of non-antibiotic treatment and prevention methods, such as behavioural changes (e.g. improved hydration), probiotics *(*e.g. *Lactobacillus spp.)* or dietary supplements (e.g. ascorbic acid, cranberry extract) (Sihra *et al.* 2018).

6.1.2.2. Antibiotic persistence

It is estimated that 1 in 4 women who undergo successful antibiotic treatment will present with a recurring UTI (RUTI) within 6 months of initial diagnosis (Foxman 1990). Currently, the underlying cause of RUTIs (i.e., re-infection or presence of persister cells in the bladder) is poorly understood. Several studies reported that the majority of RUTIs are caused by recurring infection with the same UPEC strain (Foxman *et al.* 1995; Russo *et al.* 1995; Luo *et al.* 2012), pointing towards the latter. However, it is important to note that in the aforementioned studies strain identification was based on pulsed-field gel electrophoresis, rather than genome sequencing which limited their sensitivity in detecting small genomic differences. To the best of authors knowledge, application of next-generation sequencing to demonstrate whether RUTIs are caused by persistence (i.e., infection caused by bacterial cells isogenic to the original infection strain) or re-infection (i.e., infection caused by bacterial cells not isogenic to the original infection strain) has not yet been done.

6.1.2.3. Biofilm formation

Biofilm formation is common during UTIs. It can either occur on the surface of bladder cells (UPEC and *K. pneumoniae)* (Anderson *et al.* 2003; Rosen *et al.* 2007, 2008) or on the surface of urinary catheters (UPEC, *K. pneumoniae, P. mirabilis* and *P. aeruginosa*)

(Curtis Nickel, Downey and William Costerton 1989; Ohkawa *et al.* 1990; Jones *et al.* 2007). Although fluoroquinolones have been shown to decrease biofilm formation in UPEC (González *et al.* 2017) and *P. mirabilis* (Przekwas *et al.* 2022), complete inhibition was not observed at physiologically relevant concentrations. Eradication of an already matured biofilm is even more challenging, as it usually involves induction of biofilm dispersal which in turn can cause a spread of infection to new sites (Fleming and Rumbaugh 2018).

Biofilms create a favourable environment for persister cell formation through nutrient starvation and diauxie shifts. These conditions activate expression of the stringent response which results in extended lag phase and subsequently transient tolerance to antibiotics (Amato and Brynildsen; 2014; Mok *et al.*, 2018), as described in more detail in chapter 2 of this thesis. It has been shown that persister cells are the major factor contributing to biofilm antimicrobial tolerance, at least in *Klebsiella pneumoniae* (Anderl *et al.*, 2003) *Staphylococcus aureus* (Fux, Wilson and Stoodley 2004), and *P. aeruginosa* (Nguyen *et al.* 2011). Moreover, it has been suggested that the biofilm extracellular matrix (EPS) acts as a barrier between biofilm persisters and the host's immune system, making it impossible for the host to clear these remaining cells following antibiotic treatment, resulting in recurring infections (Lewis 2005). Therefore, eradication of biofilm persisters, without the need for biofilm dispersion, or biofilm formation inhibition could be investigated as an alternative approach for treatment of RUTIs.

6.2. Methods

Please refer to Chapter 3 for the description of general methods. Please refer to Methods Appendix for buffer and media composition.

6.2.1. Strain collection

Uropathogenic *E. coli* (UPEC) were a kind gift from Prof. Roberto la Ragione (UK1 – UK5) and Prof. Kylie Mansfield (AU1-AU3). These strains were originally isolated by culture from mid-stream urine samples of hospital patients suffering from an acute urinary tract infection.

6.2.2. Antibiotic susceptibility screening

6.2.2.1. Minimum inhibitory concentration assay on UK isolates

Bacterial stocks (25% glycerol in Mueller Hinton (MH) broth) were kept at -80^{o}C, streaked on MH *(Sigma Aldrich)* agar plates and incubated for 16-24 hrs at 37^{o}C. Sensitire EU Surveillance *Salmonella*/*E. coli* EUVSEC plates were purchased from ThermoFisher Scientific (Figure 6.1). Starter cultures were prepared by mixing bacterial colonies in deionized H_20 to the density of 0.5 McFarland standard. Those were subsequently diluted 1:100 into MH broth to a final concentration of 10^6 CFU/mL, according to manufactures instructions (*ThermoFisher Scientific*). 50 µL/well of the cell suspension was then added to the antibiotic plate. Plates were sealed and incubated at 37^{o}C for 18hrs. The MIC value was determined as the lowest concentration of the antibiotic which inhibited bacterial growth i.e., did not result in turbidity following incubation. Resistance cut-off values were obtained from the European Committee on Antibiotic Susceptibility (EUCAST) version 9 MIC breakpoint table (EUCAST 2019).

	1	2	3	4	5	6	7	8	9	10	11	12
A	**SMX** 1024	**TMP** 32	**CIP** 8	**TET** 64	**MERO** 16	**AZI** 64	**NAL** 128	**CHL 128**	**TGC** 8	**COL** 16	**AMP** 64	**GEN** 32
B	**SMX** 512	**TMP** 16	**CIP** 4	**TET** 32	**MERO** 8	**AZI** 32	**NAL** 64	**CHL 64**	**TGC** 4	**COL** 16	**AMP** 32	**GEN** 16
C	**SMX** 256	**TMP** 8	**CIP** 2	**TET** 16	**MERO** 4	**AZI** 16	**NAL** 32	**CHL 32**	**TGC** 2	**COL** 16	**AMP** 16	**GEN** 8
D	**SMX** 128	**TMP** 4	**CIP** 1	**TET** 8	**MERO** 2	**AZI** 8	**NAL** 16	**CHL 16**	**TGC** 1	**COL** 16	**AMP** 8	**GEN** 4
E	**SMX** 64	**TMP** 2	**CIP** 0.5	**TET** 4	**MERO** 1	**AZI** 4	**NAL** 8	**CHL 8**	**TGC** 0.5	**COL** 16	**AMP** 4	**GEN** 2
F	**SMX** 32	**TMP** 1	**CIP** 0.25	**TET** 2	**MERO** 0.5	**AZI** 2	**NAL** 4	**FOT 1**	**TGC** 0.25	**TAZ** 2	**AMP** 2	**GEN** 1
G	**SMX** 16	**TMP** 0.5	**CIP** 0.125	**CIP** 0.03	**MERO** 0.25	**MERO** 1	**FOT** 4	**FOT 0.5**	**TAZ** 8	**TAZ** 1	**AMP** 1	**GEN** 0.5
H	**SMX** 8	**TMP** 0.25	**CIP** 0.0625	**CIP** 0.015	**MERO** 0.125	**MERO** 0.03	**FOT** 2	**FOT 0.025**	**TAZ** 4	**TAZ** 0.5	**POS** X	**POS** X

Figure 6.1 EUVSEC* MIC *plate layout. *Antibiotic concentrations are in µg/mL. SMX – sulfametoxazole, TMP – trimethoprim, CIP – ciprofloxacin, TET – tetracycline, MERO – meropenem, AZI – azithromycin, NAL – nalidixic acid, FOT – cefotaxime, CHL – chloramphenicol, TGC – tigecycline, TAZ – ceftazidime, COL – colistin, AMP – ampicillin, GEN – genatmicin, POS – positive control (no antibiotic). Adapted from Sensitire Plate Guide (ThermoFisher Scientific).*

6.2.2.2. Antibiotic susceptibility of Australian isolates

Antibiotic susceptibility profiles of Australian UPEC isolates were obtained from Ogenovska and colleagues (Ognenovska *et al.* 2022), with the exception of meropenem and colistin where MIC assay was performed as described in section 3.3. As above, the MIC value was determined as the lowest concentration of the antibiotic which inhibited bacterial growth i.e., did not result in turbidity following incubation, and resistance cut-off values were determined from the EUCAST v.9 MIC breakpoint table (EUCAST 2019).

6.2.3. Time-kill assays

Time kill assays were done as described in section 3.2. 25X MIC of meropenem (0.75 µg/mL) and 25X MIC of colistin (25 µg/mL) was used. Colistin and meropenem MICs were determined experimentally as described above. Cultures were grown in either LB Miller broth or M9-GLUCOSE broth adjusted to pH 6 with HCl, 1mL in 5mL culture tubes, with shaking at 200rpm. At T=24hrs suspected colistin resistant isolates were plated on 25X MIC colistin LB Miller agar plates at specified pH (6, 7 or 8).

6.2.4. Biofilm biomass quantification (crystal violet assay)

6.2.4.1.Biofilm formation on polystyrene

Bacterial stocks (25% glycerol in LB Miller) were kept at -80^{o}C, streaked on fresh LB Miller plates *(Sigma Aldrich)* and incubated for 16-24 hrs at 37^{o}C. Afterwards, single colonies were inoculated in 1mL of LB Miller broth with or without 0.5% v/v glucose *(Sigma Aldrich)* and incubated at 37^{o}C overnight (~18hrs), with shaking at 200rpm. Next, overnight cultures were diluted 1:50 with fresh media or synthetic urine (MP-AU) (Sarigul, Korkmaz and Kurultak 2019) into a 96-well, flat-bottom, lidded, tissue-culture treated plate (100 µL/well). The plates were sealed and incubated statically or with shaking at 50rpm at 37^{o}C for 24-48hrs. For 48hr incubations, media change was performed at 24hrs, which involved replacing half of the spent media with fresh media, as it was found to produce robust biofilms (Vyas *et al.,* 2021). Biofilm staining protocol was adapted from George O'Toole (O'Toole 2011). First, planktonic cells were removed from wells. Next, wells were rinsed with sterile MQ H_20 three times. 125 µL of 0.1% crystal violet in 0.2% ethanol solution was added to each well. Plates were incubated for 15 minutes at room temperature and crystal violet was removed from the wells. Afterwards wells were rinsed with sterile MQ H_20 three times, tapped on a paper towel to remove

remaining liquid and dried upside-down for ~15 minutes. Stained biofilm was solubilised with either 30% acetic acid or 1% SDS for 10 minutes at room temperature. Biofilm biomass was quantified by reading absorbance at 550nm on a plate reader (Clariostar, *BMG Labtech*), in precise mode. Prior to reading the plate was shaken at 300rpm for 10 seconds (double orbital mode). A strain was classified as non biofilm-producing if OD_{550} sample ≤ OD_{550} negative control, low biofilm producing if OD_{550} negative control < OD_{550} sample ≤ 2 × OD_{550} negative control , moderate biofilm producing if 2 × OD_{550} negative control < OD_{550} sample ≤ 4 × OD_{550} negative control and strong biofilm producing if 4 x OD_{550} negative control < OD_{550} sample. (Lajhar, Brownlie and Barlow 2018). Uninoculated (culture medium only) wells stained following the same protocol were used as the negative controls, and to correct biofilm biomass values for background staining.

6.2.4.2. Biofilm formation on fixed cell monolayer

Madin-Darby canine kidney (MDCK) cells were routinely cultured in Roswell Park Memorial Institute (RPMI) 1640 complete medium, at 37°C, with 5% CO_2 and split 1:5 every 4 days. Cell monolayers were prepared following the method adapted from Vyas *et al.* (Vyas, McArthur and Sanderson-Smith 2021). Cells were grown in a T75 flask *(ThermoFisher Scientific)* to ~100% confluency and seeded into four 96-well tissue-culture treated plates, 100 µL/well (seeding density ~ 1^10^4 cells/well). Plates were then returned to the incubator and left for 24hrs, resulting in a final well confluency of 95%-100%. Afterwards, culture media was removed, the plates were washed once with PBS and fixed with 4% paraformaldehyde (PFA) for 20 minutes (50 µL/well). Next, PFA was removed, and the plates were washed twice with PBS. Intact structure of the monolayer was confirmed by optical microscopy and fixed monolayers were stored in PBS (100 µL/well), at 4°C for up to 14 days. Prior to use, the plates were washed once with PBS.

Overnight bacterial cultures were prepared as described in above section. Next, overnight cultures were diluted 1:50 with LB-Miller supplemented with 0.5% v/v glucose (LB-Glu) or MP-AU and transferred into the fixed cell monolayer plates (100 µl/well). Plates were sealed and incubated at 37°C for 48hrs, with 50rpm shaking and a media change was performed at 24hrs, as described in above section. Biofilm was stained and quantified as described in above section. Uninoculated (MDCK monolayer and culture medium) wells stained following the same protocol were used as the negative controls, and to correct biofilm biomass values for background staining.

6.3. Results

6.3.1. Multidrug resistance is common in UPEC

UPEC strains investigated in this study were isolated from urine samples of hospital patients suffering from acute urinary tract infection in United Kingdom (UK1-UK5) and New South Wales, Australia (AU1-AU3). Their susceptibility to a panel of commonly prescribed antibiotics (table 6.1) was provided by Dr Maria Getino and Dr Marwa Hassan at the University of Surrey (UK isolates) and Ognenovska and colleagues (Ognenovska *et al.* 2022) (Australian isolates), with the exception of meropenem and colistin susceptibility.

As can be seen in table 6.1, multidrug resistance was common feature of UPEC, with 5/8 isolates (highlighted in yellow) classified as multidrug resistant, i.e., resistant to at least one antibiotic from three or more antibiotic classes (Magiorakos *et al.* 2012). Furthermore, two isolates (UK1 and UK4) were found to be resistant to 9/13 antibiotics from the susceptibility panel, including third generation cephalosporins cefotaxime and ceftazidime. As expected, the highest levels of resistance were observed to trimethoprim and sulfamethoxazole/sulfafurazole (7/8 isolates), and ciprofloxacin/norfloxacin (5/8 isolates) as these antibiotics are commonly used in the treatment of UTI in both United Kingdom and Australia. Interestingly, all Australian isolates were susceptible to nitrofurantoin, which is also used to treat UPEC infections, although less frequently in Australia than in the UK (Jarvis, Chan and Gottlieb 2014; NIHCE, 2018). Finally, all screened isolates were susceptible to 'last-resort' antibiotics: carbapenems (meropenem/imipenem) and polymyxins (colistin). However, it is important to note that the standard MIC assays do not detect the presence of persister cells, as a positive result is determined by growth in the presence of an antibiotic, rather than survival of antibiotic exposure (Balaban *et al.*, 2019).

Table 6.1 Antibiotic susceptibility of UPEC isolates investigated in this thesis. *Orange signifies resistance, blue signifies susceptibility and grey signifies that given antibiotic was not part of the panel. Highlighted in yellow are multidrug resistant isolates. Antibiotics with the same resistance mechanism were grouped. Resistance breakpoints are based on EUCAST v. 9 MIC breakpoint table (EUCAST 2019).*

	UK1	UK2	UK3	UK4	UK5	AU1	AU2	AU3
Amikacin								
Amoxicillin/Ampicillin								
Amoxicillin and Clavulanic acid								
Cefepime/Ceftriaxone								
Cefotaxime								
Ceftazidime								
Cephalexin								
Chloramphenicol								
Ciprofloxacin/Norfloxacin								
Colistin								
Gentamycin								
Meropenem/Imipenem								
Nalidixic Acid								
Nitrofurantoin								
Sulfamethoxazole/Sulfafurazole								
Tetracycline								
Tigecycline								
Trimethoprim								

6.3.2. Efficacy of colistin and meropenem against persister cells is dependent on environmental conditions

In this chapter, two 'last-resort antibiotics', meropenem and colistin, were selected for evaluation of their anti-persister efficacy. For comparison, time-kill assays were done in standard rich media (LB Miller broth, pH 7.5), as well as minimal media (M9-GLUCOSE broth) adjusted to the average pH of human urine (pH 6) (Worcester *et al.* 2018). It is noted that M9-GLUCOSE still contains glucose as the carbon source, which is not present in healthy human urine. However, the growth rate of UPEC in this medium was significantly lower (Figure 6.S1) than in LB Miller, which is more representative of a nutrient-limited environment of a UTI.

6.3.2.1. In field-standard in vitro incubation conditions colistin is significantly more effective against persister cells than meropenem

Time-kill assays in this medium followed the expected bi-phasic killing dynamics, except UK1 and *E. coli* ATCC25922 (control strain) where the kill curve shape following exposure meropenem was more characteristic of a tolerant population (Figures 6.S2 and 2.1). However, as can be seen in Figure 6.2, colistin was significantly more effective in eradicating the persister subpopulation than meropenem. This is likely due to its mechanism of action, as colistin is a membrane pore-forming peptide whose antimicrobial activity is independent of cell growth state, in contrast to cell wall synthesis inhibitor meropenem (Meletis 2016; Andrade *et al.* 2020). Interestingly, there was no significant difference in persister cell abundance to a given antibiotic in between strains, despite the differences in their antibiotic resistance profiles. This suggests that multidrug resistance does not correlate with increased antibiotic persistence.

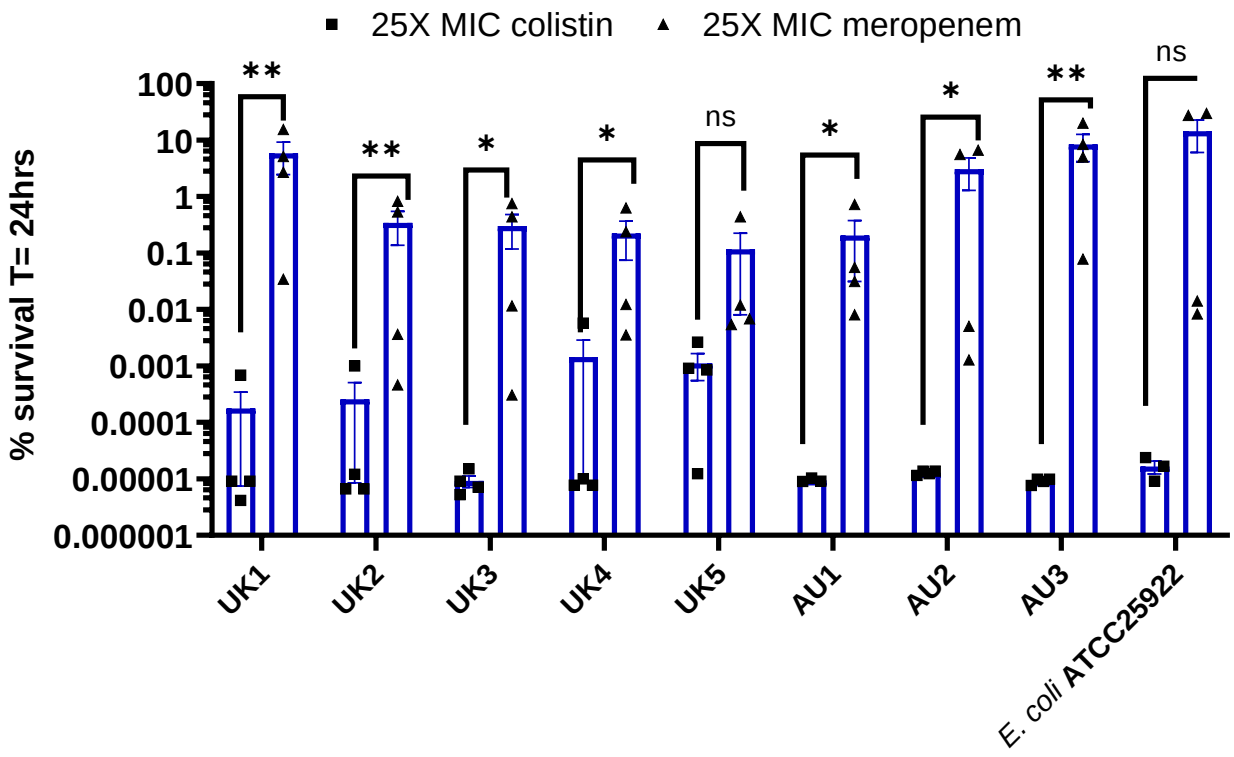

Figure 6.2. Frequency of antibiotic persister cells following 24hr exposure to 25x MIC colistin and 25x MIC meropenem in LB Miller broth (pH=7.5); *n=4 from two independent experiments, error bars are SEM; limit of detection was 100 CFU/mL; * = p< 0.05, ** =p< 0.01, and q < 0.05 by one way ANOVA with Benjamini, Kreuger and Yekutieli false discovery control method.*

6.3.2.2. Colistin resistance and high-persistence to meropenem is induced in UTI-mimicking conditions

Similarly to LB Miller, meropenem time-kill assays in M9-GLUCOSE broth followed the classical bi-phasic killing dynamics, except for UK1 and *E. coli* ATCC25922 (control strain) where the kill curve shape resembled a tolerant population (Figure 6.S3 and Figure 2.1). Frequency of meropenem persister cells was higher in M9-GLUCOSE broth than in LB Miller broth, however this difference was statistically significant for only one of the UPEC isolates (UK1) (Figure 6.3a). The observed increased persistence was likely a consequence of a slower growth rate in this medium (Figure 6.S1), resulting in reduced susceptibility to meropenem.

Interestingly, although colistin was effective in eradicating the vast majority of the persister subpopulation in LB Miller, in M9-GLUCOSE broth (pH 6) resistance, i.e. regrowth in the presence of the antibiotic, was observed following 5hrs of exposure (Figure 6.3b and Figure 6.S3). However, when the suspected resistant replicates were plated on 25X MIC colistin agar plates, colonies formed only on plates where the agar pH was adjusted to acidic (Figure 6.3b). Colistin is a positively charged peptide which exerts its antimicrobial activity by binding to negatively charged lipopolysaccharides on the cell membrane (LPS) (Andrade *et al.* 2020). It is hypothesized that in the presence of a high concentration of H+ ions (i.e., at low pH) the peptide is not able to bind to LPS, resulting in transient resistance to colistin, rather than a genetic adaptation as initially suspected.

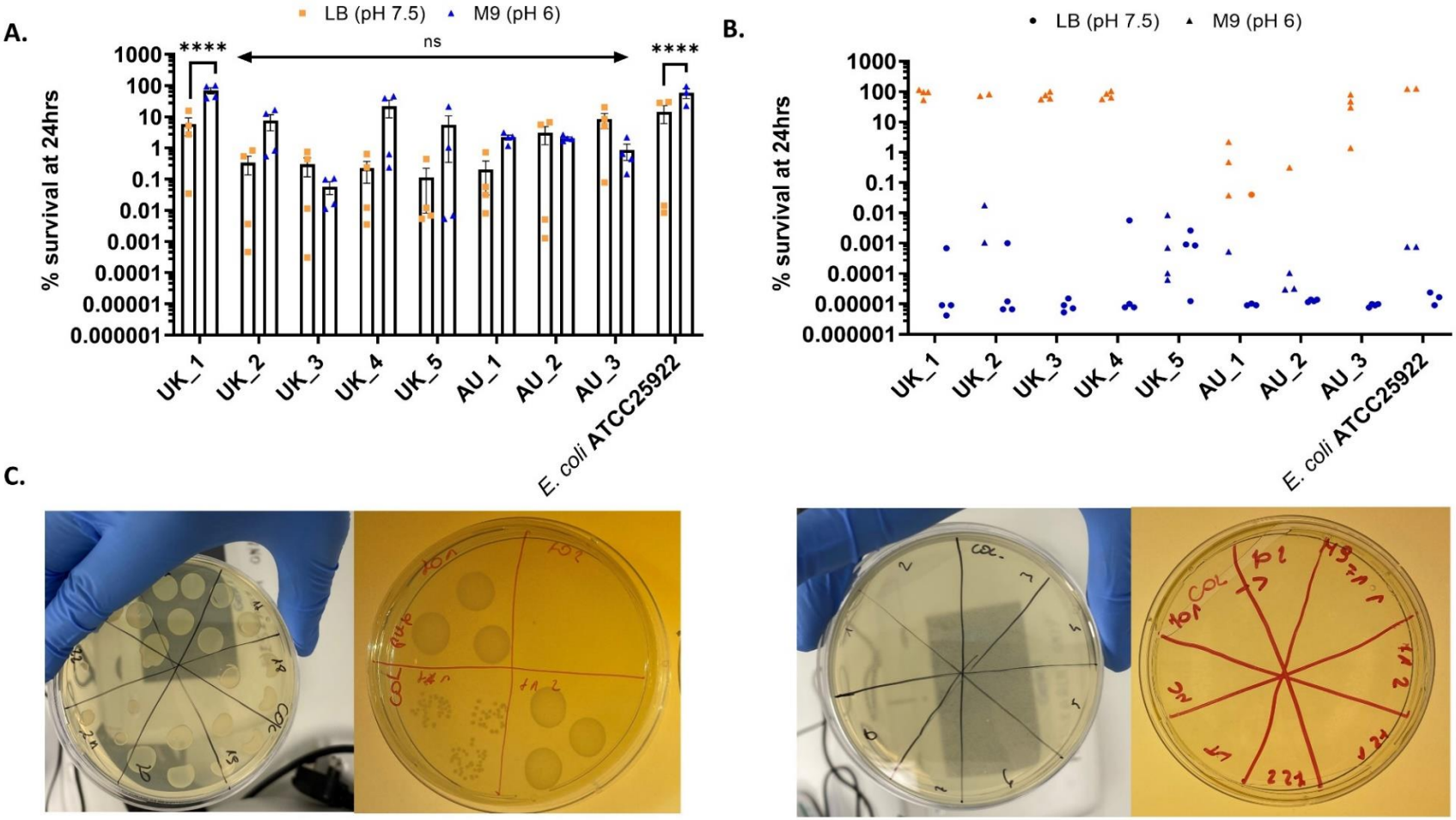

Figure 6.3 A. % survival following 24hr exposure to 25x MIC meropenem in LB Miller broth (pH 7.5) and M9-GLUCOSE broth (pH 6). *N=4 from two independent experiments, error bars are SEM; *** = p and q < 0.0001 by two way ANOVA (antibiotic vs. strain) with Benjamini, Kreuger and Yekutieli false discovery control method.* ***B. % survival following 24hr exposure to 25x MIC colistin in LB Miller broth (pH 7.5) and M9-GLUCOSE broth (pH 6).*** *N=4 from two independent experiments; blue – susceptible and orange – resistant.* ***C. Growth of suspected resistant replicates on 25X MIC colistin agar plates at pH < 7 (left) and pH > 7.5 (right).***

6.3.3. UPEC biofilm formation is surface dependent

6.3.3.1. Biofilm formation on polystyrene

Capability of UPEC strains to form a biofilm was first evaluated following the 'gold-standard' method, in 96-well polystyrene plates (O'Toole 2011). As can be seen in Figure 6.4, there was no significant difference in the amount of biofilm biomass between incubation in rich media (LB Miller, pH 7.5) or minimal media adjusted to urine pH (M9-GLUCOSE, pH6) except in *P. aeruginosa* positive control, where it was significantly increased in the latter. All investigated UPEC isolates were classified as weak biofilm formers in LB Miller, with the exception of UK4 which was classified as non biofilm-forming. UK3 and UK4 were classified as weak-biofilm forming in M9-GLUCOSE whilst the rest of the isolates did not form a biofilm in this medium. It is important to note that biofilm formation is dependent on incubation conditions. When the isolates were incubated in expected biofilm-inducing environment: LB Miller supplemented with 0.5% v/v glucose (Lade *et al.* 2019) or synthetic urine, and incubation time increased to 48hrs (Figure 6.S4), the biofilm biomass increased. However, this increase was not statistically significant, and all isolates were classified as weak biofilm formers in either medium.

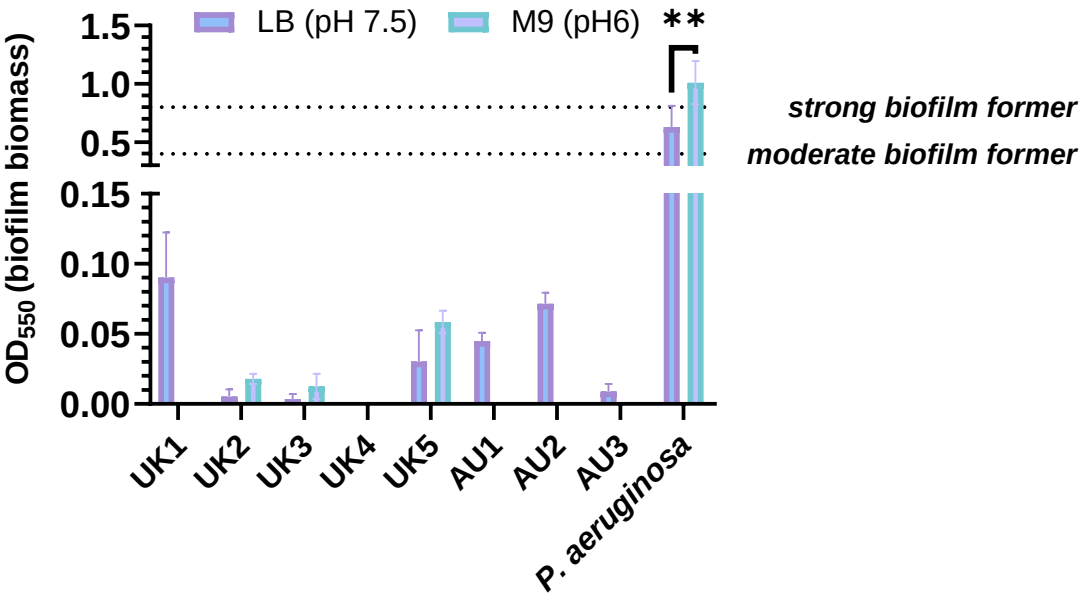

Figure 6.4. UPEC biofilm formation on polystyrene *in LB Miller broth (pH 7.5) and M9-GLUCOSE broth (pH6), following 24hr incubation. N=2, error bars are SEM. Absorbance values were baseline-corrected for absorbance of negative control (uninoculated wells). Weak biofilm former: OD_{550} < OD_{550} negative control, moderate biofilm former: 0 < OD_{550} < 2 x OD_{550} negative control, strong biofilm former: OD_{550} > 4 x OD_{550} negative control* (Lajhar, Brownlie and Barlow 2018)*. ** = p and q < 0.01 by two-way ANOVA (medium vs. strain) with with Benjamini, Kreuger and Yekutieli false discovery control method.*

6.3.3.2. Biofilm formation on kidney tubule epithelial cell monolayer

Next, ability of Australian UPEC isolates to form a biofilm on the surface of PFA-fixed Madin-Darby Canine Kidney (MDCK) cells was investigated. As can be seen on Figure 6.5a, biofilm biomass of biofilms grown on a cell monolayer was approximately double that of biofilms formed on polystyrene, however this difference was not statistically significant. Nevertheless, AU1 isolate would be classified as a strong biofilm former and AU2 would be classified as moderate biofilm former based on MDCK cell monolayer biofilm formation, in contrast to polystyrene where both isolates were classified as weak biofilm formers. Classification of AU3 remained as weak biofilm former regardless of surface. Interestingly, *P. aeruginosa* positive control was able to break down the MDCK cell monolayer resulting in biofilm formation on the side of the wells, in contrast to UPEC biofilms which formed on the surface of the monolayer (Figures 6.5b and 6.5c)

A.

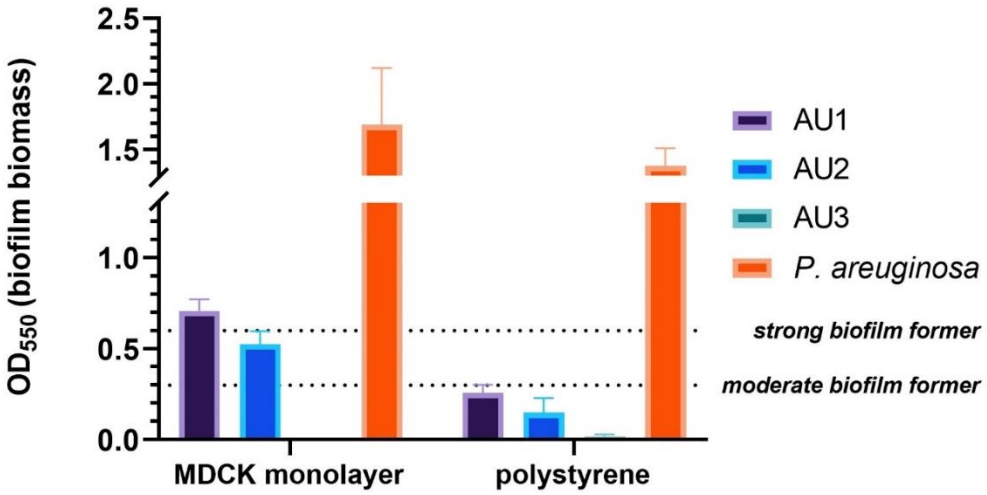

B.

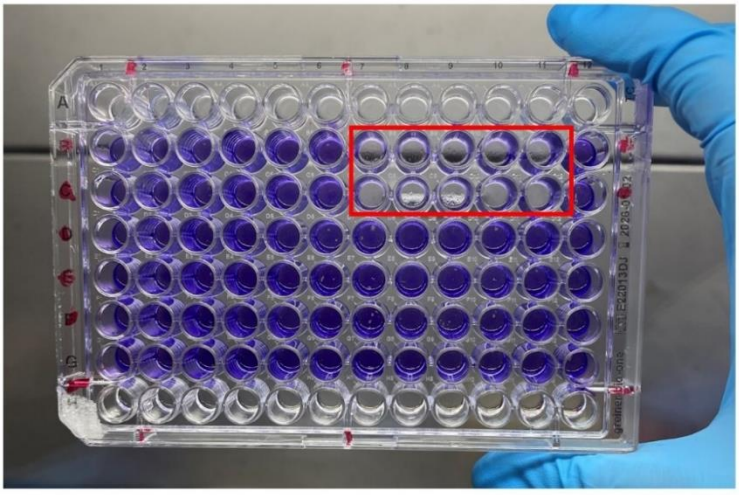

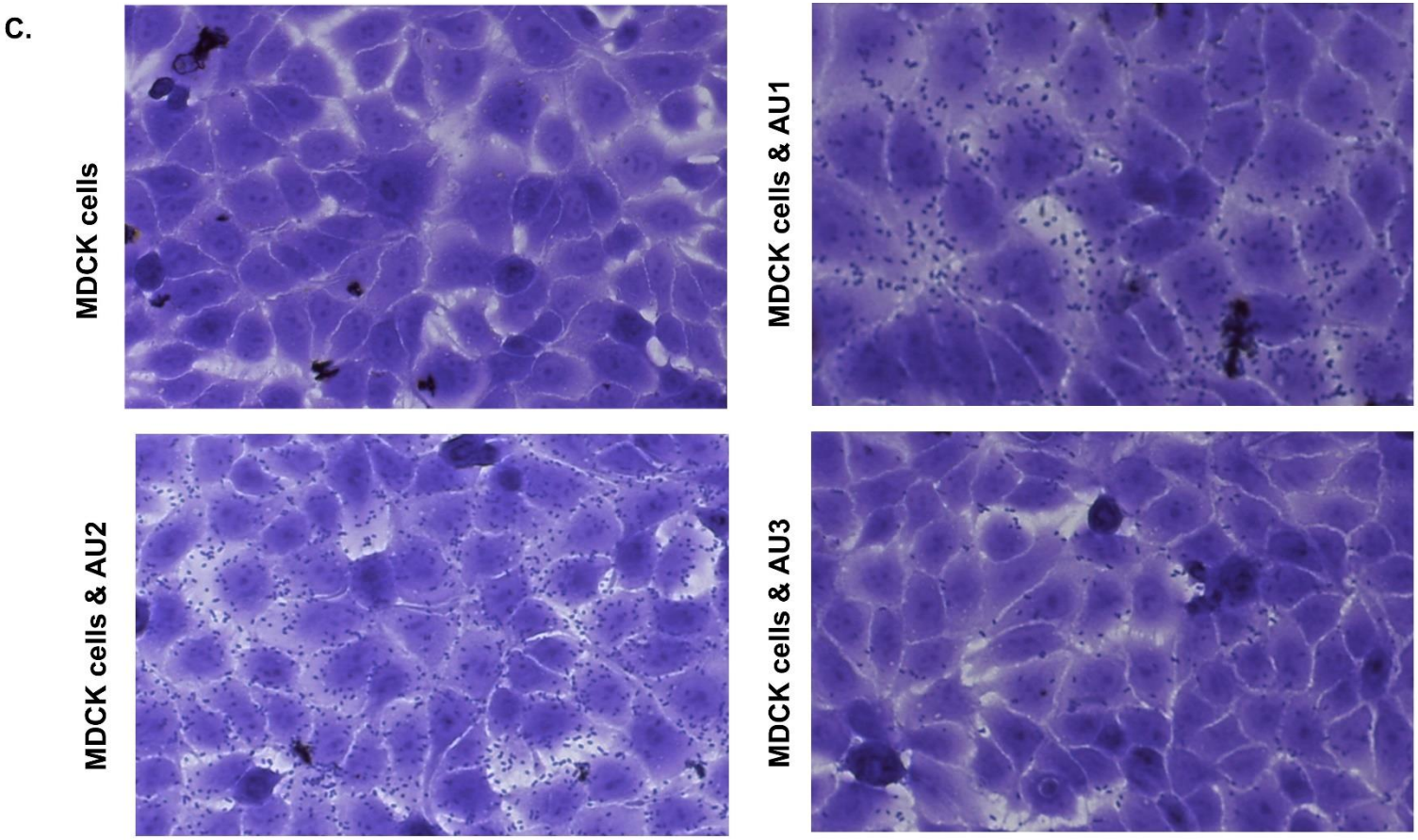

Figure 6.5. A. UPEC Biofilm and MDCK cell monolayer stained with crystal violet*. P. aeruginosa wells are highlighted in red.* ***B. Biofilm formation on MDCK cell monolayer and polystyrene in LB Miller broth (pH 7.5, 0.5% v/v glucose), following 48hr incubation****. N=4 from two independent experiments, error bars are SEM. Absorbance values were baseline-corrected to stained MDCK cell monolayer, except for P. aeruginosa which was baseline-corrected to the negative control (uninoculated media only wells). Weak biofilm former:* $OD_{550} < OD_{550}$ *negative control , moderate biofilm former:* $0 < OD_{550} < 2 \times OD_{550}$ *negative control, strong biofilm former:* $OD_{550} > 4 \times OD_{550}$ *negative control* (Lajhar, Brownlie and Barlow 2018)*; p and q > 0.05 by two-way ANOVA (medium vs. strain) with Benjamini, Kreuger and Yekutieli false discovery control method.* ***C. 48hr biofilm on the surface of MDCK cell monolayer (200x magnification).***

6.4. Discussion

6.4.1. Summary of findings presented in this chapter

The scope of this chapter was to characterize multidrug resistance, antibiotic persistence, and biofilm formation of a panel UPEC isolated from hospital patients in the United Kingdom and Australia. First, we conducted an antibiotic susceptibility screen and demonstrated that multidrug resistance is a common feature of UPEC, which supported our initial hypothesis. Next, we evaluated antibiotic persistence to two 'last-resort' antibiotics: meropenem and colistin. As hypothesized, we observed high levels of persistence to meropenem, especially in UTI-mimicking incubation conditions. Furthermore, we showed that although colistin is significantly more effective in eradicating the persister subpopulation than meropenem, transient resistance to this antibiotic develops rapidly at acidic (urine) pH in a subpopulation of cells. Finally, we compared biofilm formation in field-standard conditions (attachment to polystyrene) and on the surface of a kidney epithelial cell monolayer. We confirmed that biofilm formation is surface dependent and that isolates classified as 'weak' biofilm formers on polystyrene were able to form moderate and strong biofilms when grown on cell monolayers.

6.4.2. UPEC multidrug resistance

Antibiotic resistance is considered to be the biggest threat to public health globally. The widely cited 2014 AMR report commissioned by the UK government (O'Neil, 2014) has estimated that by 2050 10 million people will die each year as a consequence of pan-drug resistant infections if the issue is not addressed. In this chapter we evaluated resistance of UPEC to a panel of antibiotics and found an alarmingly high levels of resistance to commonly-prescribed drugs. We found 88% of screened isolates to be resistant to trimethoprim and sulfafurazole/sulfamethoxazole, compared to the national average of 33% in the UK and 20% in Australia. Similarly, resistance to fluoroquinolones was significantly higher, 80% and 33% for UK and Australian isolates respectively, compared to the expected 13%. In line with previous research, we didn't detect nitrofurantoin resistance, although this antibiotic was only included in the Australian susceptibility panel (AQSHC, 2021; Tutone *et al.*, 2022). It is important to note that the sample size in this study was relatively small (8 isolates) and restricted to a single hospital location in United Kingdom and Australia. Therefore, we cannot exclude a potential selection bias, with multidrug resistant isolates being more likely to be isolated by hospital pathology departments once the patient presented with

treatment failure. Nevertheless, the presence of multidrug-resistant isolates in a hospital setting is of concern, as those can contribute to the high mortality of nosocomial infections. Furthermore, if the multidrug resistance is encoded on a mobile genetic element (e.g. a plasmid), those have the potential to spread rapidly to other pathogens circulating in the hospital, resulting in previously reported 'plasmid-mediated' outbreaks (Ledda *et al.* 2020; Peter *et al.* 2020; Marí-Almirall *et al.* 2021).

6.4.3. UPEC persistence to colistin and meropenem

In this chapter we investigated the frequency of antibiotic persister cells to meropenem and colistin. Meropenem is a broad-spectrum carbapenem (β-lactam ring antibiotic). It is effective against extended-spectrum β-lactamase expressing strains, and due to a low level or resistance it is classified as a last-resort antibiotic used to treat multi-drug resistant infections (Meletis 2016). Colistin is a former veterinary antimicrobial pore-forming peptide currently used as last resort antibiotic for human infections with multidrug resistant Gram negative bacteria. (Andrade *et al.* 2020). Both aforementioned antibiotics are classified as 'critical in human medicine' (category B) by European Medicines Agency (EMA, 2020). Since, as described in more detail in chapter 2, antibiotic peristence is a 'stepping stone' to development of genetic AMR (Windels *et al.* 2019), any isolates displaying high levels of peristence to either of the aforementioned antibiotics would be of concern to public health.

Here, we demonstrated that although all investigated isolates were sensitive to meropenem and colistin, persistence to meropenem was high amongst clinical isolates, on average 2% (up to 20%) when the cells were grown in rich media and on average 15% (up to 100%) when cells were grown in nutrient restricted media adjusted to urine pH. Since meropenem is a cell wall synthesis inhibitor, we hypothesize that in conditions which restrict cell division (i.e. growth in nutrient-limited medium) there was a higher frequency of slower growing/non-growing cells, resulting in a higher frequency of meropenem persisters. This has clinical implications since UPEC replication *in vivo* is slower that in *in vitro* rich media growth (Haugan *et al.* 2019). Meropenem is prescribed as a treatment for complicated UTI/kidney infections, however relapse has been reported following successful treatment (Cox, Holloway and Geckler 1995). Our results suggest that the presence of persister cells can be a contributing factor to the observed infection recurrence.

It has previously been shown that colistin displays synergy with other antibiotic classes against persisters (Cui *et al.* 2016), however its potential as a combination therapy component is limited to high-risk, multi-drug resistant infections due to its nephrotoxicity (Spapen *et al.* 2011). Our results suggest that colistin on its own is also an effective anti-persister compound, as it was capable of eradicating > 99.9% of UPEC cells following exposure. However, when the cultures were incubated at acidic pH, we observed a regrowth of the population after 5hrs from antibiotic addition, which we subsequently linked to low extracellular pH. Increased MIC of colistin in acidic pH has been previously reported (Loose *et al.* 2020), however our results suggest that it is a subpopulation feature as the initial rapid-kill phase was still observed following colistin exposure even though the cultures were pre-grown at low pH. From the clinical perspective, this feature of colistin could affect its efficacy in the treatment of UTIs, as the pH of the bladder is generally slightly acidic (Worcester *et al.* 2018). We note that his acidic pH can be raised as a result of replication of urea-digesting pathogens, e.g. *Proteus mirabilis* (Lai *et al.* 2021) which can explain why colistin has successfully been used in the treatment of UTIs (Krakkattu, Jismy *et al.* 2017; Sorlí *et al.* 2019).

6.4.4. UPEC biofilm formation

As explained in detail in the introduction to this chapter, biofilm is an important virulence factor of UPEC. Surface attachment, the first step of biofilm formation, in *E. coli* is mediated by curli and fimbriae. In UPEC specifically, M (*papAH*, *bmaE*) and S fimbriae (*sfas*) were found to be overexpressed in strong biofilm formers when biofilms were formed on polystyrene (Zamani and Salehzadeh 2018). In contrast, curli overexpression was found to increase adhesion to MDCK cell surface (Elpers and Hensel 2020). Here we evaluated the ability of UPEC isolates to form biofilms on both polystyrene and MDCK cell monolayers. We showed that the biofilm biomass doubled when bacterial cells were are able to attach to the epithelial cell surface, changing their classification from weak to moderate or strong biofilm formers. This highlights the importance of *in vivo*-relevant model choice for evaluation of biofilm formation capability of clinical isolates.

7. Conclusions and Future Directions

Antibiotic persistence is a concern to public health globally as it both contributes to treatment failure and accelerates development of genetic AMR. The purpose of this thesis was to investigate molecular mechanisms which regulate formation of persister cells in *Escherichia coli,* and their clinical relevance.

First, function of the transcription factor YdcI, a proposed persistence regulator (Hingley-Wilson *et al.*, 2020), was investigated. Our results suggested that *ydcI* does not regulate persistence to β-lactams or fluoroquinolones. We also found that a defective allele of this gene was not present in the highly-persistent strain *E. coli* HipQ (Wolfson *et al.*, 1990), both contrary to previous observations (Hingley-Wilson *et al.*, 2020). Instead, we found multiple novel non-synonymous substitutions in the HipQ genome, including known persistence regulators. Therefore, we concluded that the increased persistence of *E. coli* HipQ to β-lactams and fluoroquinolones is likely multifactorial. Moreover, we demonstrated that *E. coli* HipQ displays a growth defect in rich media, suggesting that high persistence can incur a fitness cost and be selected for/against in a manner similar to multidrug resistance (Melnyk, Wong and Kassen, 2015). Finally, we found further supporting evidence for the previously reported reduced phenotypic inheritance (RPI) feature of the HipQ strain (Hingley-Wilson *et al.*, 2020), however we were unable to link it directly to increased antibiotic persistence. Therefore, we suggest that future work investigating the mechanisms involved in high-persistence of *E. coli* HipQ focuses on single-cell observations in a microfluidics system, where RPI can be tracked across cell lineages, as has been previously done for other *E. coli* strains (Balaban *et al.*, 2004; Hingley-Wilson *et al.*, 2020) These observations would potentially result in identification of YdcI-independent pathways that regulating phenotypic inheritance, and subsequently antibiotic susceptibility. Furthermore, the proposed persistence regulators identified by whole genome sequencing of the *E. coli* HipQ genome could be further investigated. The role of these gene in antibiotic persistence and/or tolerance could be elucidated with the use of either gene deletion models or CRISPR recombineering, as was done for YdcI in this thesis. This would subsequently allow for identification alternative drug targets which could be effective against persister cells, since YdcI was demonstrated to not be a promising target by our work.

Next, we looked into the role of NADH homeostasis in antibiotic persistence and tolerance. We have previously shown that *E. coli* HipQ carries a mutation in the Glyceraldehyde-3-phosphate dehydrogenase *(gap)* gene, a component of the glycolysis

pathway (Wang *et al.*, 2020). Therefore, we hypothesised that cellular respiration rate plays a role in persister cell formation. In order to investigate this on a single-cell level we employed a [NADH:NAD+] biosensor. We subsequently demonstrated that HipQ ciprofloxacin-tolerant cells undergo respiration at a lower rate than antibiotic-tolerant cells of its parental strain, supporting our initial hypothesis. However, in our study we were not able to distinguish antibiotic persisters from viable but non culturable (VBNC) cells, which constituted the majority of the antibiotic tolerant subpopulation. Therefore, for future work we suggest implementation of microfluidics, capable of separating the aforementioned subpopulations, as demonstrated previously by Orman and colleagues (Orman and Brynildsen, 2013a and 2015; Bamford *et al.*, 2017). Additionally, we evaluated dysregulated NADH homeostasis as a potential marker for antibiotic tolerance and showed that the antibiotic tolerant subpopulation differs significantly from the bulk population in their cytosolic [NADH:NAD+]. We note that the biggest limitation of our study is that we were not able to determine whether this dysregulation occurs as cause or effect of antibiotic tolerance (in other words, whether antibiotic-tolerant cells showed this NAD(H) homeostasis dysregulation prior to antibiotic exposure). To expand on the observations presented here, we suggest employing fluorescence-activated cell sorting (FACS), in order to sort populations based on [NADH:NAD+] prior to antibiotic exposure, which would allow to answer the aforementioned research question, and subsequently to demonstrate whether [NADH:NAD+] can be used as antibiotic tolerance biomarker Furthermore, the observations presented in this thesis could be easily expanded on to other non-lytic antibiotics and/or bacterial species, following the method we established and validated here.

Lastly, we assessed the clinical impact of antibiotic persistence through characterisation of a panel of uropathogenic *E. coli.* Our results suggest that high-persistence and multidrug resistance is common amongst clinical isolates and that the ‘gold standard’ time-kill assays are not necessarily representative of *in vivo* killing dynamics. We note that our sample size was relatively small (8 isolates), and limited to two collection locations, and therefore we suggest expanding the number of clinical isolates evaluated for antibiotic persistence in the future work.

Furthermore, we proposed a mechanism through which incubation at low pH induces transient colistin resistance by altering peptide - cell membrane interactions and demonstrated that this transient resistance is a subpopulation feature. To expand on this work, we propose to validate this mechanism through measurements of bacterial surface charge, as demonstrated by Wilhelm and colleagues (Wilhelm *et al.*, 2021), and its relationship to colistin sensitivity in infection-mimicking growth conditions. Furthermore,

the effect of external pH on bacterial LPS structure can be investigated in UPEC, as was done previously in *Vibrio spp.* (Schwartzman *et al.,* 2019)

Next, we investigated surface attachment and biofilm formation of UPEC and found that it doubled on kidney epithelial cell monolayers, compared to 'gold-standard' polystyrene (O'Toole 2011). This highlights the importance of *in vivo* relevant models for investigation of clinical isolates. If our work is expanded on by including live-tissue or animal biofilm models, it would add to our understanding on how surface attachment affects biofilm biomass, and subsequently improve biofilm testing models currently used in the clinical setting.

Finally, genome or RNA sequencing of these clinical isolates was outside of the scope of this thesis; however, it would allow to link the observed phenotypes with genetic and/or transcriptomic changes (i.e., potentially identify novel 'persistence' and 'biofilm formation'- regulating genes). Therefore, we suggest that it is carried out as a part of future work.

Overall, antibiotic persistence remains a complex phenomenon, where genetic mutations, stochastic variation in gene expression, and local environmental conditions influence the frequency and phenotype of individual persister cells. Furthermore, the co-existence of other functionally distinct antibiotic-recalcitrant subpopulations, such as VBNC cells, or transiently (phenotypically) resistant cells, makes the development of drugs effective against antibiotic-tolerant cells a significant challenge.

However, it is imperative that potential therapeutic strategies continue to be researched into, in order to combat the increasing rates of treatment failure and slow down the development of genetic AMR. Several approaches discussed in detail in this thesis have already shown significant promise *in vitro,* validating the relevance of antibiotic persistence/tolerance research.

8. References

1. Abranches J, Martinez AR, Kajfasz JK*et al.* The Molecular Alarmone (p)ppGpp Mediates Stress Responses, Vancomycin Tolerance, and Virulence in *Enterococcus faecalis. J Bacteriol*. 2009;191:2248–56.
2. Ahmed H, Farewell D, Jones HM *et al.* Incidence and antibiotic prescribing for clinically diagnosed urinary tract infection in older adults in UK primary care, 2004-2014. Arez AP (ed.). *PLoS ONE* 2018;13:e0190521.
3. Allison KR, Brynildsen MP, Collins JJ. Metabolite-enabled eradication of bacterial persisters by aminoglycosides. *Nature*. 2011;473:216.
4. Amato SM, Brynildsen MP. Nutrient Transitions Are a Source of Persisters in Escherichia coli Biofilms. Beloin C (ed.). *PLoS ONE 2014*;9:e93110.
5. Anderson GG, Palermo JJ, Schilling JD *et al.* Intracellular Bacterial Biofilm-Like Pods in Urinary Tract Infections. *Science* 2003;301:105–7.
6. Andrade FF, Silva D, Rodrigues A *et al.* Colistin Update on Its Mechanism of Action and Resistance, Present and Future Challenges. *Microorganisms* 2020;8:1716.
7. Andrews JM. Determination of minimum inhibitory concentrations. *Journal of Antimicrobial Chemotherapy* 2001;48:5–16.
8. Australian Commission on Safety and Quality in Health Care. Kidney infections and urinary tract infections. 2018. Available from: https://www.safetyandquality.gov.au/our-work/healthcare-variation/fourth-atlas-2021/chronic-disease-and-infection-potentially-preventable-hospitalisations/24-kidney-infections-and-urinary-tract-infections (Accessed: 09/09/22).
9. Avarbock A, Avarbock D, Teh JS*et al.*. Functional regulation of the opposing (p)ppGpp synthetase/hydrolase activities of RelMtb from *Mycobacterium tuberculosis*. Biochemistry. 2005;44:9913–23.
10. Ayrapetyan M, Williams T, Oliver JD. Relationship between the Viable but Nonculturable State and Antibiotic Persister Cells. Margolin W (ed.). *J Bacteriol* 2018;200, DOI: 10.1128/JB.00249-18.
11. Baba T, Ara T, Hasegawa M *et al.* Construction of *Escherichia coli* K-12 in-frame, single-gene knockout mutants: the Keio collection. *Mol Syst Biol* 2006;2, DOI: 10.1038/msb4100050.
12. Baek MS, Chung ES, Jung DS*et al.*. Effect of colistin-based antibiotic combinations on the eradication of persister cells in *Pseudomonas aeruginosa*. *J Antimicrob Chemother*. 2020;75:917–24.

13. Balaban NQ, Helaine S, Lewis K *et al.* Definitions and guidelines for research on antibiotic persistence. *Nat Rev Microbiol* 2019;17:441–8.
14. Balaban NQ, Merrin J, Chait R *et al.* Bacterial Persistence as a Phenotypic Switch. *Science* 2004;305:1622–5.
15. Bamford RA, Smith A, Metz J *et al.* Investigating the physiology of viable but non-culturable bacteria by microfluidics and time-lapse microscopy. *BMC Biol* 2017;15:121.
16. Barraud N, Buson A, Jarolimek W*et al.* Mannitol Enhances Antibiotic Sensitivity of Persister Bacteria in Pseudomonas aeruginosa Biofilms. *PLoS One*. 2013;8:e84220.
17. Beletskii A, Bhagwat AS. Transcription-induced mutations: Increase in C to T mutations in the nontranscribed strand during transcription in *Escherichia col2. Proc Natl Acad Sci USA* 1996;93:13919–24.
18. Bergmiller T, Andersson AMC, Tomasek K *et al.* Biased partitioning of the multidrug efflux pump AcrAB-TolC underlies long-lived phenotypic heterogeneity. *Science* 2017;356:311–5.
19. Bernier SP, Lebeaux D, DeFrancesco AS*et al.* Starvation, Together with the SOS Response, Mediates High Biofilm-Specific Tolerance to the Fluoroquinolone Ofloxacin*. PLos Genet.* 2013;9:e1003144.
20. Bhaskar A, De Piano C, Gelman E *et al.* Elucidating the role of (p)ppGpp in mycobacterial persistence against antibiotics. *IUBMB Life*. 2018;70:836–44.
21. Bhat SA, Iqbal IK, Kumar A. Imaging the NADH:NAD+ Homeostasis for Understanding the Metabolic Response of *Mycobacterium* to Physiologically Relevant Stresses. *Front Cell Infect Microbiol* 2016;6.
22. Bigger JW. Treatment of staphylococcal infections with penicillin - By intermittent sterilisation. *Lancet North Am Ed*. 1944;244:497–500.
23. Blacker TS, Mann ZF, Gale JE *et al.* Separating NADH and NADPH fluorescence in live cells and tissues using FLIM. *Nat Commun* 2014;5:3936.
24. Brown DR. Nitrogen Starvation Induces Persister Cell Formation in *Escherichia col2. J Bacteriol. 2019;*201(3)
25. Cai L, Friedman N, Xie XS. Stochastic protein expression in individual cells at the single molecule level. *Nature*. 2006;440:358–62.
26. Cai YL, Liu HY, Wei X*et al.*. Efficacy of relacin combined with sodium hypochlorite against *Enterococcus faecalis biofilms. J Appl Oral Sc2.* 2018;26
27. Caleffi-Ferracioli KR, Amaral RC, Demitto FO*et al.* Morphological changes and differentially expressed efflux pump genes in *Mycobacterium tuberculosis* exposed to a rifampicin and verapamil combination. *Tuberculosis.* 2016;97:65–72.

28. Cañas-Duarte S, Perez-Lopez M, Herrfurth C *et al.* An Integrative Approach Points to Membrane Composition as a Key Factor *in E. Coli* Persistence. *Microbiology*. 2020.
29. Cantón R, Morosini M-2. Emergence and spread of antibiotic resistance following exposure to antibiotics. *FEMS Microbiol Rev*. 2011;35:977–91.
30. Center for Disease Control and Prevention. 2019. About Chronic Diseases. Available at: www.cdc.gov/chronicdisease/about/index.html. (Accessed: 07/2020)
31. Chen XH, Hashizume H, Tomishige T*et al.* Delamanid Kills Dormant *Mycobacteria* In Vitro and in a Guinea Pig Model of Tuberculosis. *Antimicrob Agents Chemother*. 2017;61:e02402–16.
32. Chen ZY, Gao YY, Lv BY*et al.* Hypoionic Shock Facilitates Aminoglycoside Killing of Both Nutrient Shift- and Starvation-Induced Bacterial Persister Cells by Rapidly Enhancing Aminoglycoside Uptake. *Front Microbiol*. 2019;10:2028.
33. Chowdhury N, Kwan BW, Wood TK. Persistence Increases in the Absence of the Alarmone Guanosine Tetraphosphate by Reducing Cell Growth. *Sci Rep*. 2016;6:20519.
34. Chua SL, Yam JKH, Hao PL*et al.*. Selective labelling and eradication of antibiotic-tolerant bacterial populations in *Pseudomonas aeruginosa* biofilms. *Nat Commun*. 2016;7:10750.
35. Cirz RT, Jones MB, Gingles NA*et al.*. Complete and SOS-mediated response of *Staphylococcus aureus* to the antibiotic ciprofloxacin. *J Bacteriol*. 2007;189:531–9.
36. Clinical and Laboratory Standards Institute. CLSI Guidelines M100-S26 Document., 2019. Available at: https://www.fda.gov/media/108180/download (Accessed: 09/2021).
37. Cohen NR, Lobritz MA, Collins JJ. Microbial Persistence and the Road to Drug Resistance*. Cell Host and Microbe*. 2013;13:632–42.
38. Cosma A. The Nightmare of a Single Cell: Being a Doublet. *Cytometry* 2020;97:768–71.
39. Cox CE, Holloway WJ, Geckler RW. A Multicenter Comparative Study of Meropenem and Imipenem/Cilastatin in the Treatment of Complicated Urinary Tract Infections in Hospitalized Patients. *Clinical Infectious Diseases* 1995;21:86–92.
40. Cui P, Niu H, Shi W *et al.* Disruption of Membrane by Colistin Kills Uropathogenic *Escherichia coli* Persisters and Enhances Killing of Other Antibiotics. *Antimicrob Agents Chemother* 2016;60:6867–71.
41. Curtis Nickel J, Downey JA, William Costerton J. Ultrastructural study of microbiologic colonization of urinary catheters. *Urology* 1989;34:284–91.

42. Dahl JL, Kraus CN, Boshoff HIM*et al.* The role of Rel(Mtb)-mediated adaptation to stationary phase in long-term persistence of *Mycobacterium tuberculosis* in mice. *Proc Natl Acad Sci*, 2003;100:10026–31.
43. de Steenwinkel JE, de Knegt GJ, ten Kate MT*et al.*. Time-kill kinetics of anti-tuberculosis drugs, and emergence of resistance, in relation to metabolic activity of *Mycobacterium tuberculosis*. *J Antimicrob Chemother*. 2010;65:2582–9.
44. Dong K, Pan HX, Yang D*et al.*. Induction, detection, formation, and resuscitation of viable but non-culturable state microorganisms. *Compr Rev Food Sci Food Saf*. 2020;19:149–83.
45. Dorr T, Lewis K, Vulic M. SOS response induces persistence to fluoroquinolones in *Escherichia col2. PLos Genet*. 2009;5:e1000760.
46. Dorr T, Vulic M, Lewis K. Ciprofloxacin Causes Persister Formation by Inducing the TisB toxin in *Escherichia col2. PLoS Biol*. 2010;8:e1000317.
47. Durfee T, Nelson R, Baldwin S *et al.* The Complete Genome Sequence of *Escherichia coli* DH10B: Insights into the Biology of a Laboratory Workhorse. *J Bacteriol* 2008;190:2597–606.
48. Dwyer DJ, Belenky PA, Yang JH *et al.* Antibiotics induce redox-related physiological alterations as part of their lethality. *Proc Natl Acad Sci USA* 2014;111, DOI: 10.1073/pnas.1401876111.
49. Elowitz MB, Levine AJ, Siggia ED*et al.*. Stochastic gene expression in a single cell. Science. 2002;297:1183–6.
50. Elpers L, Hensel M. Expression and Functional Characterization of Various Chaperon-Usher Fimbriae, Curli Fimbriae, and Type 4 Pili of Enterohemorrhagic *Escherichia coli* O157:H7 Saka2. *Front Microbiol* 2020;11:378.
51. EUCAST. Breakpoint tables for interpretation of MICs and zone diameters. Version 9.0. Available at: https://www.eucast.org/clinical_breakpoints (Accessed: 10/2022)
52. European Medicines Agency. Categorisation of antibiotics used in animals promotes responsible use to protect public and animal health. 2020. Available at: https://www.ema.europa.eu/en/news/categorisation-antibiotics-used-animals-promotes-responsible-use-protect-public-animal-health (Accessed: 09/2022)
53. Ezaki B, Ogura T, Niki H*et al.*. Partitioning of a mini-F plasmid into anucleate cells of the mukB null mutant. *J Bacteriol*. 1991;173:6643–6.
54. Falkow S. Molecular Koch's postulates applied to bacterial pathogenicity — a personal recollection 15 years later. *Nat Rev Microbiol* 2004;2:67–72.
55. Feng J, Weitner M, Shi WL*et al.* Identification of Additional Anti-Persister Activity against *Borrelia burgdorferi* from an FDA Drug Library. *Antibiotics*. 2015;4:397–410.

56. Fleming D, Rumbaugh K. The Consequences of Biofilm Dispersal on the Host. *Sci Rep* 2018;8:10738.
57. Flores-Mireles AL, Walker JN, Caparon M *et al.* Urinary tract infections: epidemiology, mechanisms of infection and treatment options. *Nat Rev Microbiol* 2015;13:269–84.
58. Foxman B, Zhang L, Tallman P *et al.* Virulence Characteristics of *Escherichia coli* Causing First Urinary Tract Infection Predict Risk of Second Infection. *Journal of Infectious Diseases* 1995;172:1536–41.
59. Foxman B. Recurring urinary tract infection: incidence and risk factors. *Am J Public Health* 1990;80:331–3.
60. Fux CA, Wilson S, Stoodley P. Detachment Characteristics and Oxacillin Resistance of *Staphyloccocus aureus Biofilm* Emboli in an In Vitro Catheter Infection Model. *J Bacteriol* 2004;186:4486–91.
61. Gao Y, Yurkovich JT, Seo SW *et al.* Systematic discovery of uncharacterized transcription factors in *Escherichia coli* K-12 MG1655. *Nucleic Acids Research* 2018, DOI: 10.1093/nar/gky752.
62. Garcia P, Martinez B, Rodriguez L*et al.*. Synergy between the phage endolysin LysH5 and nisin to kill Staphylococcus aureus in pasteurized milk. *Int J Food Microbiol*. 2010;141:151–5.
63. Gerdes K, Maisonneuve E. Bacterial persistence and toxin-antitoxin loc2. *Annu Rev Microbiol.* 2012;66:103–23.
64. Germain E, Castro-Roa D, Zenkin N*et al.* Molecular mechanism of bacterial persistence by HipA. Mol Cell. 2013;52:248–54.
65. González MJ, Robino L, Iribarnegaray V *et al.* Effect of different antibiotics on biofilm produced by uropathogenic *Escherichia coli* isolated from children with urinary tract infection. *Pathogens and Disease* 2017;75, DOI: 10.1093/femspd/ftx053.
66. Goode O, Smith A, Zarkan A *et al.* Persister *Escherichia coli* Cells Have a Lower Intracellular pH than Susceptible Cells but Maintain Their pH in Response to Antibiotic Treatment. Balaban N, Levin BR (eds.). *mBio* 2021;12:e00909-21.
67. Goode O, Smith A, Łapińska U *et al.* Heterologous Protein Expression Favors the Formation of Protein Aggregates in Persister and Viable but Nonculturable Bacteria. *ACS Infect Dis* 2021;7:1848–58.
68. Goormaghtigh F, Fraikin N, Putrins M*et al.*. Reassessing the Role of Type II Toxin-Antitoxin Systems in Formation of *Escherichia coli* Type II Persister Cells. *mBio*. 2018;9:e00640–18.

69. Goormaghtigh F, Van Melderen L. Single-cell imaging and characterization of *Escherichia coli* persister cells to ofloxacin in exponential cultures. *Sci Adv*. 2019;5:eaav9462. [
70. Greenwood DJ, Dos Santos MS, Huang S*et al.*. Subcellular antibiotic visualization reveals a dynamic drug reservoir in infected macrophages. *Science*. 2019;364:1279–82.
71. Guptasarma P. Does Replication-Induced Transcription Regulate Synthesis of the Myriad Low Copy Number Proteins of *Escherichia col2. Bioessays.* 1995;17:987–97.
72. Gutierrez D, Ruas-Madiedo P, Martinez B*et al.*. Effective Removal of Staphylococcal Biofilms by the Endolysin LysH5. *PLoS One*. 2014;9.
73. Harms A, Fino C, Sorensen MA*et al.*. Prophages and Growth Dynamics Confound Experimental Results with Antibiotic-Tolerant Persister Cells. *mBio*. 2017;8:e01964–17.
74. Haugan, Hertz, Charbon *et al.* Growth Rate of *Escherichia coli* During Human Urinary Tract Infection: Implications for Antibiotic Effect. *Antibiotics* 2019;8:92.
75. Healy J, Ekkerman S, Pliotas C *et al.* Understanding the Structural Requirements for Activators of the Kef Bacterial Potassium Efflux System. *Biochemistry* 2014;53:1982–92.
76. Hingley-Wilson SM, Ma N, Hu Y *et al.* Loss of phenotypic inheritance associated with *ydcI* mutation leads to increased frequency of small, slow persisters in *Escherichia col2. Proc Natl Acad Sci USA* 2020;117:4152–7.
77. Hobby GL, Meyer K, Chaffee E. Observations on the mechanism of action of penicillin. *Exp Biol Med.* 1942;50:281–5.
78. Hu Y, Coates AR. Enhancement by novel anti-methicillin-resistant *Staphylococcus aureus* compound HT61 of the activity of neomycin, gentamicin, mupirocin and chlorhexidine: in vitro and in vivo studies. *J Antimicrob Chemother*. 2013;68:374–84.
79. Hu Y, Kwan BW, Osbourne Do *et al.* Toxin YafQ increases persister cell formation by reducing indole signalling. *Environ Microbiol* 2015;17:1275–85.
80. Hu YM, Pertinez H, Liu Y*et al.* Bedaquiline kills persistent *Mycobacterium tuberculosis* with no disease relapse: an in vivo model of a potential cure. *J Antimicrob Chemother*. 2019;74:1627–33.
81. Hubbard AT, Barker R, Rehal R*et al.* Mechanism of Action of a Membrane-Active Quinoline-Based Antimicrobial on Natural and Model Bacterial Membranes. *Biochemistry.* 2017;56:1163–74.
82. Hung YP, Albeck JG, Tantama M *et al.* Imaging Cytosolic NADH-NAD+ Redox State with a Genetically Encoded Fluorescent Biosensor. *Cell Metabolism* 2011;14:545–54.

83. IHME. Global Burden of Disease (GBD) 2019 Report. Available at: https://ghdx.healthdata.org/ (Accessed: 09/2022)
84. Ishikawa M, Tanaka Y, Suzuki R *et al.* Real-time monitoring of intracellular redox changes in *Methylococcus capsulatus* (Bath) for efficient bioconversion of methane to methanol. *Bioresource Technology* 2017;241:1157–61.
85. Jain P, Weinrick BC, Kalivoda EJ*et al.*. Dual-Reporter Mycobacteriophages (Phi(DRMs)-D-2) Reveal Pre-existing *Mycobacterium tuberculosis* Persistent Cells in Human Sputum*. mBio.* 2016;7:e01023–16.
86. Jarvis T, Chan L, Gottlieb T. Assessment and management of lower urinary tract infection in adults. *Aust Prescr* 2014;37:7–9.
87. Jawetz E, Gunnison JB, Speck RS. Studies on Antibiotic Synergism and Antagonism - the Interference of Aureomycin, Chloramphenicol and Terramycin with the Action of Streptomycin. *Am J Med Sc2.* 1951;222:404–12.
88. Jennings ME, Quick LN, Soni A *et al.* Characterization of the *Salmonella enterica* Serovar Typhimurium *ydcI* Gene, Which Encodes a Conserved DNA Binding Protein Required for Full Acid Stress Resistance. *J Bacteriol* 2011;193:2208–17.
89. Jiang Y, Chen B, Duan C *et al.* Multigene Editing in the *Escherichia coli* Genome via the CRISPR-Cas9 System. Kelly RM (ed.). *Appl Environ Microbiol* 2015;81:2506–14.
90. Johnson PJ, Levin BR. Pharmacodynamics, population dynamics, and the evolution of persistence in *Staphylococcus aureus*. *PLos Genet.* 2013;9:e1003123.
91. Jones SM, Yerly J, Hu Y *et al.* Structure of *Proteus mirabilis* biofilms grown in artificial urine and standard laboratory media. FEMS Microbiology Letters 2007;268:16–21.
92. Keren I, Shah D, Spoering A*et al.*. Specialized persister cells and the mechanism of multidrug tolerance in *Escherichia col2. J Bacteriol.* 2004;186:8172–80.
93. Kepiro IE, Marzuoli I, Hammond K *et al.* Engineering Chirally Blind Protein Pseudocapsids into Antibacterial Persisters. *ACS Nano 2020*;14:1609–22.
94. Khare A, Tavazoie S. Extreme Antibiotic Persistence via Heterogeneity-Generating Mutations Targeting Translation. *mSystems.* 2020;5:e00847–19.
95. Khodakaram-Tafti A, Farjanikish G. Persistent bovine viral diarrhea virus (BVDV) infection in cattle herds. *Iranian Journal of Veterinary Research*. 2017;18:154–63.
96. Kim W, Zhu W, Hendricks GL*et al.* A new class of synthetic retinoid antibiotics effective against bacterial persisters. *Nature.* 2018;556:103–7.
97. Kohanski MA, Dwyer DJ, Hayete B*et al.*. A common mechanism of cellular death induced by bactericidal antibiotics. *Cell.* 2007;130:797–810.
98. Korch SB, Henderson TA, Hill TM. Characterization of the hipA7 allele of *Escherichia coli* and evidence that high persistence is governed by (p)ppGpp synthesis. *Mol Microbiol*. 2003;50:1199–213.

99. Korch SB, Hill TM. Ectopic overexpression of wild-type and mutant hipA genes in *Escherichia coli*: effects on macromolecular synthesis and persister formation. *J Bacteriol*. 2006;188:3826–36.
100. Koskiniemi S, Lamoureux JG, Nikolakakis KC *et al.* Rhs proteins from diverse bacteria mediate intercellular competition. *Proc Natl Acad Sci USA* 2013;110:7032–7.
101. Krakkattu, Jismy, Mohan, Anisha, James, Emmanuel *et al.* Effectiveness and Safety of Colistin in Multi Drug Resistant Urinary Tract Infections*. J App Pharm Sci* 2017, DOI: 10.7324/JAPS.2017.70920.
102. Kvist M, Hancock V, Klemm P. Inactivation of Efflux Pumps Abolishes Bacterial Biofilm Formation*. Appl Environ Microbiol*. 2008;74:7376–82.
103. Kwan BW, Chowdhury N, Wood TK. Combatting bacterial infections by killing persister cells with mitomycin C. *Environ Microbiol*. 2015;17:4406–14.
104. Lade H, Park JH, Chung SH *et al.* Biofilm Formation by *Staphylococcus aureus* Clinical Isolates is Differentially Affected by Glucose and Sodium Chloride Supplemented Culture Media. *JCM* 2019;8:1853.
105. Lai H-C, Chang S-N, Lin H-C *et al.* Association between urine pH and common uropathogens in children with urinary tract infections. *Journal of Microbiology, Immunology and Infection* 2021;54:290–8.
106. Lajhar SA, Brownlie J, Barlow R. Characterization of biofilm-forming capacity and resistance to sanitizers of a range of *E. coli* O26 pathotypes from clinical cases and cattle in Australia. *BMC Microbiol* 2018;18:41.
107. Lamers RP, Cavallari JF, Burrows LL. The efflux inhibitor phenylalanine-arginine beta-naphthylamide (PAbetaN) permeabilizes the outer membrane of gram-negative bacteria. *PLoS One*. 2013;8:e60666.
108. Lapinska U, Glover G, Capilla-Lasheras P*et al.*. Bacterial ageing in the absence of external stressors. *Philosophical Transactions of the Royal Society B: Biological Sciences.* 2019;374:20180442.
109. Łapińska U, Voliotis M, Lee KK *et al.* Fast bacterial growth reduces antibiotic accumulation and efficacy*. eLife* 2022;11:e74062.
110. LeBel M. Ciprofloxacin: Chemistry, Mechanism of Action, Resistance, Antimicrobial Spectrum, Pharmacokinetics, Clinical Trials, and Adverse Reactions. *Pharmacotherapy: The Journal of Human Pharmacology and Drug Therapy* 1988;8:3–30.
111. Ledda A, Cummins M, Shaw LP *et al.* Hospital Outbreak of Carbapenem-Resistant Enterobacteriales Associated with an OXA-48 Plasmid Carried Mostly by *Escherichia coli* ST399. *Evolutionary Biology,* 2020.

112. Levine E, Hwa T. Stochastic fluctuations in metabolic pathways. *Proc Natl Acad Sc2.* 2007;104:9224–9.
113. Lewis K. Persister cells and the riddle of biofilm survival. *Biochemistry (Moscow)* 2005;70:267–74.
114. Li H, Durbin R. Fast and accurate short read alignment with Burrows-Wheeler transform. *Bioinformatics* 2009;25:1754–60.
115. Liu J, Gefen O, Ronin I*et al.*. Effect of tolerance on the evolution of antibiotic resistance under drug combinations. *Science.* 2020;367:200–4.
116. Liu YG, Matsumoto M, Ishida H*et al.* Delamanid: from discovery to its use for pulmonary multidrug-resistant tuberculosis (MDR-TB). Tuberculosis. 2018;111:20–30.
117. Loose M, Naber KG, Coates A *et al.* Effect of Different Media on the Bactericidal Activity of Colistin and on the Synergistic Combination With Azidothymidine Against mcr-1-Positive Colistin-Resistant *Escherichia col2. Front Microbiol* 2020;11:54.
118. Luo Y, Ma Y, Zhao Q *et al.* Similarity and Divergence of Phylogenies, Antimicrobial Susceptibilities, and Virulence Factor Profiles of *Escherichia coli* Isolates Causing Recurrent Urinary Tract Infections That Persist or Result from Reinfection. *J Clin Microbiol* 2012;50:4002–7.
119. Magiorakos A-P, Srinivasan A, Carey RB *et al.* Multidrug-resistant, extensively drug-resistant and pandrug-resistant bacteria: an international expert proposal for interim standard definitions for acquired resistance. *Clinical Microbiology and Infection* 2012;18:268–81.
120. Manina G, Dhar N, McKinney JD. Stress and host immunity amplify *Mycobacterium tuberculosis* phenotypic heterogeneity and induce nongrowing metabolically active forms. *Cell Host and Microbe*. 2015;17:32–46. [PubMed] [Google Scholar]
121. Manuse S, Shan Y, Canas-Duarte SJ *et al.* Bacterial persisters are a stochastically formed subpopulation of low-energy cells. Bollenbach T (ed*.). PLoS Biol* 2021;19:e3001194.
122. Marí-Almirall M, Ferrando N, Fernández MJ *et al.* Clonal Spread and Intra- and Inter-Species Plasmid Dissemination Associated With Klebsiella pneumoniae Carbapenemase-Producing Enterobacterales During a Hospital Outbreak in Barcelona, Spain. *Front Microbiol* 2021;12:781127.
123. Markossian S, Grossman A, Brimacombe K. Assay Guidance Manual. Bethesda (MD): Eli Lilly and Company and the National Center for Advancing Translational Sciences, 2021.

124. Marques CNH, Morozov A, Planzos P*et al.*. The Fatty Acid Signaling Molecule cis-2-Decenoic Acid Increases Metabolic Activity and Reverts Persister Cells to an Antimicrobial-Susceptible State. *Appl Environ Microbiol*. 2014;80:6976–91.
125. Martincorena I, Luscombe NM. Non-random mutation: The evolution of targeted hypermutation and hypomutation. *Bioessays* 2013;35:123–30.
126. Massudi H, Grant R, Guillemin GJ *et al.* NAD + metabolism and oxidative stress: the golden nucleotide on a crown of thorns. *Redox Report* 2012;17:28–46.
127. Masuda H, Awano N, Inouye M. ydfD encodes a novel lytic protein in *Escherichia col2.* Calendar R (ed.). *FEMS Microbiology Letters* 2016;363:fnw039.
128. McCune RM, Feldmann FM, Lambert HP *et al.* MICROBIAL PERSISTENCE. *Journal of Experimental Medicine* 1966;123:445–68.
129. McCune RM, Tompsett R, Mcdermott W. The Fate of *Mycobacterium tuberculosis* in Mouse Tissues as Determined by the Microbial Enumeration Technique .2. The Conversion of Tuberculous Infection to the Latent State by the Administration of Pyrazinamide and a Companion *Drug. J Exp Med*. 1956;104:763–802.
130. McKenzie GJ, Harris RS, Lee PL*et al.*. The SOS response regulates adaptive mutation. *Proc Natl Acad Sc2.* 2000;97:6646–51.
131. Meletis G. Carbapenem resistance: overview of the problem and future perspectives. *Therapeutic Advances in Infection* 2016;3:15–21.
132. Mensa B, Howell GL, Scott R*et al.*. Comparative Mechanistic Studies of Brilacidin, Daptomycin, and the Antimicrobial Peptide LL16. *Antimicrob Agents Chemother*. 2014;58:5136–45.
133. Mensa B, Kim YH, Choi S*et al.*. Antibacterial Mechanism of Action of Arylamide Foldamers. *Antimicrob Agents Chemother*. 2011;55:5043–53. [
134. Miles AA, Misra SS, Irwin JO. The estimation of the bactericidal power of the blood. *Epidemiol Infect* 1938;38:732–49.
135. Mohiuddin SG, Hoang T, Saba A *et al.* Identifying Metabolic Inhibitors to Reduce Bacterial Persistence. *Front Microbiol* 2020;11:472.
136. Mok WW, Park JO, Rabinowitz JD*et al.* RNA Futile Cycling in Model Persisters Derived from MazF Accumulation. *mBio.* 2015;6:e01588–01515.
137. Mok WWK, Brynildsen MP. Timing of DNA damage responses impacts persistence to fluoroquinolones. *Proc Natl Acad Sc2.* 2018;115:E6301–9.
138. Moyed HS, Bertrand KP. hipA, a newly recognized gene of *Escherichia coli* K-12 that affects frequency of persistence after inhibition of murein synthesis. *J Bacteriol* 1983;155:768–75

139. Narayanaswamy VP, Keagy LL, Duris K*et al.*. Novel Glycopolymer Eradicates Antibiotic- and CCCP-Induced Persister Cells in *Pseudomonas aeruginosa*. *Front Microbiol*. 2018;9:1724.
140. National Institute for Health and Care Excellence (NIHCE). Mitomycin. Available from: https://cks.nice.org.uk/drugs/mitomycin (Accessed 07/2021)
141. National Institute for Health and Care Excellence (NIHCE). Urinary tract infection (lower): antimicrobial prescribing 2018.
Available from: https://cks.nice.org.uk/topics/urinary-tract-infection-lower-women/ (Accessed: 09/2022)
142. Ngan JYG, Pasunooti S, Tse W *et al.* HflX Controls Hypoxia-Induced Non-Replicating Persistence in Slow Growing Mycobacteria. *Microbiology*, 2020.
143. Nguyen D, Joshi-Datar A, Lepine F *et al.* Active Starvation Responses Mediate Antibiotic Tolerance in Biofilms and Nutrient-Limited Bacteria. *Science* 2011;334:982–6.
144. Nicolau SE, Lewis K. The Role of Integration Host Factor in *Escherichia coli* Persister Formation. Ballard JD (ed.). *mBio* 2022;13:e03420-21.
145. O'Toole GA. Microtiter Dish Biofilm Formation Assay. JoVE 2011:2437.
146. Ognenovska S, Mukerjee C, Sanderson-Smith M *et al.* Virulence Mechanisms of Common Uropathogens and Their Intracellular Localisation within Urothelial Cells. *Pathogens* 2022;11:926.
147. Ohkawa M, Sugata T, Sawaki M *et al.* Bacterial and Crystal Adherence to the Surfaces of Indwelling Urethral Catheters. Journal of Urology 1990;143:717–21.
148. Orman MA, Brynildsen MP. Dormancy Is Not Necessary or Sufficient for Bacterial Persistence. *Antimicrob Agents Chemother* 2013;57:3230–9.
149. Orman MA, Brynildsen MP. Inhibition of stationary phase respiration impairs persister formation in *E. col2.* Nat Commun 2015;6:7983.
150. Patridge EV, Ferry JG. WrbA from *Escherichia coli* and *Archaeoglobus fulgidus* Is an NAD(P)H:Quinone Oxidoreductase. *J Bacteriol* 2006;188:3498–506.
151. Peter S, Bosio M, Gross C *et al.* Tracking of Antibiotic Resistance Transfer and Rapid Plasmid Evolution in a Hospital Setting by Nanopore Sequencing. Bradford PA (ed.). *mSphere* 2020;5:e00525-20.
152. Pisu D, Provvedi R, Espinosa DM*et al.*. The Alternative Sigma Factors SigE and SigB Are Involved in Tolerance and Persistence to Antitubercular Drugs. *Antimicrob Agents Chemother*, 2017;61:e01596–17.
153. Przekwas J, Gębalski J, Kwiecińska-Piróg J *et al.* The effect of fluoroquinolones and antioxidans on biofilm formation by *Proteus mirabilis* strains. Ann *Clin Microbiol Antimicrob* 2022;21:22.

154. Pu Y, Zhao Z, Li Y*et al.*. Enhanced Efflux Activity Facilitates Drug Tolerance in Dormant Bacterial Cells. *Mol Cell*. 2016;62:284–94.
155. Pyne ME, Moo-Young M, Chung DA *et al.* Coupling the CRISPR/Cas9 System with Lambda Red Recombineering Enables Simplified Chromosomal Gene Replacement in *Escherichia col2.* Kivisaar M (ed.). *Appl Environ Microbiol* 2015;81:5103–14.
156. Quandt EM, Gollihar J, Blount ZD *et al.* Fine-tuning citrate synthase flux potentiates and refines metabolic innovation in the Lenski evolution experiment. *eLife* 2015;4:e09696.
157. Radzikowski JL, Vedelaar S, Siegel D*et al.*. Bacterial persistence is an active sigmaS stress response to metabolic flux limitation. *Mol Syst Biol*. 2016;12:882.
158. Raj A, van Oudenaarden A. Nature, nurture, or chance: stochastic gene expression and its consequences. *Cell*. 2008;135:216–26.
159. Ram Y, Dellus-Gur E, Bibi M *et al.* Predicting microbial growth in a mixed culture from growth curve data. *Proc Natl Acad Sci USA* 2019;116:14698–707.
160. Rang CU, Peng AY, Chao L. Temporal dynamics of bacterial aging and rejuvenation. *Curr Biol*. 2011;21:1813–6.
161. Ray A, Malin D, Nicolau DP*et al.* Antibiotic Tissue Penetration in Diabetic Foot Infections A Review of the Microdialysis Literature and Needs for Future Research. *J Am Podiatr Med Assoc*. 2015;105:520–31.
162. Reniere ML. Reduce, Induce, Thrive: Bacterial Redox Sensing during Pathogenesis. *J Bacteriol* 2018;200, DOI: 10.1128/JB.00128-18.
163. Reygaert W. An overview of the antimicrobial resistance mechanisms of bacteria. *AIMS Microbiology* 2018;4:482–501.
164. Robinson JT, Thorvaldsdóttir H, Winckler W *et al.* Integrative genomics viewer. *Nat Biotechno*l 2011;29:24–6.
165. Rocco A, Kierzek AM, McFadden J. Slow Protein Fluctuations Explain the Emergence of Growth Phenotypes and Persistence in Clonal Bacterial Populations. *PLoS One*. 2013;8:e54272.
166. Romiyo V, Wilson JW. Phenotypes, transcriptome, and novel biofilm formation associated with the *ydcI* gene. *Springer Nature* 2020;113:1109–22.
167. Rosen DA, Hooton TM, Stamm WE *et al.* Detection of Intracellular Bacterial Communities in Human Urinary Tract Infection. Opal SM (ed.). *PLoS Med* 2007;4:e329.
168. Rosen DA, Pinkner JS, Jones JM *et al.* Utilization of an Intracellular Bacterial Community Pathway in Klebsiella pneumoniae Urinary Tract Infection and the Effects of FimK on Type 1 Pilus Expression. *Infect Immun* 2008;76:3337–45.

169. Russo TA, Stapleton A, Wenderoth S *et al.* Chromosomal Restriction Fragment Length Polymorphism Analysis of *Escherichia coli* Strains Causing Recurrent Urinary Tract Infections in Young Women*. Journal of Infectious Diseases* 1995;172:440–5.
170. Sanchez-Torres V, Hu H, Wood TK. GGDEF proteins YeaI, YedQ, and YfiN reduce early biofilm formation and swimming motility in *Escherichia col2. Appl Microbiol Biotechnol* 2011;90:651–8.
171. Sanger F, Coulson AR. A rapid method for determining sequences in DNA by primed synthesis with DNA polymerase. *Journal of Molecular Biology* 1975;94:441–8.
172. Santi I, Dhar N, Bousbaine D*et al.*. Single-cell dynamics of the chromosome replication and cell division cycles in mycobacteria. *Nat Commun*. 2013;4:2470.
173. Sarigul N, Korkmaz F, Kurultak İ. A New Artificial Urine Protocol to Better Imitate Human Urine. *Sci Rep* 2019;9:20159.
174. Schellhorn HE. Function, Evolution, and Composition of the *RpoS* Regulon in *Escherichia col2. Front Microbiol* 2020;11:560099.
175. Scholar E. Chloramphenicol. XPharm: The Comprehensive Pharmacology Reference. Elsevier, 2007, 1–7.
176. Schramm FD, Schroeder K, Jonas K. Protein aggregation in bacteria. *FEMS Microbiology Reviews* 2020;44:54–72.
177. Schumacher MA, Balani P, Min JK*et al.*. HipBA-promoter structures reveal the basis of heritable multidrug tolerance. *Nature*. 2015;524:59–U108.
178. Schwartzman, J.A., Lynch, J.B., Flores Ramos, S., Zhou, L., Apicella, M.A., Yew, J.Y. and Ruby, E.G. (2019), Acidic pH promotes lipopolysaccharide modification and alters colonization in a bacteria–animal mutualism. Mol Microbiol, 112: 1326-1338.
179. Sebastian J, Swaminath S, Nair RR*et al.*. De Novo Emergence of Genetically Resistant Mutants of *Mycobacterium tuberculosis* from the Persistence Phase Cells Formed against Antituberculosis Drugs In Vitro. *Antimicrob Agents Chemother*. 2017;61:e01343–16.
180. Seemann T. Prokka: rapid prokaryotic genome annotation*. Bioinformatics* 2014;30:2068–9.
181. Semanjski M, Germain E, Bratl K*et al.*. The kinases HipA and HipA7 phosphorylate different substrate pools in *Escherichia coli* to promote multidrug tolerance. *Sci Signal.* 2018;11:eaat5750. [
182. Senoh M, Ghosh-Banerjee J, Ramamurthy T *et al.* Conversion of viable but nonculturable enteric bacteria to culturable by co-culture with eukaryotic cells: Culturability of VBNC enteric bacteria. *Microbiology and Immunology* 2012;56:342–5.

183. Sihra N, Goodman A, Zakri R *et al.* Nonantibiotic prevention and management of recurrent urinary tract infection. *Nat Rev Urol* 2018;15:750–76.
184. Singh M, Jadaun GPS, Ramdas*et al.* Effect of efflux pump inhibitors on drug susceptibility of ofloxacin resistant *Mycobacterium tuberculosis* isolates. *Indian J Med Res*. 2011;133:535–40. [PMC free article] [PubMed] [Google Scholar]
185. Slatkin M. Hedging one's evolutionary bets*. Nature.* 1974;250:704–5. [Google Scholar]
186. Smith A, Kaczmar A, Bamford RA*et al.*. The Culture Environment Influences Both Gene Regulation and Phenotypic Heterogeneity in *Escherichia col2. Front Microbiol*. 2018;9:1739.
187. Solomon L, Shah A, Hannagan S *et al.* Bacterial Genus-Specific Tolerance for *ydcI* Expression. *Curr Microbiol* 2014;69:640–8.
188. Sorlí L, Luque S, Li J *et al.* Colistin for the treatment of urinary tract infections caused by extremely drug-resistant *Pseudomonas aeruginosa*: Dose is critical. Journal of Infection 2019;79:253–61.
189. Spapen H, Jacobs R, Van Gorp V *et al.* Renal and neurological side effects of colistin in critically ill patients. *Ann Intensive Care* 2011;1:14.
190. Stevanovic M, Boukéké-Lesplulier T, Hupe L *et al.* Nutrient Gradients Mediate Complex Colony-Level Antibiotic Responses in Structured Microbial Populations. Front Microbiol 2022;13:740259.
191. STRING Database v. 11.5. Available at: https://string-db.org/. (Accessed 08/2022)
192. Sulaiman JE, Lam H. Proteomic Investigation of Tolerant *Escherichia coli* Populations from Cyclic Antibiotic Treatment*. J Proteome Res* 2020;19:900–13.
193. Sun QG, Li XJ, Perez LM*et al.*. The molecular basis of pyrazinamide activity on *Mycobacterium tuberculosis* PanD. *Nat Commun*. 2020;11:339.
194. Surre J, Saint-Ruf C, Collin V *et al.* Strong increase in the autofluorescence of cells signals struggle for survival. *Sci Rep* 2018;8:12088.
195. Swaminath S, Paul A, Pradhan A*et al.*. *Mycobacterium smegmatis* moxifloxacin persister cells produce high levels of hydroxyl radical, generating genetic resisters selectable not only with moxifloxacin but also with ethambutol and isoniazid, *Microbiology*. 2020;166:180–98.
196. Syal K, Bhardwaj N, Chatterji D. Vitamin C targets (p)ppGpp synthesis leading to stalling of long-term survival and biofilm formation in *Mycobacterium smegmatis*. *FEMS Microbiol Lett*. 2017;364:fnw282.
197. Tashiro Y, Eida H, Ishii S *et al.* Generation of Small Colony Variants in Biofilms by *Escherichia coli* Harboring a Conjugative F Plasmid. *Microbes and environments* 2017;32:40–6.

198. Tejwani V, Schmitt F-J, Wilkening S *et al.* Investigation of the NADH/NAD + ratio in *Ralstonia eutropha* using the fluorescence reporter protein Peredox. *Biochimica et Biophysica Acta (BBA) - Bioenergetics* 2017;1858:86–94.
199. Tiwari P, Arora G, Singh M*et al.*. MazF ribonucleases promote *Mycobacterium tuberculosis* drug tolerance and virulence in guinea pigs. *Nat Commun*. 2015;6:6059
200. Torrey HL, Keren I, Via LE*et al.*. High Persister Mutants in *Mycobacterium tuberculosis*. *PLoS One.* 2016;11:e0155127.
201. Tuomanen E, Cozens R, Tosch W*et al.*. The rate of killing of *Escherichia coli* by beta-lactam antibiotics is strictly proportional to the rate of bacterial growth. *J Gen Microbiol.* 1986;132:1297–304.
202. Tutone M, Bjerklund Johansen TE, Cai T *et al.* SUsceptibility and Resistance to Fosfomycin and other antimicrobial agents among pathogens causing lower urinary tract infections: findings of the SURF study. *International Journal of Antimicrobial Agents* 2022;59:106574.
203. UniProt. 2020. Available at: https://www.uniprot.org/
204. Van den Bergh B, Fauvart M, Michiels J. Formation, physiology, ecology, evolution and clinical importance of bacterial persisters. *FEMS Microbiology Reviews* 2017;41:219–51.
205. Vijay S, Nair RR, Sharan D*et al.*. Mycobacterial Cultures Contain Cell Size and Density Specific Sub-populations of Cells with Significant Differential Susceptibility to Antibiotics, Oxidative and Nitrite Stress. *Front Microbiol.* 2017;8:463.
206. Vijay S, Vinh DN, Hai HT*et al.* Influence of Stress and Antibiotic Resistance on Cell-Length Distribution in *Mycobacterium tuberculosis* Clinical Isolates. *Front Microbiol*. 2017;8:2296.
207. Vilcheze C, Hartman T, Weinrick B*et al.*. Enhanced respiration prevents drug tolerance and drug resistance in *Mycobacterium tuberculosis*. *Proc Natl Acad Sc2.* 2017;114:4495–500.
208. Vilcheze C, Jacobs WR. The Isoniazid Paradigm of Killing, Resistance, and Persistence in *Mycobacterium tuberculosis*. *J Mol Biol*. 2019;431:3450–61
209. Vilcheze C, Kim J, Jacobs WR. Vitamin C Potentiates the Killing of *Mycobacterium tuberculosis* by the First-Line Tuberculosis Drugs Isoniazid and Rifampin in Mice. *Antimicrob Agents Chemother.* 2018;62:e02165–17.
210. Vogwill T, Comfort AC, Furio V*et al.*. Persistence and resistance as complementary bacterial adaptations to antibiotics. *J Evol Biol*. 2016;29:1223–33
211. Vyas HKN, McArthur JD, Sanderson-Smith ML. An optimised GAS-pharyngeal cell biofilm model. *Sci Rep* 2021;11:8200.

212. Wakamoto Y, Dhar N, Chait R*et al.*. Dynamic persistence of antibiotic-stressed mycobacteria. *Science*. 2013;339:91–5.
213. Wang C, Yang L, Shah AA *et al.* Dynamic interplay of multidrug transporters with TolC for isoprenol tolerance in *Escherichia col2. Sci Rep* 2015;5:16505.
214. Wang S, Chen H, Tang X *et al.* The Role of Glyceraldehyde-3-Phosphate Dehydrogenases in NADPH Supply in the Oleaginous Filamentous Fungus *Mortierella alpina*. *Front Microbiol* 2020;11:818.
215. Wexselblatt E, Kaspy I, Glaser G*et al.*. Design, synthesis and structure-activity relationship of novel Relacin analogs as inhibitors of Rel proteins. *Eur J Med Chem*. 2013;70:497–504.
216. WHO 2019. WHO guidelines on tuberculosis infection prevention and control 2019 update. Available at: https://apps.who.int/iris/handle/10665/311259 (Accessed: 05/2020)
217. Wilmaerts D, Bayoumi M, Dewachter L*et al.*. The Persistence-Inducing Toxin HokB Forms Dynamic Pores That Cause ATP Leakage. *Mbio.* 2018;9.
218. Windels EM, Michiels JE, Fauvart M *et al.* Bacterial persistence promotes the evolution of antibiotic resistance by increasing survival and mutation rates. *ISME J* 2019;13:1239–51.
219. Wolfson JS, Hooper DC, Mchugh GL*et al.* Mutants of Escherichia-Coli K-12 Exhibiting Reduced Killing by Both Quinolone and Beta-Lactam Antimicrobial Agents. *Antimicrob Agents Chemother*. 1990;34:1938–43.
220. Worcester EM, Bergsland KJ, Gillen DL *et al.* Mechanism for higher urine pH in normal women compared with men. *American Journal of Physiology-Renal Physiology* 2018;314:F623–9.
221. World Health Organization (WHO) (2019). Global action plan on AMR. Available at: https://www.who.int/antimicrobial-resistance/global-action-plan/en/. (Accessed 09/2019)
222. Yang X, Chen H, Zheng Y *et al.* Disease burden and long-term trends of urinary tract infections: A worldwide report. *Front Public Health* 2022;10:888205.
223. Zamani H, Salehzadeh A. Biofilm formation in uropathogenic *Escherichia coli*: association with adhesion factor genes. *Turk J Med Sci* 2018;48:162–7.
224. Zarkan A, Matuszewska M, Trigg SB *et al.* Inhibition of indole production increases the activity of quinolone antibiotics against *E. coli* persisters. *Sci Rep* 2020;10:11742.
225. Zeiler HJ. Evaluation of the in vitro bactericidal action of ciprofloxacin on cells of *Escherichia coli* in the logarithmic and stationary phases of growth. *Antimicrob Agents Chemother* 1985;28:524–7.

226. Zhang Y, Kepiro I, Ryadnov MG *et al.* Single Cell Killing Kinetics Differentiate Phenotypic Bacterial Responses to Different Antibacterial Classes*. Kim M (ed.). Microbiol Spectr 2*023;11:e03667-22.

227. Zumla A, Memish ZA, Maeurer M*et al.*. Emerging novel and antimicrobial-resistant respiratory tract infections: new drug development and therapeutic options*. Lancet Infect Dis.* 2014;14:1136–49.

Methods Appendix

LB Lennox broth
10g/L Tryptone
5 g/L NaCl
5 g/L Yeast Extract

LB Miller broth

10g/L Tryptone
10 g/L NaCl
5 g/L Yeast Extract

MP Artificial Urine (MP-AU) (Sarigul, Korkmaz and Kurultak 2019)
11.965mM Na_2SO_4
1.487mM $C_5H_4N4O_3$
2.450mM $Na_3C_6H_5O_7x2H_2O$
7.791mM $C_4H_7N_3O$
249.750mM CH_4N_2O
30.953mM KCl
30.053mM NaCl
1.663mM $CaCl_2$
23.667mM NH_4Cl
0.19mM $K_2C_2O_4xH_2O$
4.389mM $MgSO_4x7H_2O$
18.667mM $NaH_2PO_4x2H_2O$
4.667mM $Na_2HPO_4x2H_2O$

Muller-Hinton broth
2g/L Beef Extract
17.5g/L Acid Hydrolysate of Casein
1.5g/L Starch

M9-GLUCOSE
minimal medium
10.5g/L M9-GLUCOSE broth powder
0.4% wt/v glucose
2mM $MgSO_4$
0.1% v/v vitamin B1 (thiamine)
100 µM $CaCl_2$
0.05g/L $FeSO_4$
0.4% wt/v casamino acids

RPMI 1640 complete medium
2 mM L-glutamine
10 mM 4-(2-hydroxyethyl)-1-piperazineethanesulfonic acid (HEPES)
1 mM sodium pyruvate
4500 mg/L glucose
1500 mg/L sodium bicarbonate
10% v/v heat-inactivated foetal bovine serum (FBS)
1% v/v 5000U/mL penicillin-streptomycin solution *(ThermoFisher Scientific)*

TCM
10 mM Tris/HCl pH 7.5
10 mM $MgCl_2$
10 mM $CaCl_2$

Transport and storage solution (TSS)
LB Miller base
10% PEG 3350 or 8000
20mM $MgSO_4$
5% dimethyl sulphoxide

Chapter 4 Appendix

1. Primer sequences: (all primers were ordered from *Sigma Aldrich*)

Full forward: 5'ATGAAAAAAATAGTCTGTTTAGT3'

Full reverse: 5'TCAGAACGGCATTGATTTTC3'

PAM forward: 5'AACTTTGGGACGCGCGGC3'

PAM reverse: 5'GCCGCGCGTCCCAAAGTT3'

2. PCR conditions

Table 4.S1. E. coli ydcI gene PCR amplification conditions. *1 refers to reaction with full forward/full reverse primer pair, 2 refers to full forward/PAM reverse and 3 refers to PAM forward/full reverse; GC enhancer (New England Biolabs) was added to reactions 2 and 3.*

STEP	TEMPERATURE	TIME
Initial Denaturation	98^{o}C	30 seconds
Denaturation	98^{o}C	10 seconds
Annealing	58^{o}C^{1}, 58^{o}C^{2}, 61^{o}C^{3},	20 seconds
Extension	72^{o}C	20 seconds
Final Extension	72^{o}C	2 minutes
Hold	8^{o}C	until collected

3. Plasmid maps

A.

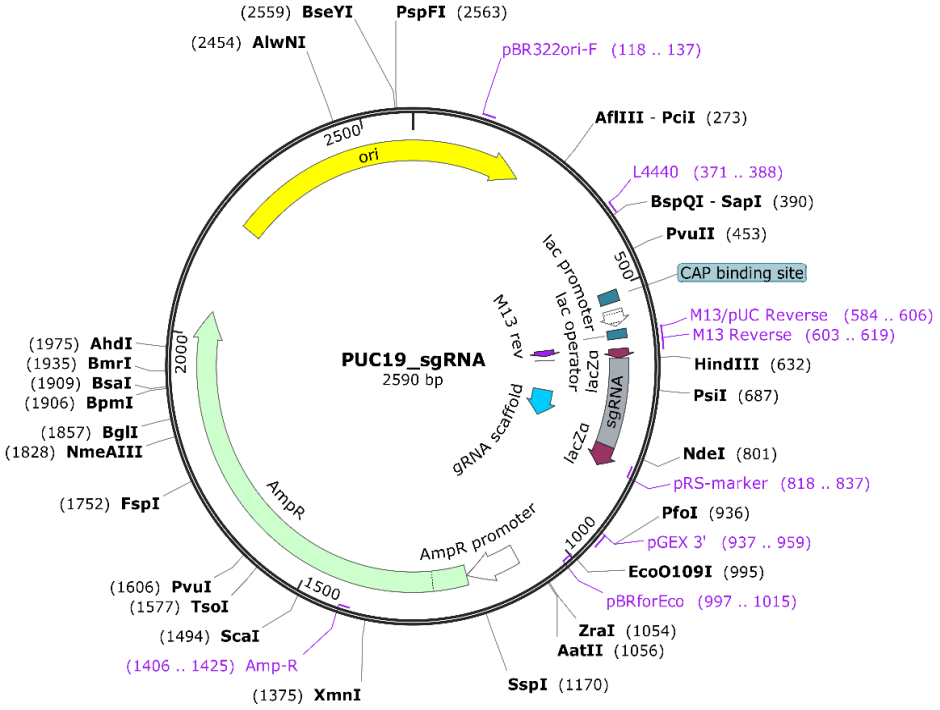

B.

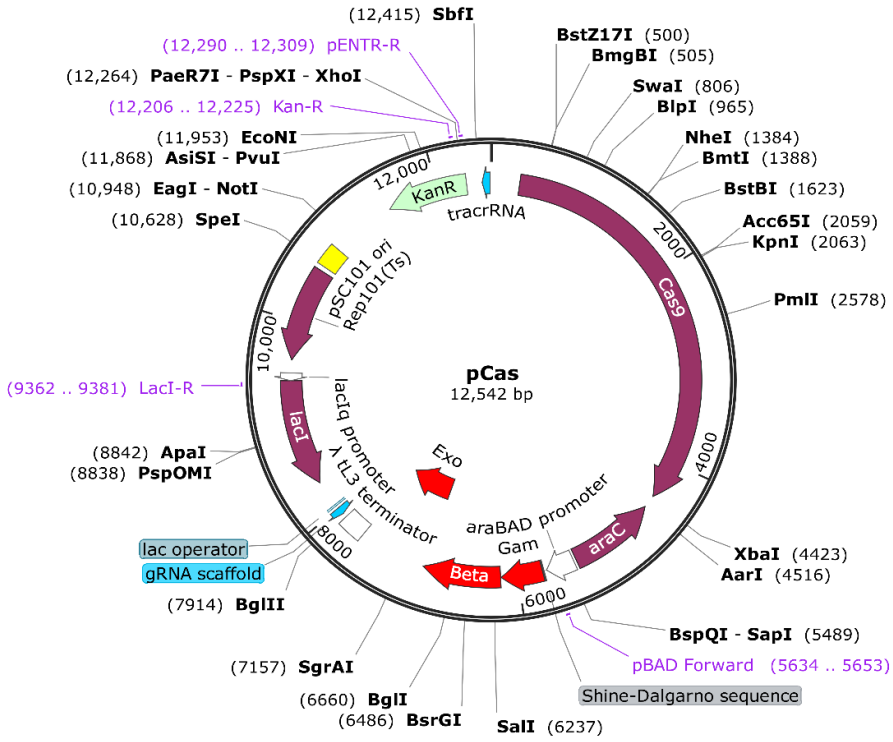

Figure 4.S1 Plasmid maps of vectors used in CRISPR recombineering. *A. psgRNA plasmid map (synthesised and verified by Biobasic UK). B. pCas plasmid map (Addgene plasmid # 62225).*

4. *E. coli Δydcl* genotype and phenotype confirmation

A.

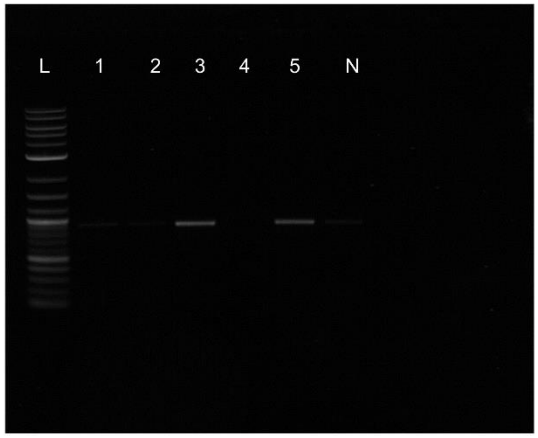

B.

E. coli Δydcl

ONPG	ADH	LDC	ODC	CIT	H2S	URE	TDA	IND	VP	GEL	GLU	MAN	INO	SOR	RHA	SAC	MEL	AMY	ARA
N	N	P	N	N	N	N	P	P	X	N	P	N	N	P	N	N	N	N	N

E. coli BW25113 (Δydcl parental strain)

ONPG	ADH	LDC	ODC	CIT	H2S	URE	TDA	IND	VP	GEL	GLU	MAN	INO	SOR	RHA	SAC	MEL	AMY	ARA
N	N	P	N	N	N	N	P	P	X	N	P	P	N	P	N	N	N	N	N

E. coli K12

ONPG	ADH	LDC	ODC	CIT	H2S	URE	TDA	IND	VP	GEL	GLU	MAN	INO	SOR	RHA	SAC	MEL	AMY	ARA
P	P	P	P	N	N	N	P	P	X	N	P	P	N	P	P	N	P	N	P

Figure 4.S2 Δydcl strain genotype and phenotype confirmation. *A. 1% agarose gel electrophoresis of E. coli Δydcl colony PCR with full forward/full reverse primers; from left to right: L- 1kb plus ladder (New England Biolabs) 1,2,4 – Δydcl colonies, 3,5 – positive control (parental strain) colonies, N- no template control; ydcl gene size is 924bp. B 20E API strip (BioMerieux) results on E. coli Δydcl and its parental strain BW25113; P – positive test result, N- negative test result, X – test not performed; ONPG: β-galactosidase, ADH: arginine dihydrolase, LDC: lysine decarboxylase, ODC: ornithine decarboxylase, CIT : use of citrate as sole carbon source, H2S : hydrogen sulfide production, URE : urease, TDA: tryptophan deaminase enzyme, IND: tryptophanase, VP : detection of acetoin produced by fermentation of glucose by bacteria using the butylene glycol pathway, GEL : gelatinase, GLU : glucose fermentation, MAN: mannose fermentation, INO : fermentation of inositol fermentation, SOR: sorbitol fermentation, RHA : rhamnose fermentation, SAC : sucrose fermentation; E. coli BW25113 and E. coli Δydcl carry deletions in arabinose (ARA), B-galactosidase (ONPG) and rhamnose (RHA) operons (highlighted in blue) (Baba et al., 2004).*

5. *E. coli* Δ*ydcI* ampicillin time-kill assays in different conditions:

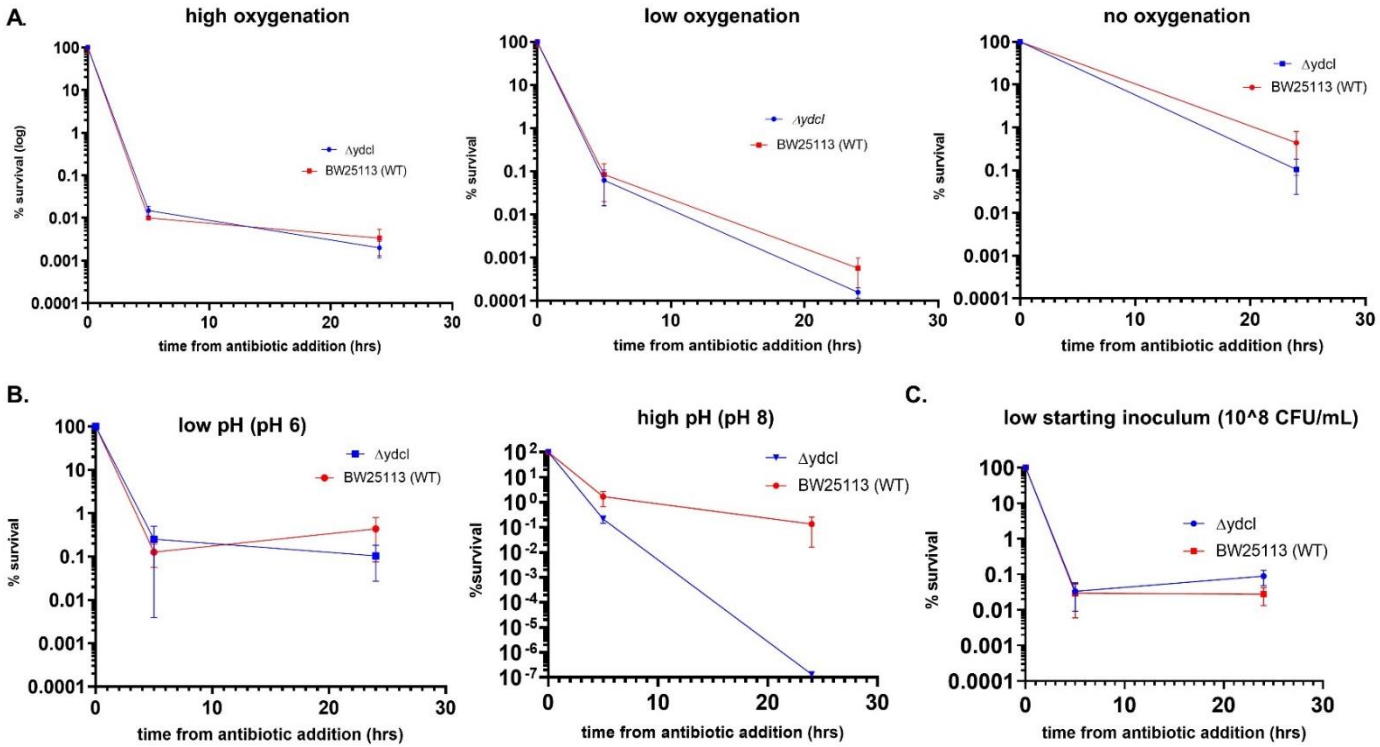

Figure 4.S3. Ampicillin time kill assays on E. coli Δydc2. *A. Effect of media oxygenation on frequency of persister cells in LB Miller broth ; from left to right: 50mL culture in 200mL conical flask, 250rpm shaking, 150rpm shaking, no shaking. B Effect of pH on frequency of persister cells in M9-GLUCOSE broth (buffered medium); C. Effect of low starting inoculum on frequency of persister cells in LB Miller broth (10-fold lower than standard time-kill assays in this chapter) n=3, error bars are SEM; p and q > 0.05 by two-way ANOVA (strain vs. time) with and Benjamini, Kreuger and Yekutieli false discovery control method.*

6. MIC assays

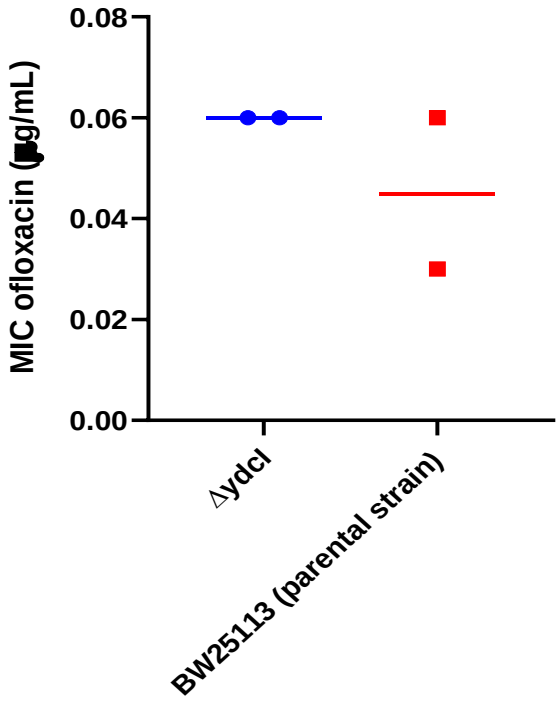

Figure 4.S4 Ofloxacin minimum inhibitory concentration for E. coli ΔydcI and its parental strain BW25113. *n=2; MIC was determined as the lowest concentration of the antibiotic that inhibited growth of all technical replicates of a biological replicate. (n).*

7. Single read analysis of *E. coli* HipQ and its parental strain KY sequencing data

Table II2.S2: Single read variant comparison between published E. coli HipQ and its parental strain (KY) whole-genome sequencing data and whole-genome sequencing data obtained as part of this project. *SAMN13648604 and SAMN136486050 raw reads were downloaded from BioSample. Presence of variants in HipQ (this project) and HipQ (published sequence) which are absent in KY would points towards published genome originating from a mixed colony.*

	KY (SAMN13648604)	**HipQ** (SAMN136486050)	**HipQ** (this project)
variants > 0.3% frequency in raw (unfiltered) reads	**136**	**139**	**514**
common variants with KY		**114**	**89**
common variants with HipQ (published sequence)	**114**		**88**

Variants present in HipQ (this project), HipQ (published sequence) absent in KY: 0

Chapter 5 Appendix

1. Primer sequences: (all primers were ordered from *Sigma Aldrich*)

T7 polymerase forward: 5'GCTATCCCGTTCAACACTC3'

T7 polymerase reverse: 5'TTTCACTTCCTCAAACCAGTC3'

2. PCR conditions

Table 5.S1. T7 polymerase gene PCR amplification conditions.

STEP	TEMPERATURE	TIME
Initial Denaturation	98^{o}C	30 seconds
Denaturation	98^{o}C	10 seconds
Annealing	63^{o}C	20 seconds
Extension	72^{o}C	20 seconds
Final Extension	72^{o}C	2 minutes
Hold	8^{o}C	until collected

3. NADH biosensor plasmid map

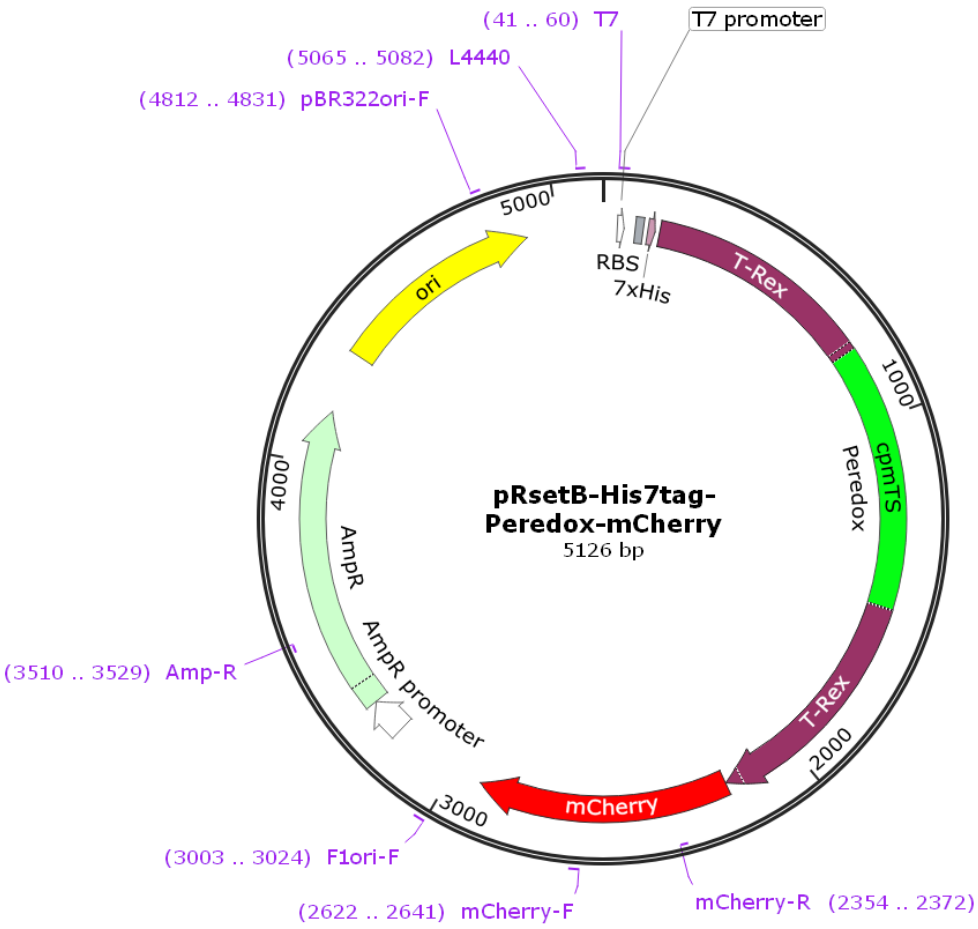

Figure 5.S1 pRsetB-Peredox plasmid map (Addgene plasmid #32382).

4. T7 polymerase gene PCR

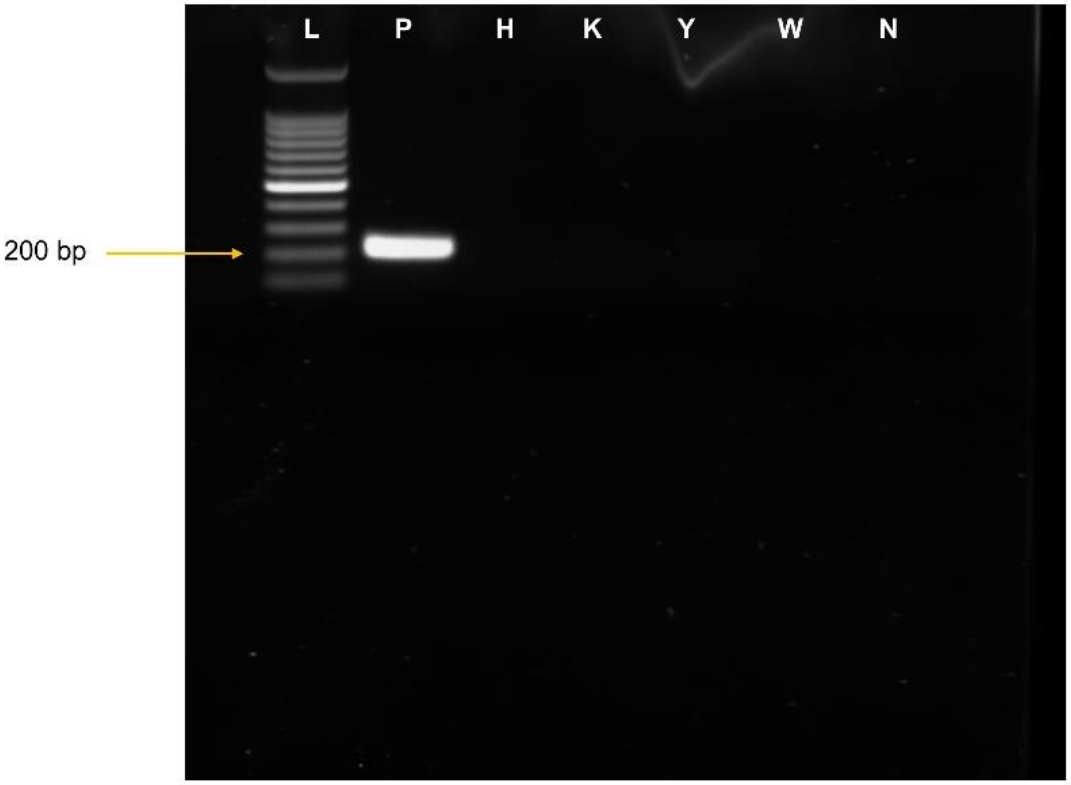

Figure 5.S2. 2% agarose gel electrophoresis of T7 polymerase gene detection PCR. *From left to right: L - 100bp DNA ladder (Promega), P - positive control (E. coli BL21(DE3)), H - E. coli HipQ, K - E. coli KY, Y - E. coli ΔydcI, W – E. coli BW25113, N – no template control; expected band size was 228bp.*

5. Optical density growth curves of NADH biosensor expressing and untransformed *E. coli*

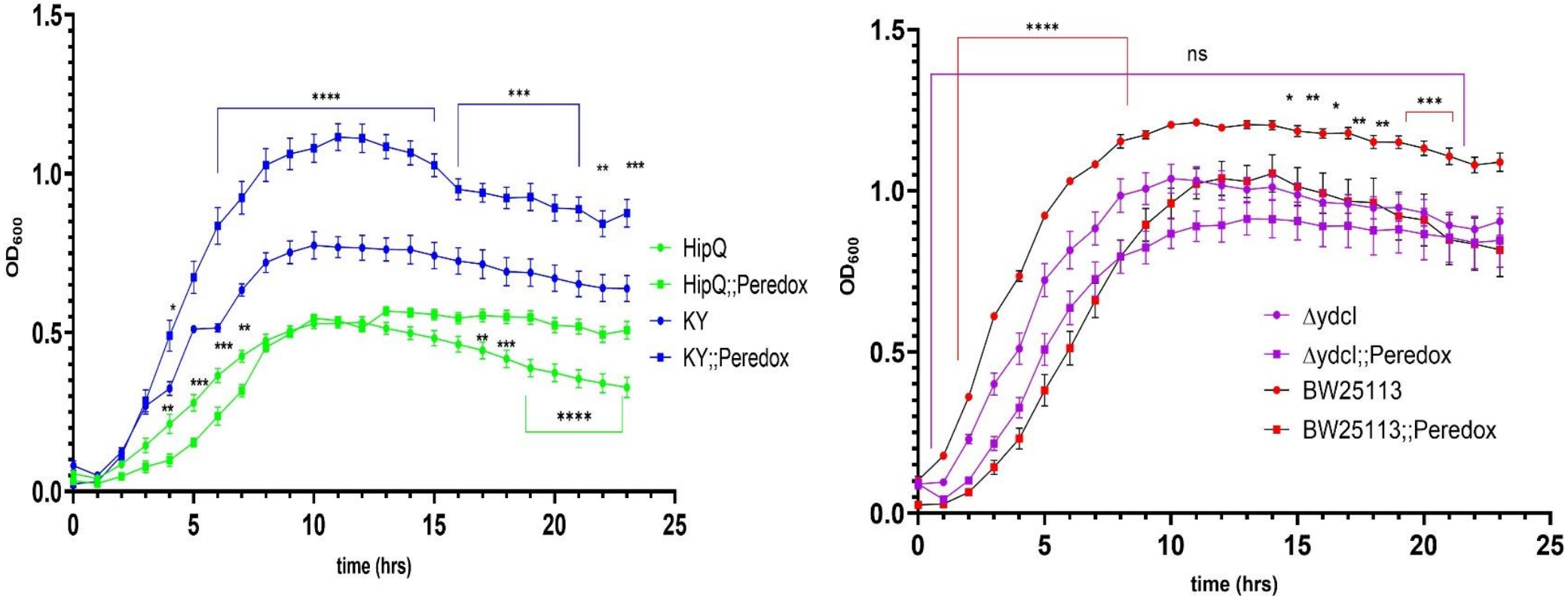

Figure 5.S3. Optical density (OD_{600}) of NADH biosensor expressing E. coli and their respective untransformed controls. *n=3, error bars are SEM; * = p<0.05, ** = p<0.01, *** = p<0.001 and q < 0.05 by two-way ANOVA (strain vs. time) with Benjamini, Kreuger and Yekutieli false discovery control method.*

6. Live/dead cell discrimination histograms

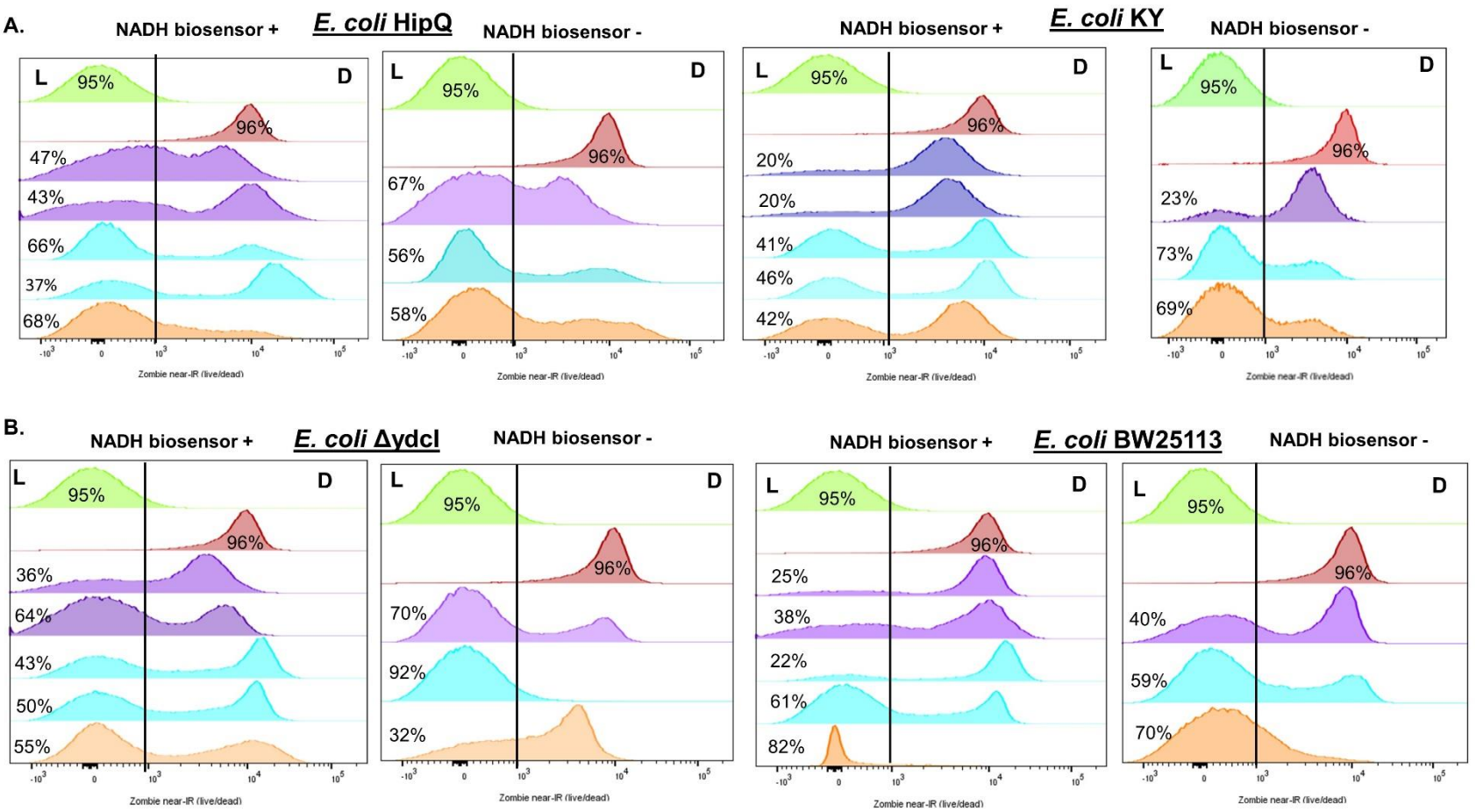

Figure 5.S4. Live/dead cell discrimination of A. E. coli HipQ and its parental strain KY and B. E coli Δydcl and its parental strain BW25113 following 24hr exposure to 25X MIC of ciprofloxacin. *All panels: green – negative control (live cells) and red – positive control (heat-killed cells). Each histogram represents a biological replicate, 100 000 events/replicate were collected; matched replicates (biosensor + and – from the same independent experiment) are colour coded . L – 'live' population, D – 'dead' population.*

7. 405/520nm (green) autofluorescence of *E. coli*

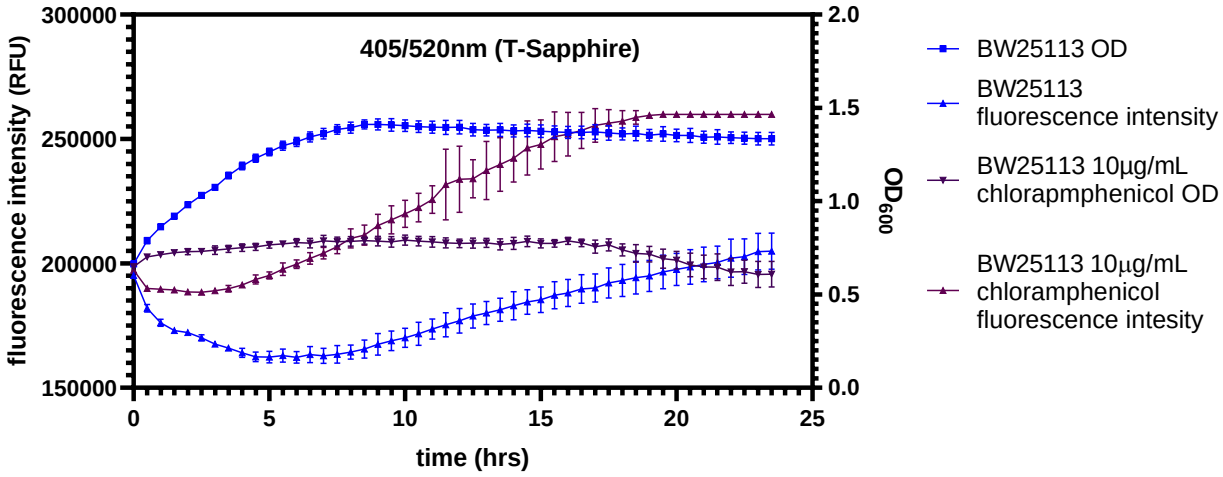

Figure 5.S5. Green (405/520nm) autofluorescence (left Y axis) relative to optical density (OD, right Y axis) of chloramphenicol-exposed and unexposed E. coli BW25113*. error bars are SD, each datapoint is an average of 6 technical replicates.*

A.

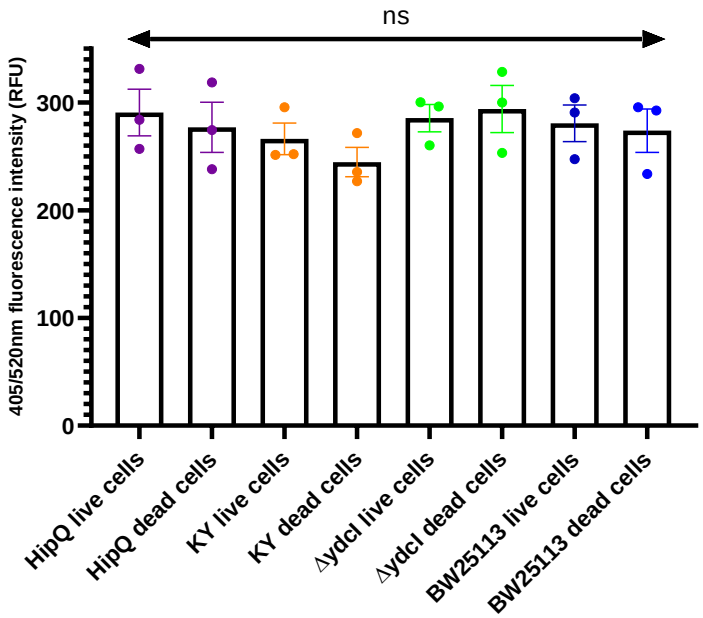

B.

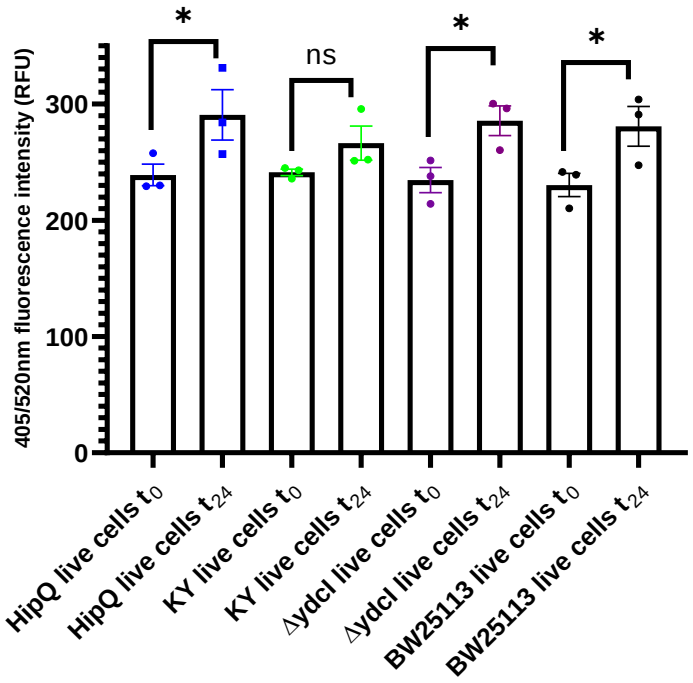

Figure 5.S6 405/520nm (T-Sapphire) autofluorescence intensity of A. live (persisters and VBNCs) and dead and B. live at t=0hrs and t=24hrs of E. coli cells following 24hr exposure to 25X MIC of ciprofloxacin. *n=3 from three independent experiments, error bars are SEM; 100 000 events/replicate were collected; * = p<0.05 by repeated measures ANOVA with Geiser-Greenhouse correction and with Benjamini, Kreuger and Yekutieli false discovery control method, values were matched within experiment.*

8. Intracellular NAD:NAD+ on single-cell level

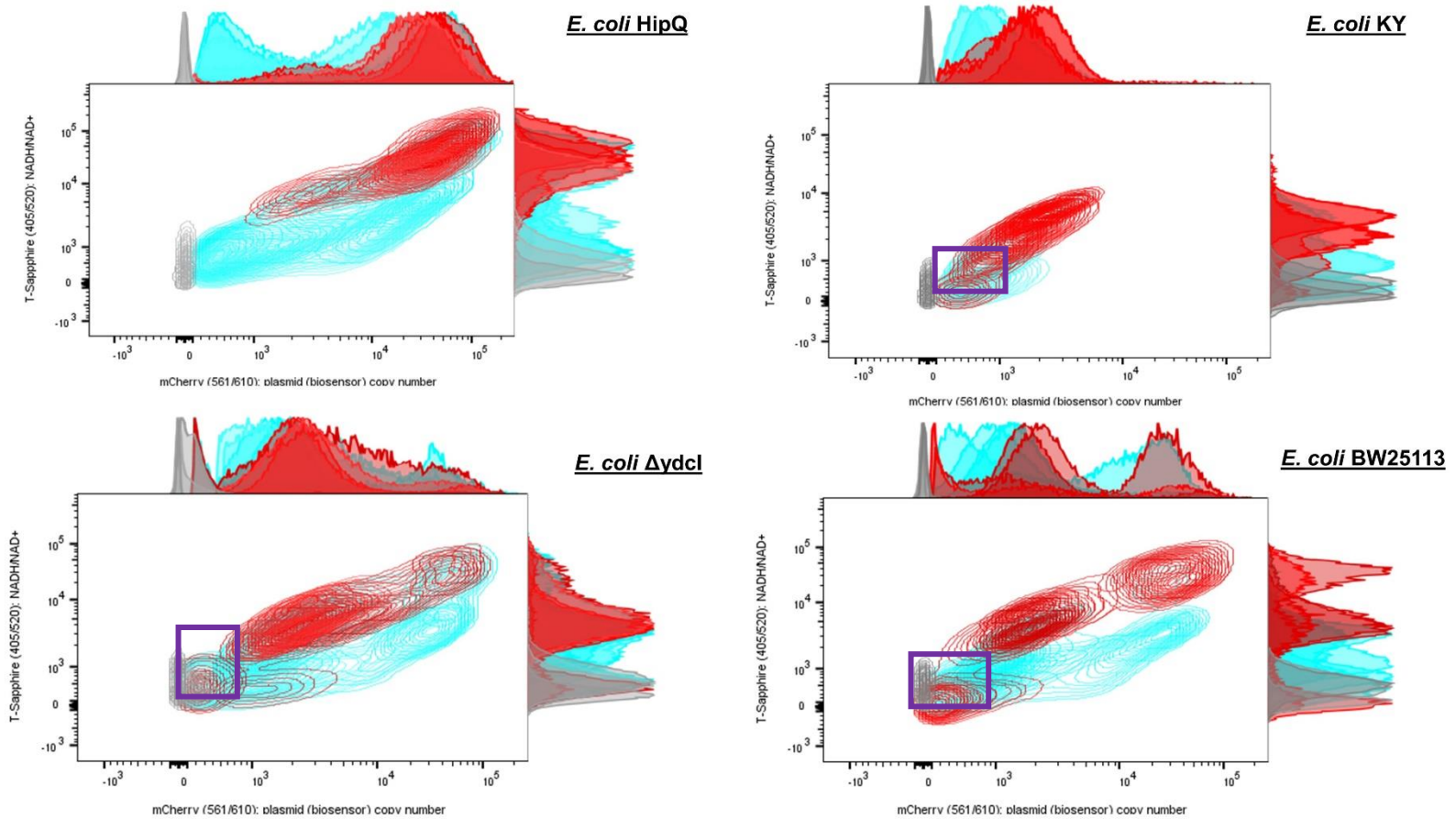

Figure 5.S7. Intracellular NADH:NAD+ of E. coli cells 24hrs post exposure to 25X MIC of ciprofloxacin. *In blue are dead cells, in red are live cells, and in grey is autofluorescence (cultures not expressing the NADH biosensor), 'zombie' subpopulation is highlighted in purple. Higher NADH/NAD+ ratio corresponds to higher rate of cellular respiration. n=5 from 3 independent experiments; 1000k events per sample were collected.*

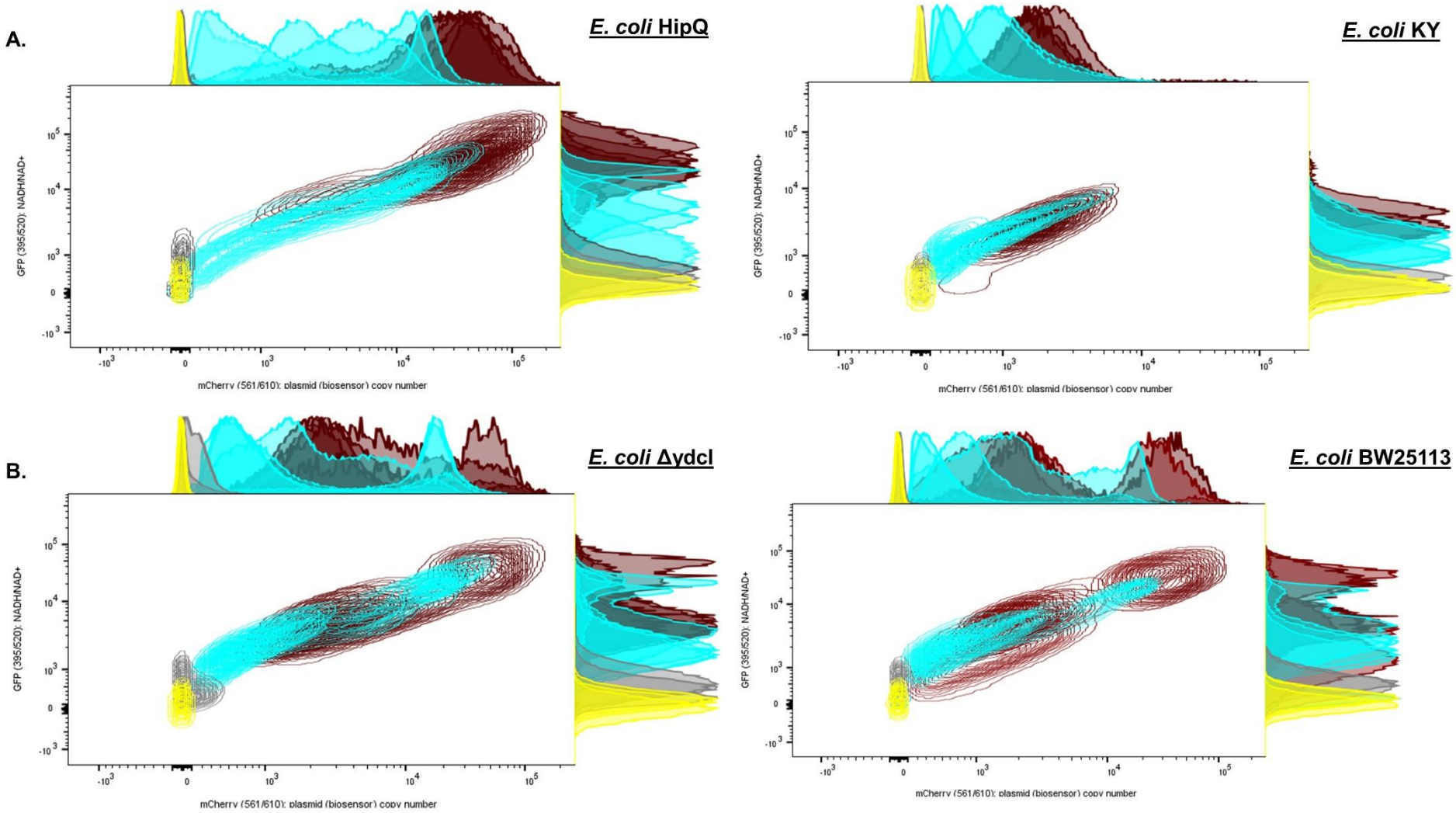

Figure 5.S8. Intracellular NADH:NAD+ of live E. coli prior (blue) and post (red, excluding the zombie subpopulation) 24hrs post exposure to 25X MIC of ciprofloxacin. *In blue are dead cells, in red are live cells, in yellow is autofluorescence at t=0hrs and in grey is autofluorescence at t=24hrs of antibiotic exposure (cultures not expressing the NADH biosensor). Higher NADH/NAD+ ratio corresponds to higher rate of cellular respiration. n=5 from 3 independent experiments; 1000k events per sample were collected.*

Chapter 6 Appendix

1. Time-kill assay starting inoculum CFU/mL in LB Miller and M9-GLUCOSE media

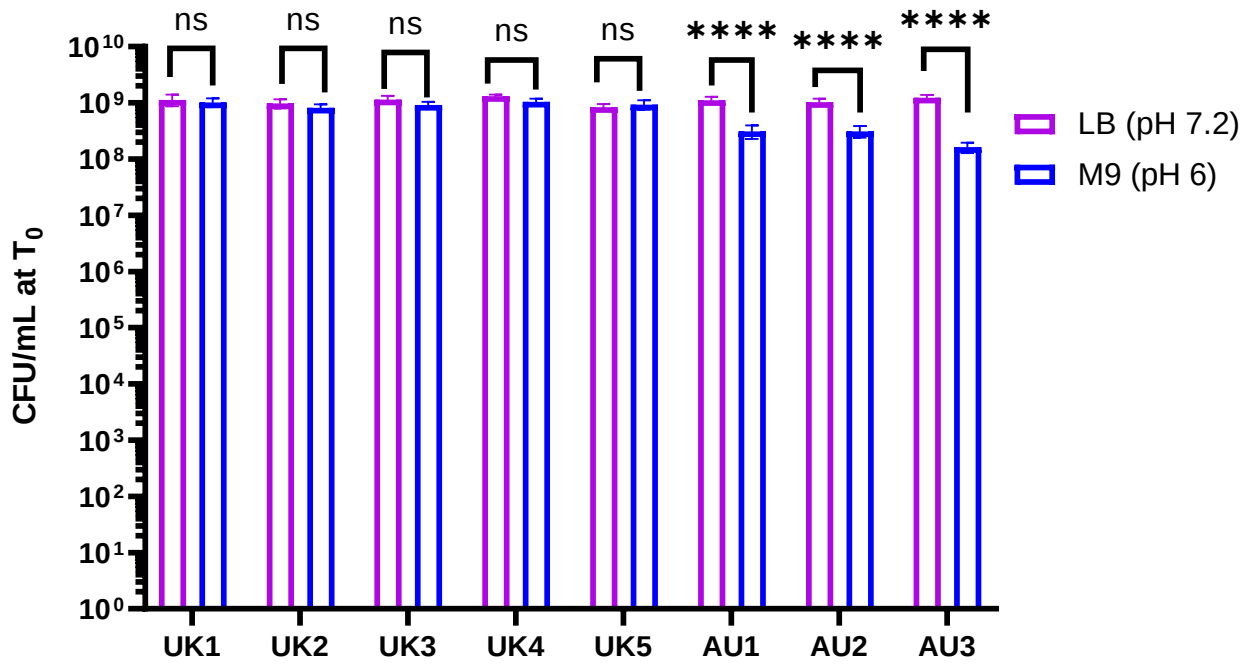

Figure 6.S1. Starting inoculum (T=0hrs) size in time-kill assays. *UK1-UK5 had the starting inoculum size adjusted by incubating M9-GLUCOSE broth cultures for additional 30minutes prior to taking the CFU/mL measurement and AU1-AU3 had measurements were taken at the same incubation time for both media. n=4/media type, from two independent experiments, error bars are SEM.*

1. **LB Miller time-kill assays**

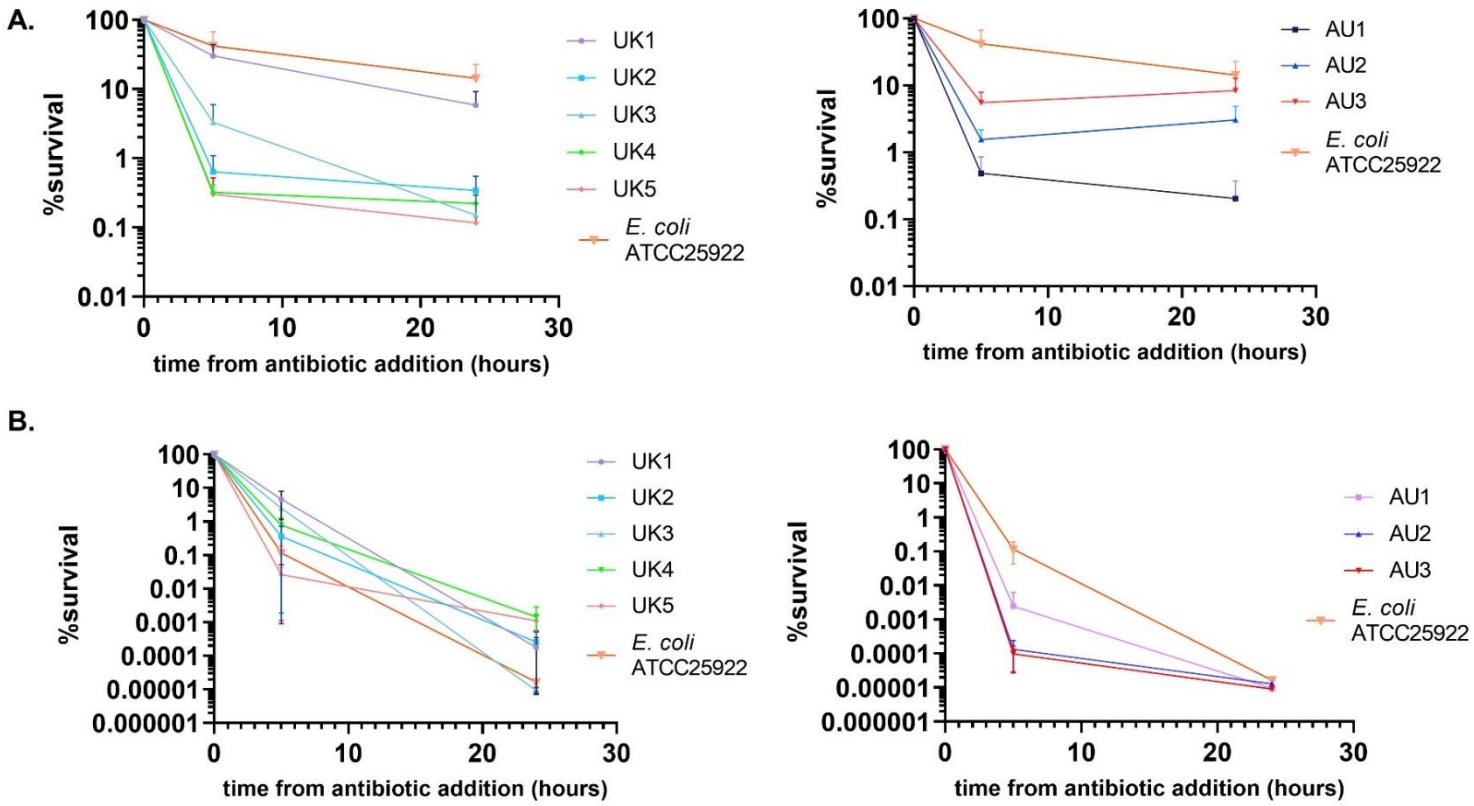

Figure 6.S2 Time-kill assay following exposure to A.25X MIC meropenem and B. 25X MIC colistin in LB Miller broth (pH 7.5). *n=4 from two independent experiments, except UK3 meropenem and AU1 colistin where n=3 due to exclusion a resistant replicate; error bars are SEM. Limit of detection was 100 CFU/mL.*

2. **M9-GLUCOSE time-kill assays**

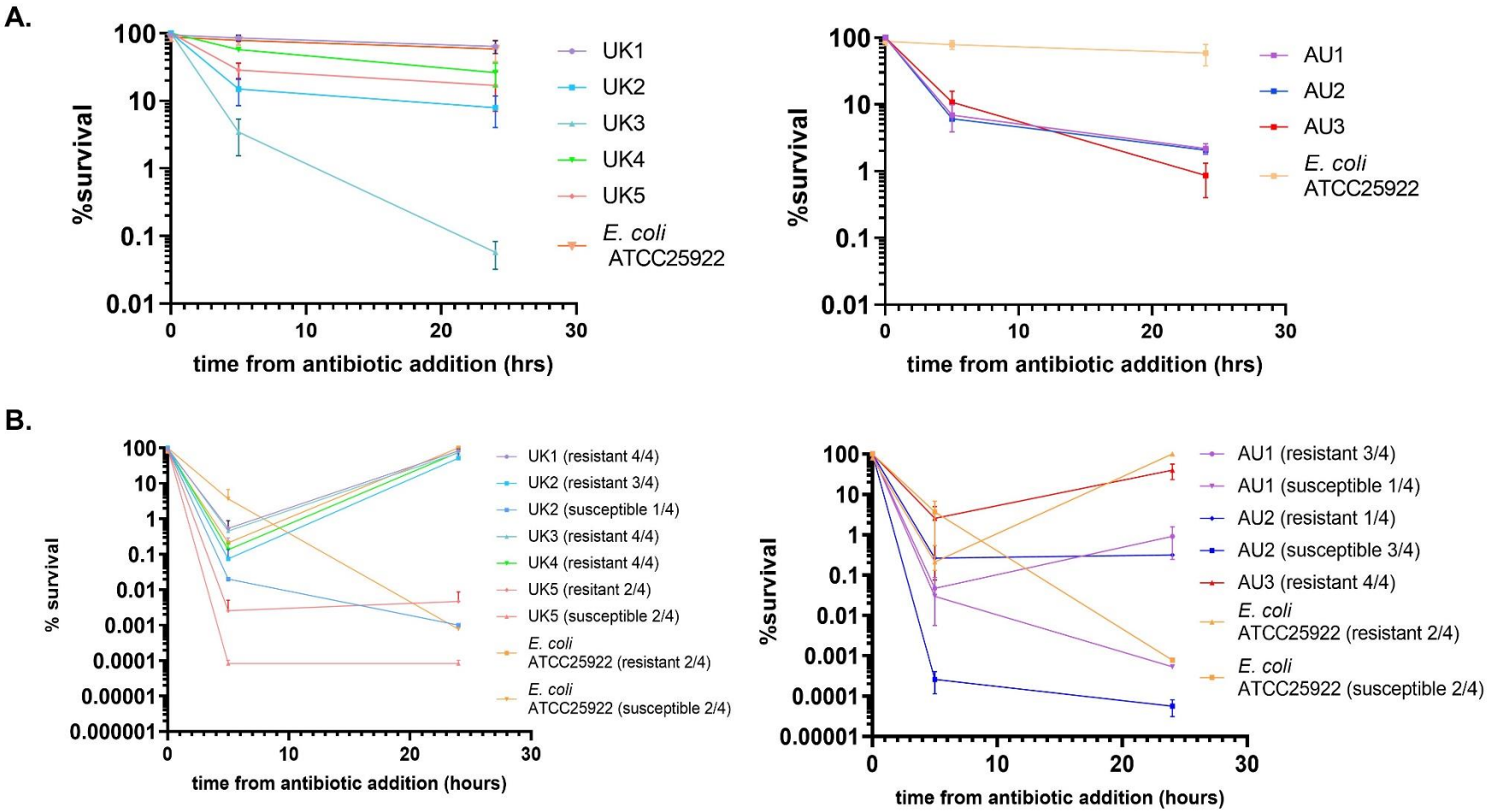

Figure 6.S3 Time-kill assay following exposure to A.25X MIC meropenem and B. 25X MIC colistin in M9-GLUCOSE broth (pH 6). *n=4 from two independent experiments; error bars are SEM. Limit of detection was 100 CFU/mL.*

3. UPEC biofilm biomass quantification

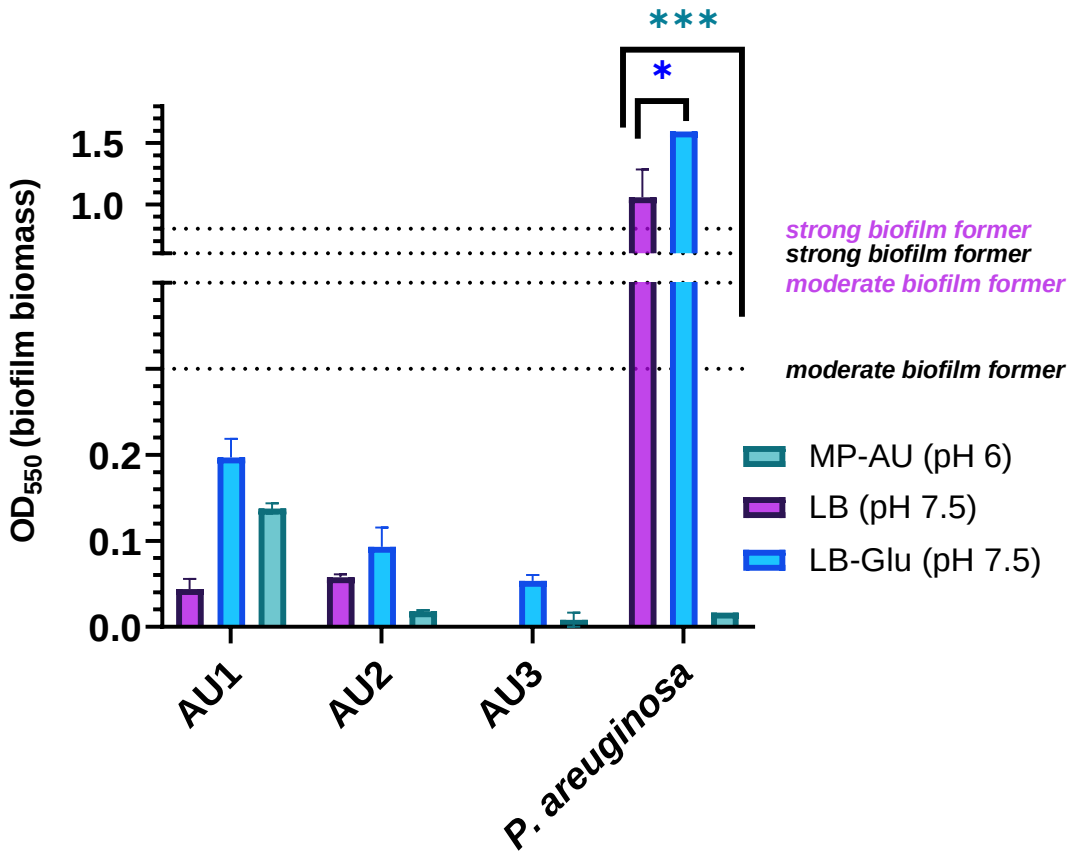

Figure 6.S4 Biofilm formation of UPEC in standard conditions (LB Miller broth, pH 7.5), LB Miller broth supplemented with 0.5% v/v glucose (LB-Glu, pH 7.5) and artificial urine (MP-AU, pH 6), following 48hr incubation*. n=2, error bars are SEM. Absorbance values were baseline-corrected for absorbance of negative control (uninoculated wells). Weak biofilm former: OD_{550} < OD_{550} negative control, moderate biofilm former: 0 < OD_{550} < 2 x OD_{550} negative control, strong biofilm former: OD_{550} > 4 x OD_{550} negative control (Lajhar, Brownlie and Barlow 2018). *= p and q < 0.05, *** = p < 0.001 by two-way ANOVA (medium vs. strain) with Benjamini, Kreuger and Yekutieli false discovery control method.*